A KINETIC STUDY OF THE T CELL RECOGNITION MECHANISM

A Thesis
Presented to
The Academic Faculty

by

Jun Huang

In Partial Fulfillment
of the Requirements for the Degree
Doctor of Philosophy in the
School of Biomedical Engineering

Georgia Institute of Technology
December 2008

A KINETIC STUDY OF THE T CELL RECOGNITION MECHANISM

Approved by:

Dr. Cheng Zhu, Advisor
Department of Biomedical Engineering
Georgia Institute of Technology and Emory university

Dr. Julia E. Babensee
Department of Biomedical Engineering
Georgia Institute of Technology and Emory University

Dr. Brian D. Evavold
Department of Microbiology and Immunology
Emory University

Dr. Michael L. Dustin
Department of Pathology
New York University

Dr. Hanjoong Jo
Department of Biomedical Engineering
Georgia Institute of Technology and Emory University

Date Approved: August 14, 2008

I DEDICATE THIS THESIS TO

MY PARENTS: 黄玉平 赵兴琳

MY WIFE: YING XIA

MY DAUGHTER: ISABELLA ROUWEN HUANG

ACKNOWLEDGMENTS

I would like to express my appreciation to the following people who helped me to make this thesis possible in my five-year PhD study.

I firstly thank my advisor, Dr. Cheng Zhu, for his guidance, encouragement, understanding, patience and support for these five years. He makes the Zhu lab a great place for us to enjoy the beauty of science. I also thank my committee members Drs. Babensee, Evavold, Dustin, and Jo for monitoring the process of my thesis.

Special thanks to my collaborators, Dr. Evavold and Lindsay Edwards. I thank Dr. Evavold for his guidance, motivation and encouragement to my PhD research. Thank Lindsay Edwards for her tremendous work in purifying T cells for my experiments.

I thank Zhu lab members for making the lab a nice place to come. Thank Veronika Zarnistyna for her encouragement and helpful discussion in T cell research; Ning Jiang for her foundation work on T cell; Fang Zhang and Yan Zhang for technical support; Tao Wu, Wei Chen and Jack Wei Chen, we came to Zhu lab at same year and will graduate together, you helped and supported me a lot in this long journey; Fang kong for donating blood; Timothy Tolentino for his kindness and patience. My acknowledgements also go to Jizhong Lou, Xue Xiang, William Madison Parks, Larissa Doudy, Jiangguo Lin, Christina Royce, Jun Yang, Krishna Sarangapani, Annica Wayman, and Brandy Rogers.

I would like to thank all the staff of the IBB building. Special thanks to Mr. Chris Ruffin and Mr. Johnafel Crowe.

I also thank my former advisor Dr. Mian Long for his support and encouragement.

TABLE OF CONTENTS

LIST OF TABLES

LIST OF FIGURES

LIST OF SYMBOLS AND ABBREVIATIONS

2D	Two dimension(al)
3D	Three dimension(al)
A_c	Contact area
APL	Altered peptide ligand
APC	Antigen presenting cell
BSA	Bovine serum albumin
CD	Cluster of differentiation
CD45 inhibitor	N-(9,10-Dioxo-9,10-dihydro-phenanthren-2-yl)-2,2-dimethyl-propionamide
CTL	Cytotoxic T lymphocytes
CTLA4	Cytotoxic T-lymphocyte antigen 4
EAS45	Experimental additive solutions 45
EC_{50}	Half maximal effective concentration
EDTA	Ethylenediamine tetraacetic Acid
FACS	Fluorescence-activated cell sorting
FBS	Fetal bovine serum

FRET	Fluorescence resonance energy transfer
ICAM-1	Intercellular adhesion molecule-1
ITAMs	Immunoreceptor tyrosine based activation motifs
K_a	Affinity
K_d	Dissociation constant
k_r	Off-rate (reverse rate)
k_{on}	On-rate (forward rate)
LAT	Linker for activation of T cells
Lck	Src kinase $p56^{lck}$
LFA-1	lymphocyte function-associated antigen-1
mAb	Monoclonal antibody
MHC	Major histocompatibility complex
m_l	Site density of ligand
m_r	Site density of receptor
P_a	Adhesion probability (frequency)
PBS	Phosphate buffered saline
PFA	Paraformaldehyde

PY	Phosphorylated tyrosine
PE	Phycoerythrin
pMHC	Peptide complexed with MHC
PP2	4-amino-5-(4-chloro-phenyl)-7-(*t*-butyl) pyrazolo [3,4-*d*] pyrimidine
PTK	Protein tyrosine kinase
PTP	Protein tyrosine phosphatase
RBC	Red blood cell
SEM	Standard error of the mean
SDS-PAGE	Sodium dodecyl sulfate polyacrylamide gel electrophoresis
SO	Sodium orthovanadate
SPR	Surface plasmon resonance
T_C	Cytotoxic T cell
TCR	T cell receptor
T_H	Helper T cell
WT	Wild type
ZAP-70	Zeta-chain-associated protein kinase 70

SUMMARY

The mechanism of T cell recognition is the central but unsolved puzzle of adaptive immunology. The difficulties come from the multichain structure of TCR/CD3, the binate binding structure of the pMHC molecule, the diversity of the peptides presented on the APC, the critical role of coreceptor CD4/8, the communication between TCR and coreceptor CD4/8, the complex environment of interactions taking place and the binding and signaling coupled process of recognition. Most studies were using the 3D kinetic measurements or biological functional assays to address the mechanism of the T cell recognition. However, those assays are usually either lacking of physiology relevance or missing of the initial recognition signals. Here a 2D micropipette adhesion assay with high temporal resolution (~second) was used to address the *in situ* kinetics of molecular interaction at the membrane of live T cells. The aim of this project is to advance our understanding to the T cell recognition mechanism.

The micropipette adhesion assay was firstly used to address a simple case, the resting state pMHC-CD8 interaction. In the absence of TCR-pMHC interaction, the pMHC-CD8 interaction has a very low affinity that depends on the MHC alleles and the lipid rafts of the T cell membrane where CD8 resides, but not on the peptide complexed to the MHC and whether the CD8 is an $\alpha\alpha$ homodimer or an $\alpha\beta$ heterodimer.

For cognate pMHC, following the initial observation in the F5 T cell system, the binding also displays a two-step curve in the OTI T cell system. The first-step binding occurs before one second and has a very fast on-rate and off-rate ($>2s^{-1}$), and the second-step binding follows immediately but reaches a much higher level of binding. It was

identified that the first-step binding is mediated by the TCR-pMHC interaction, and the second-step binding is triggered by the TCR-pMHC interaction but mediated by CD8-pMHC binding. The two-step binding is the unique property of cognate pMHC, and it can be abolished by disrupting the lipid rafts, inhibiting the Src family protein tyrosine kinases (PTK) or protein tyrosine phosphatase (PTP). The finding of two-step binding identifies a CD8-dependent signaling amplification pathway. The data also indicated the active communication between TCR and CD8 in the antigen recognition.

The crosstalk between TCR and CD8 was further dissected using two anti-CD8 antibodies 53.6.7 and CT-CD8a. 53-6.7 can significantly enhance the binding of pMHC to the T cell. Although the enhancement is directly mediated by MHC-CD8 interaction, the enhancing role of this antibody is TCR dependent. Blocking the TCR-pMHC interaction on OTI T cell or expressing CD8 alone on a hybridoma abolished the enhancement. The enhancement is also dependent on the integrity of lipid rafts and the normal function of PTP. In contrast, the antibody CT-CD8 can inhibit the binding of pMHC to the T cells and interfere with the TCR-pMHC interaction. The enhancing or inhibitory role of these two anti-CD8 antibodies is reversely correlated with the affinities of TCR-pMHC interactions. Only 53-6.7, but not CT-CD8 antibody, can phosphorylate and activate Lck. The data demonstrated a dual way crosstalk between TCR and CD8, and indicated the importance of cooperation of TCR and CD8 in antigen recognition.

In the physiology condition, the TCR must accurately and efficiently recognize the cognate peptide from thousands of surrounding endogenous peptides. There is an argument regarding whether the endogenous peptides plays a role in helping the TCR recognition. Our results demonstrated that the nonstimulatory peptides can significantly

enhance the T cell recognition sensitivity. In the presence of nonstimulatory peptide, the TCR can efficiently detect a single antigenic pMHC. The enhancement of recognition is due to the CD8 binding to the nonstimulatory pMHC. Blocking the CD8 binding can paralyze the enhancement. In contrast, it was found that the presence of antagonist can inhibit the binding of agonist pMHC to the T cells, and the inhibition occurs in the initial recognition step. Based on the data, an "amplification and competition" model was proposed to explain the molecular mechanism of the enhancement and inhibition function of the nonstimulatory and antagonist peptides in the T cell recognition, respectively.

CHAPTER 1

OBJECTIVES

How a T cell recognizes antigen presented on an APC surface is the central question of adaptive immunology. The complexity of this recognition process includes interactions between/among surface molecules on the cell membrane, signaling across the cell membrane and inside of the cells, and the proper physiology environment. The following aims were proposed to investigate the T cell recognition mechanism using a 2D micropipette adhesion assay.

1. Measure the resting state kinetics of MHC-CD8 interaction at cell membrane;

The co-receptor CD8 is composed of either homodimer CD8αα or heterodimer CD8αβ, binds to the invariant α3 domain of polymorphic MHC molecule. The specific MHC-CD8 binding was isolated and measured from trimolecular interaction of TCR-pMHC-CD8 by blocking the TCR-pMHC binding. The binding dependence of MHC-CD8 interaction on peptide complexed to MHC molecule, the CD8 composition, the MHC allele, the type of T cell and lipid rafts are characterized respectively.

2. Investigate the role of CD8 in helping the TCR's antigen recognition;

Though the TCR is the only molecule that can discriminate a foreign antigen from self proteins, its recognition efficiency is greatly reduced without the help of coreceptor CD8. Therefore how the CD8 amplifies the initial TCR recognition signal was investigated by comparing the binding difference of CD8-MHC in the absence and

presence of TCR-pMHC interaction, and studying the cooperation and signaling between CD8 and TCR during antigen recognition process.

3. Further characterize the crosstalk between TCR and CD8;

The communication and cooperation between TCR and CD8 is important in the antigen recognition process. The TCR and CD8 binding to pMHC initiates a complex signaling process leading to the CTL activation and the antigen elimination. It was found that some anti-CD8 mAbs can either enhance or inhibit the tetramer staining of CTLs. With the help of these anti-CD8 mAbs, we designed a series of experiments to examine the crosstalk between TCR and CD8 using the micropipette adhesion assay.

4. Study the diversity of peptides affecting the antigen recognition.

In the physiology condition, the antigenic peptide is surrounded with numerous of self nonstimulatory peptides. Whether and how these nonstimulatory peptides play a role in help TCR recognition of antigenic peptide is not clear. Similarly, the inhibitory mechanism of antagonist in the TCR recognition is not fully understood. The roles of the nonstimulatory and the antagonist peptides affecting the TCR recognition of antigen were studied using the micropipette adhesion assay. Also, the mechanisms of enhancing role of nonstimulatory peptide and the inhibitory function of antagonist were specifically addressed.

CHAPTER 2

BACKGROUND

2.1 T Cell Immunology

2.1.1 T Lymphocyte

The T lymphocyte mediated immune response is the central part of adaptive immunity. Two distinct lineages of T cells have been identified based on the T cell receptor (TCR) expressed on the T lymphocyte surface, either αβ or γδ TCR. . The αβ T cell is dominant in most mammals and is responsible for recognizing fragments of antigens (usually peptides) bound to the major histocompatibility complex (MHC) presented on the antigen presenting cell (APC) surface. The αβ T cell mediated immunology has been extensively studied, while the function of γδ T cell is much less understood (1, 2). This thesis will focus on αβ T cells and the following discussion is exclusively deal with αβ TCR bearing T cells.

The T lymphocyte plays an essential role for both the humoral (antibody-mediated) and cellular (T cell-mediated) immunity. The αβ TCR bearing T cells can be subdivided into cytotoxic T cell (T_C or CTL) and helper cell (T_H). The T_C or killer T cells typically express CD8 dimers and directly kill target cells on which they recognize foreign antigens bound to class I MHC molecules. The T_H cells express the CD4 molecule and secrete cytokines and other factors when they recognize antigens displayed on class II MHC molecules. The T_H cells can activate macrophage (by T_{H1}) to kill the intravesicular pathogens they harbor or B cells (by T_{H2}) to make antibody to eliminate antigens (2). Also, the T_C recognition and reaction to APC is much faster than the T_H (1).

2.1.2 T cell recognition

T cell are a self-referential and sensory organ, and the TCR owns a magic ability to recognize one antigenic peptide from the sea of thousands of self peptides (3). TCR only can recognize antigenic peptide complexed with MHC (pMHC) appropriately presented on the surface of APC. T cell recognition is a complicated process which includes the initial recognition of antigenic peptide, T cell activation and the lysis of the target cell. The specific interaction between TCR and pMHC ligand triggers the initial signaling leading to the recognition of an antigen in the cellular immune response. T cell becomes activated with a sustained elevation of calcium and begins to form a synapse. Then the T cell will secrete either cytokines to stimulate the cell it is recognizing (for T_H) or induce cell death (for T_C) (1).

The recognition of the T cell is determined by the specificity arising from a TCR repertoire and the diversity of MHC coming from the polymorphism, which guarantees the effectiveness and accuracy of TCR recognizing foreign antigen. Furthermore, the TCR not only binds to pMHC, but serves as part of a multicomponent signaling complex that includes the CD3, co-receptors CD4 or CD8, and other accessory molecules such as LFA-1, CD45 and CD28. Thus, the T cell recognition is consist of a series complicated chemical interactions involving binding and signaling coupled processes, and then leads to T cell development and activation (1, 4).

2.1.3 T cell development

T cell activation and development are both determined by TCR recognition of pMHC ligand. This flexibility of ligand recognition is essential for the development and function of T cells.

T cell development involves positive selection and negative selection. The positive selection ensures the T cell express functional TCRs capable of recognizing pMHC presented on APC surface, selects the right co-receptor CD4 or CD8 and determines the commitment for the appropriate class of MHC. The positive selection is mainly mediated by thymic epithelial cells. The negative selection eliminates the self-pMHC reactive T cells, and it is largely mediated by dendtritic cells and macrophage (2). In other words, a developing T cell must recognize a self pMHC in order to complete its developmental program, but once this T cell has matured, the self pMHC seen during development will be nonstimulatory and the cell will only be activated by a non-self pMHC. Self-reactive T cells are largely removed during differentiation in the thymus, hence reactivity among those that remain is generally against foreign entities. It seems that T cells are continually exposed to ligands that can bind the TCR to some degree, but how T cells are able to ignore many of these self pMHC while recognize a few foreign pMHC, and how is a self pMHC play a role in this recognition process, it is still not fully understood (2, 5, 6).

2.1.4 TCR/CD3 complex

The TCR/CD3 complex plays a critical role in the differentiation, survival, and function of T cells. TCR is a heterodimer composed of disulfide-bonded α and β chains. Each TCR chain is composed of variable and constant Ig-like domains, followed by a transmembrane domain and a short cytoplasmic tail. The variable domain is encoded by a rearranged gene comprising components of the variable (V), diversity (D) and joining (J) minigenes (D is only present in the β chain) (7, 8). TCR is assembled with the invariant chains of the CD3 complex: $\delta\varepsilon$ and $\gamma\varepsilon$ heterodimers, and the $\zeta\zeta$ homodimer (Fig. 2.1).

The assembly of TCR-CD3 complex is organized by three major assembly steps in the membrane, and each step depends on the formation of a three-helix interface between one basic and two acidic residues. The association of these three CD3 signaling dimers with TCR is driven by the highly specific polar interactions among transmembrane domains which are uniquely favorable in the lipid environment (9, 10). The TCR αβ structure itself has no intrinsic signaling capacity, while the CD3 components have immunoreceptor tyrosine based activation motifs (ITAMs) that become phosphorylated after TCR engagement with pMHC and recruit other signaling molecules to initiate a signaling cascade(2, 8, 11).

2.1.5 Peptide and MHC

The peptide, either cytosolic or endocytosed, binds to MHC I or MHC II in a specialized groove of the MHC protein respectively (8). MHC I is expressed on most cell types and is recognized by CD8+ T cells. In contrast, class II is expressed on specialized APCs and can be induced on other cells under certain conditions. Class I molecules present cytosolic peptides, and thus are particularly suited for presenting antigens from intracellular viruses. Class II molecules present peptides derived from endocytosed proteins, and thus tend to induce responses to extracellular proteins. Class I molecules comprise an α heavy chain (with α_1, α_2 and α_3 helices) and β_2 microglobulin (β_2m) light chain. The α chain encodes the two helices that form the sides and floor of the peptide binding groove. Class II molecules consist of α (α_1 and α_2 helices) and β chains (β_1 and β_2 helices); the two chains are of similar size and each contributes one side of the binding groove. Class II is recognized by CD4+ T cells. Thus, CD8+ T cells are said to be ‘class I-restricted’ and CD4+ cells ‘class II-restricted’ on the basis of the class of MHC that

their receptors recognize CD4 interacts with class II at a site away from the TCR-interaction site, and CD8 interacts with a similar region of class I; the role of this interaction is to stabilize the TCR-pMHC complex.

MHC class I and class II both have a peptide binding groove along the top (membrane-distal) face of the molecule. In class I molecules, the ends of the groove are closed so that the groove accommodates a peptide of 8–9 amino acids. Class II peptides can be much longer, since the ends of the groove are not closed, but the peptides tend to be 15–20 amino acids in length. Peptide amino acid side-chains can either interact with the MHC molecule or point out of the groove to be recognized by the TCR. Those interacting with the MHC often show 'anchor residues'; these are specific types of side-chains interacting with pockets in the floor of the binding groove. Thus, it is often possible to predict peptides that can bind to MHC molecules by searching for combinations of potential anchor residues that might fit the binding groove of a specific MHC molecule (8).

2.1.6 Co-receptor CD4/8

There are two major classes of T cells, CD4 T cell and CD8 T cell. They distinguish from each other by the surface markers CD4 or CD8 molecules. Both the CD4 and CD8 bind to the invariant parts of MHC molecules. Because CD4/CD8 helps TCR recognize antigen pMHC, they are called co-receptors. The co-receptor CD4/CD8 binding to pMHC is also a requirement for normal T cell selection (2).

CD4 is a single chain molecule composed of four immunoglobulin-like domains (Fig. 2.1). The D1 and D2 domains are packed together to form a rigid rod, which is linked with a similar rod formed by D3 and D4 domains by a flexible hinge. The

cytoplasmic domain of CD4 interacts with a tyrosine kinase Lck, which can transmit signal to the interior of T cell. CD4 binds to MHC II β_2 domain mainly via its D1 domain, and some residues of D2 domain might be also involved. Because the interaction of CD4 and MHC II is weak and the binding site is far away from the one for binding TCR on the MHC II molecule, it is not clear how CD4 plays its function by binding to MHC molecule. However, with the participation of CD4, the T cell recognition sensitivity will greatly increase and the dose for activate the T cell will be lowered ~100 folds.

CD8 is a disulfide-linked heterodimer CD8αβ or homodimer CD8αα molecule (Fig. 2.1) (12). Each single α or β chain contains a single immunoglobin-like domain linked to the membrane by an extensively glycosylated segment of extended polypeptide chain. The CD8 binds weakly to the α3 domain of MHC I molecule. The cytoplasmic of CD8α chain is noncovalently associated with Lck, while the CD8β domain is believed to facilitate the participation of CD8 into lipid raft for signaling by delivery Lck to TCR/CD3. The dimeric CD8 potentiates the reactivity of T cell and increases its sensitivity in recognizing antigen pMHC by ~100 folds (1).

The co-receptor CD4/8 binds to invariant domain of MHC molecule and is linked with Lck via its cytoplasmic domain. The CD4/8 also associates with TCR/CD3 on activated T cells. These features facilitate the signaling of T cell in early triggering and activation. Absence or blockage of the CD4/8 results in poor recognition and require much more peptide-MHC (10–100x) (1). So, it seems the co-receptor CD4 or CD8, bind to the MHC molecule and facilitate the recognition of T cell in a similar way. However,

the functions of the co-receptor CD4/8 still need to be further investigated before fully understand them.

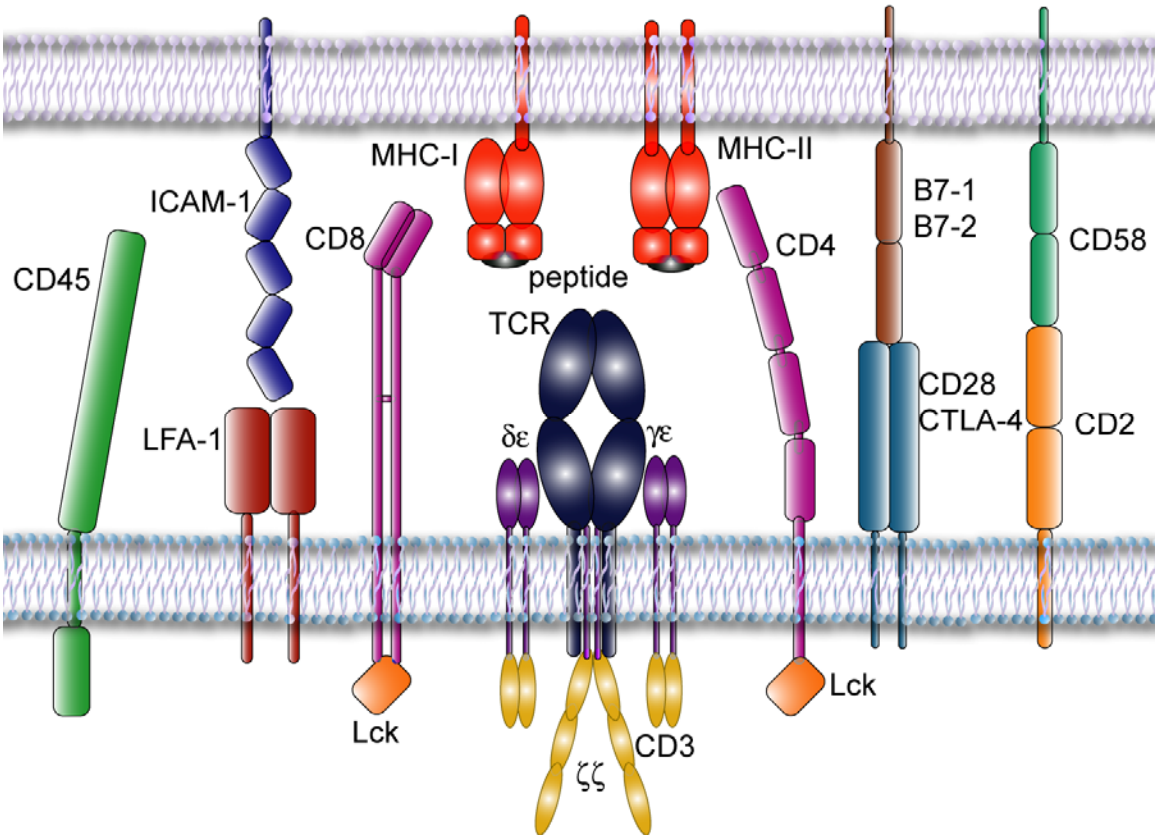

Figure 2.1 Important surface molecules expressed on either T cell or APC surface. These molecules play critical roles in the T cell recognition, and the function of each molecule was discussed in the text (1).

2.1.7 Co-stimulatory molecules

Co-stimulatory molecules play critical roles in T cell development, activation and effector function. Activation of T cell is generally thought require two signals: The first signal is delivered by TCR complex according to its specific antigen pMHC recognition, and the second signal is provided by non-specific co-stimulatory molecule engagement. Activation of T cells without co-stimulation may lead to T cell anergy, T cell deletion or the development of immune tolerance (13). We will briefly introduce some of those co-stimulatory molecules including LFA-1, CD28, CTLA-4, CD2 and CD45 (Fig. 2.1).

(1) LFA-1

LFA-1, a $\alpha_1\beta_2$ integrin molecule, can either play a role of an adhesive molecule or serve as a co-stimulatory receptor. As adhesion molecule, LFA-1' dependent adhesion is critical for immunological synapse formation (14) and triggering T cell activation (5). As a co-stimulatory molecule, LFA-1 delivers functional signals and synergises with TCR stimulation to activate T cell. LFA-1 is subjected to two-way signaling that plays a pivotal role in the regulation of its function and activity(15). LFA-1 on resting cell binds to its ligand ICAM-1, 2 and 3 with low affinity, and this binding affinity can be greatly increased by the inside-out signaling mediated by TCR (16) and chemokine receptors (17), while the outside-in signals from the LFA-1 binding to its ligands can contribute to TCR triggering (5). Recently, it was reported that the affinity of LFA/ICAM-1 can be regulated by specific TCR-pMHC interaction (18).

(2) CD28

CD28 is the principal co-stimulatory receptor that expressed on naive and primed T cell surface. CD28 is a 44 kDa glycoprotein molecule that binds to its ligand B7-1 and B7-2 on APCs. The CD28 ligation is required for the effective immune response to occur. Without the CD28 ligation, the TCR binding to the pMHC will lead to apoptosis or anergy of T cell. The co-stimulatory signal of CD28 can increase the production of cytokine and promote the T cell survival. Also, the CD28 ligation can reduce the threshold of the TCR number to trigger T cell activation (13). CD28 colocalizes with the TCR within the immunological synapse thereby triggering the active transport of cell surface molecules into the synapse (1) and increasing the local concentration of enzymes and adaptor molecules (13). The signaling mechanism of CD28 is not fully understood,

and it was suggested that the CD28 can influence nuclear transcription and block the egress of NFAT from the nucleus (1, 13).

(3) CTLA-4

Cytotoxic T-lymphocyte antigen 4 (CTLA-4) is a CD28 family receptor mainly expressed on activated T cell. CTLA-4 is ~30% homologous with CD28 and also binds to the ligands B7-1 and B7-2, but with higher affinity than CD28. Most CTLA-4 molecules are found intracellular, and it comes to the T cell surface several minutes after activation, however, in contrast to CD28 which enhances cell activation, CTLA-4 inhibits the T cell proliferation and prevents it from functioning by reducing IL-2 receptor expression and IL-2 production, and by arresting T cells at the G1 phase of the cell cycle (1, 13).

(4) CD2

CD2 is an adhesion molecule expresses on T cell that binds to CD48 (mouse) and CD58 (human) with low affinity (19-21). CD2 has been shown to set quantitative thresholds in T cell activation. The CD2 signaling pathway and network are being investigated and characterized (22).

(5) CD45

CD45 is most abundant large leukocyte cell surface glycoproteins expressed on hematopoietic cells. CD45 have different isoforms depending on the type of exon the CD45 has or not. CD45 plays a critical role in T cell thymic development, T activation and proliferation. CD45 is a large protein tyrosine phosphatase (PTP) molecule, although there is no known ligand, at least two members of the Src-family of protein tyrosine kinases (PTKs), the Lck and Fyn proteins, have been implicated as physiological substrates of CD45. This transmembrane phosphatase has a role as both positive and

negative regulator of T cell signaling through the primary initiator Lck, in particular, by regulating the phosphorylation state of tyrosine Y505 and Y394 (23-27).

2.1.8 Cytoskeleton and lipid raft

The cytoskeleton is crucial for the highly dynamic T cell in determining its shape and performing its function. Upon encountering APC in the lymph nodes or spleen, the T cells must go through several complicated cytoskeleton-dependent processes, including TCR recognition of antigen, integrin-mediated adhesion immunological-synapse formation (28), accessory receptor stimulation, cellular polarization, receptor sequestration and signaling (29), to efficiently recognize and take action to the target cells. The cytoskeleton system provides the T cell a dynamic cellular framework to rapidly deform itself against the target cell and reorient its cellular organelles to the interface between the T cell and the APC (30). The dynamic rearrangements of the cytoskeleton are crucial for T cell migration, scan the presence of antigens and recognize the infected target cells (31). In fact, treatment with inhibitors of actin polymerization results in the abolishment of T cell functions (30). Thus, the cytoskeleton plays a critical role in mediating multiple T cell functions.

Lipid rafts also play a critical role in TCR recognition, signaling and stimulation. Lipid rafts are structures known as glycosphingolipid-enriched microdomains or detergent resistant microdomains, which are formed by hydrophobic interactions between saturated fatty acid residues of their main lipid constituents sphingomyelin and glycosphingolipids (32). It has been implicated that lipid rafts are hotspots for both protein and lipid signaling pathways. These rafts accumulate several cytoplasmic lipid-modified molecules, including Src-family kinases Lck and Fyn, coreceptors CD4/8 and

transmembrane adapters LAT and PAG/Cbp, while exclude most other abundant transmembrane proteins including the protein tyrosine phosphatase CD45. The engagement of TCR promotes aggregation of lipid rafts, which facilitates colocalization of signaling proteins including Lck, LAT, and the TCR, thereby initiating the protein tyrosine phosphorylation and amplifying the downstream signaling (32-36). However, lipid rafts are still in hot debates. First, the existence and functional roles of lipid rafts remain unclear in physiological condition. Second, there are lacking direct methods for studying lipid rafts such as their composition, size and heterogeneity, as well as the dynamics of their interactions with TCRs and other immunoreceptors (32, 36).

2.2 Previous studies on T cell recognition

2.2.1 Puzzles at T cell recognition.

Although it is generally accepted that the T cell recognition goes through such a way: the engagement of TCRs with pMHCs initiates a signal, which is amplified via kinase cascade and signal protein translocation, and transmitted to the nucleus to lead the T cell activation. In sharp contrast, how the TCR engagement with a pMHC initiate the first recognition signal remains a puzzle (5, 6). Several barriers have to be overcome for T cells to recognize antigenic pMHCs effectively on the APC.

The first barrier is the diversity of the peptides presented on the APC surface. In physiological condition, a foreign antigenic peptide is surrounded by a large number of self peptides, and it is more likely randomly distributed on the APC surface with very low density, so the T cell must reliably recognize these very few antigenic pMHCs with high sensitivity (5, 37). Second one is the trimolecular binding structure of pMHC. Both the TCR and co-receptor CD4/8 can bind to pMHC. Although a lot of publications have

stressed the importance of the co-receptor in the recognition process, however, it is still controversial on how the TCR and co-receptor cooperate in binding to the pMHC (2, 3, 6, 7, 38). Third one is the complexity of TCR/CD3 structure. The association of TCR with CD3δε, γε, and ζζ signaling subunits are critical and necessary for signal transduction (9, 10, 39, 40). Fourth one is the molecular geometry. Because of the relatively small size of the TCR, 7 nm, compared to other cell surface molecules such as CD45, 40–50 nm, how the TCR overcome the sterical hindrance to interacting with pMHC need to be explained (37). Fifth one is the complicated communication environment between T cell and APC, includes the surface structure and cytoskeleton of cells, the physical forms of the surface molecules, the complex but critical co-stimulatory molecular interactions and the complicated signaling process. Sixth one is how to translate and amplify the TCR/pMHC interaction into a prolonged signal necessary for activation (37). The last one is the anchorage of molecules and the interaction dimension. It has been shown that only surface anchored pMHC, but not the soluble pMHC can efficiently activate T cells (5, 6, 41).

Due to the complexity of the T cell recognition, many studies have been done and several models have been proposed. A complete model should fulfill the following criteria. First, the model can explain how the initial recognition signal is achieved. Second, the model should explain how the signal is amplified and transmitted. Finally, it must explain how the signaling is controlled. Below, we will briefly review some of those models (37).

2.2.2 Proposed models for T cell recognition and discrimination

(1) Kinetic proofreading model.

Kinetic proofreading model was proposed to explain how T cells can discriminate among pMHC ligands based on a kinetic parameter, the ligand-receptor dissociation rate constant (42, 43). Kinetic proofreading model suggests that the potency of a pMHC is primarily determined by the off-rate of the TCR-pMHC interaction. This model explains how ligands with apparently minor differences in off-rates for the TCR could have biologically different outcomes based on the time it takes for T cells to commit to successive activation events. The TCR/pMHC complex must sustain long enough to send a complete signal to fully activate a T cell (42).

Also, Using SPR technique, it was found that there is positive correlation between the kinetic off-rate and the peptide potency in activating T cell in both CD4 and CD8 T cell system (11, 44). However, several exceptions were reported that slow off rate do not necessarily result in better activation (45-47). Also, this model does not address how the T cell overcomes the initial contact barriers caused by large surface glycoprotein such as CD45. In order to explain those exceptions and barriers, Van der Merwe et al. revised the kinetic proofreading model and proposed a kinetic-segregation model (48, 49).

(2) Conformational model

Conformational model also called allostery model, which requires conformational changes for signal transmission across the cell membrane. The conformational model suggests that upon encounter with a pMHC, the TCR can change to a conformation that induces a signal within the T cell facilitating activation. Alarcón's group has shown that the engagement of TCR with pMHC can cause the exposure of an epitope on CD3 which

can be reported by an antibody (50-53). However, except the LC13 TCR crystal structure, most TCR crystal structures do not show any direct evidence for conformational changes of the TCR following binding to pMHC-TCR complex (54, 55). To date, the challenge of the conformational model still exists: lacking of more direct evidence of TCR conformational changes.

(3) Clustering model

The clustering model proposed that the TCR dimerization or oligomerization is important in T cell recognition and signaling(56-60), based on the data that only dimeric or oligomeric pMHCs, but not soluble monomer pMHCs, can efficiently trigger the T cell activation and signaling(5, 6, 58, 60). Dustin lab found that the TCR microclusters form within seconds of T cell contact and colocalized with activated forms of Lck, ZAP-70, and LAT(61, 62), then form the immunological synapse to activate T cells(14).

(4) Pseudodimer model

Based on the heterodimer data, Davis et al. proposed a pseudodimer model. This model suggested that the binding of a first TCR to an agonist pMHC can recruit a second TCR binding to an endogenous pMHC, which is bridged by a CD4 molecule associated with the first TCR, thereby forming a stable pseudodimer to initiate activation through the kinase Lck (3, 6). In sharp contrast, using similar experimental system and method, Ma et al. obtained opposite results and conclusions. They claimed endogenous pMHCs had a negligible effect in triggering T cell activation, and the pseudodimer is not well supported by experimental data (5). Actually, the psudodimer model is lacking direct spatial resolution evidences, and it is conflict with several reports that the TCR and CD8 must bind to same pMHC in order to fully initiate the T cell activation (2, 63, 64).

(5) Other models

Those models includes thermodynamic two-step model (65), serial triggering model (66), occupancy model (67), and spare receptor model(68, 69) etc.

2.3 Significance of present project

The T cell discrimination mechanism is the central questions of adaptive immune response. Although many studied have been performed, it remains unclear. This project will provide new information and insight to advance current understanding. Therefore it has fundamental scientific importance as well as clinical application significance.

CHAPTER 3

MATERIALS AND METHODS

3.1 Cells, proteins, antibodies and chemicals

3.1.1 Cell Preparation

OTI transgenic mice expressing H-2K^b MHC-restricted OTI TCR specific for an OVA epitope (aa 257–264) of ovalbumin (44, 70, 71), P14 transgenic mice expressing H-2D^b MHC-restricted P14 TCR specific for a gp33 epitope (aa 33-41) of lymphocytic choriomeningitis virus (72) and F5 transgenic mice expressing H-2D^b MHC-restricted F5 TCR specific for an epitope (aa 366-374) of influenza nucleoprotein (73) were housed in the Emory University Department of Animal Resources facility according to a protocol approved by the Institutional Animal Care and Use Committee of Emory University. Naïve OTI, P14 and F5 T cells from transgenic mice were purified using MACS according to the manufacturer's instructions (Miltenyi Biotec, Auburn, CA). Briefly, a single cell suspension of splenocytes was incubated with anti-CD8 positive selection magnetic beads. Cells were washed, run through a magnetic column, and eluted. Purified T cells were washed and stored at 4 ^{o}C for use up to two days.

Human Red Blood Cells (RBCs) were isolated from whole blood of healthy volunteers according to a protocol approved by the Institutional Review Board of Georgia Institute of Technology as previously described (74-76). Briefly, 5 ml whole blood was collected using a sterile tube containing EDTA, then carefully layered over 3 ml of Histopaque (Sigma, St. Louis, MO), centrifuged and washed 5 times with PBS and another 3 times with experimental additive solutions 45 (EAS45) at room temperature.

The isolated RBCs were resuspended and stored in EAS45 solution at 10% hematocrit aseptically at 4 ^{o}C for further protein coating and micropipette experiments.

3.1.2 Reagents

*Peptide Major Histocompatibility Complex (pMHC):*The following peptides were custom synthesized and purified: OVA (SIINFEKL), A2 (SAINFEKL), G4 (SIIGFEKL), E1 (EIINFEKL), K4 (SIIKFEKL), R4 (SIIRFEKL), V-OVA (RGYNYEKL), VSV (RGYVYQGL) (44, 71), Mapk8 (AGYSFEKL), Stat3 (ATLVFHNL), gp33 (KAVYNFATM) (72), HIV gag (SQVTNPANI) (77) and MOG35–55 (MEVGWYRSPFSRVVHLYRNGK). Monomeric mouse MHC-I or MHC-II molecules complexed with these peptides (OVA, A2, G4, E1, K4, R4, V-OVA, VSV, Mapk8 and Stat3 for WT or CD8-null H-2K^{b}, gp33 and HIV gag for H-2D^{b}, and MOG for I-A^{b}) and tagged with a single biotin at the C-terminus were produced by the NIH Tetramer Core Facility at Emory University.

Antibodies: Rat anti-mouse CD8α (CT-CD8a) and CD8β (CT-CD8b) mAbs with or without PE conjugation were from Invitrogen (Carlsbad, CA). Rat anti-mouse Vα2 TCR (B20.1) mAb with or without PE conjugation was from BD Pharmingen (San Diego, CA) or eBioscience (San Diego, CA), respectively. PE-conjugated hamster anti-mouse CD3ε (145-2C11) mAb was from BD Pharmingen. PE-conjugated anti-mouse H-2K^{b} (3H2672) and H-2D^{b} (BCDb) mAbs were from United States Biological (Swampscott, MA) and Biocarta (San Diego, CA), respectively. PE-conjugated mouse anti-biotin (Bio3-18E7.2) mAb was from Miltenyi Biotec. Anti-Lck PY394 (Clone 9A6)

was from milliore (Billerica, MA), PE conjugated goat-anti-mouse antibody was from Sigma (St. Louis, MO)

Antibody Fragmentation: Monoclonal mAbs 145-2C11, CT-CD8a, and 53-6.7 Fab were prepared using the Fab preparation kit (Pierce Biotechnology, Inc., Rockford, IL) following the manufacture's instruction. Briefly, antibodies were incubated with immobilized papain with continuous rotation for overnight at 37^{o}C. The digested mixtures of Fab and Fc were tested by SDS-PAGE at both reduce and non-reduced conditions to ensure the completion of fragmentation.

Chemicals: PP2 (4-Amino-5-(4-chlorophenyl)-7-(t-butyl)pyrazolo[3,4-d]pyrimidine) was from Biomol (Plymouth Meeting, PA). Protein tyrosine phosphatase CD45 inhibitor (N-(9, 10-Dioxo-9, 10-dihydro-phenanthren-2-yl)-2, 2-dimethyl-propionamide) was from EMD (San Diego, CA). Cholesterol oxidase was from MP Biomedical (Santa Ana, CA) or Sigma (St. Louis, MO). Sodium orthovanadate was from Sigma.

3.2 Coupling pMHC onto RBCs

Biotin-streptavidin coupling was used to coat biotinylated pMHC monomers onto the RBC surface (76). RBCs were biotinylated using Biotin-X-NHS (Calbiochem, San Diego, CA) according to the manufacturer's instruction. Briefly, RBCs were washed three times with PBS, incubated with titrated Biotin-X-NHS at pH 7.2 for 30 min at room temperature, and washed five times with PBS/1% BSA to remove Biotin-X-NHS and stop the reaction. The biotinylation efficiency was checked via flow cytometry by using

PE-conjugated anti-biotin mAb. After three washes with EAS45/1% BSA, biotinylated RBCs were stored in EAS45 solution for further use within 3-4 weeks.

Before each experiment, biotinylated RBCs were incubated with streptavidin (Pierce, Rockford, IL) at 0.5 mg/ml for 30 min at 4 ^{o}C, washed three times with EAS45/1% BSA to remove unbound streptavidin, and incubated with biotinylated pMHC monomers for 30 min at 4 ^{o}C. After washing three times with EAS45/1% BSA, the pMHC coated RBCs were ready for site density determination and micropipette adhesion assay.

3.3 Flow cyctometry analysis

3.3.1 Determination of molecular density on cell surface

For every micropipette experiment, site densities of pMHC on RBCs and CD8 on T cells were measured by flow cytometry (Fig. 3.1). To measure the pMHC site density, RBCs were incubated with PE-conjugated mAb 3H2672 (for H-2K^{b}) or BCDb (for H-2D^{b}) at 10 μg/ml in 200 μl of FACS buffer (RPMI/5mM EDTA/1% BSA/0.02% sodium azide) on ice for 40 min. Similarly, CD8α subunit, CD8β subunit, TCR, and CD3 expressed on T cells were stained with their respective PE-conjugated mAbs. CD8 is expressed as either an αα homodimer or an αβ heterodimer (12). Therefore, it is assumed that the site density of CD8αβ equals to that of CD8β whereas the site density of CD8αα equals half of the site density difference between CD8α and CD8β.

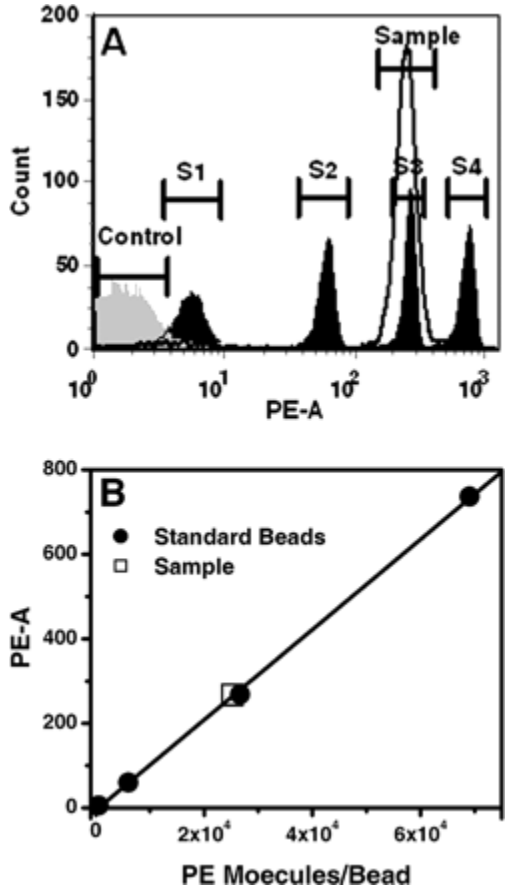

Figure 3.1 Site density determination. *A*, T cells were incubated with PE-labeled primary mAb and analyzed by flow cytometry (*sample, open histogram*) along with four standard calibration beads (*S1–S4*, *filled histograms*). The isotype control for nonspecific binding was shown for comparison (*control, shaded histogram*). *B*, A calibration curve of PE molecules/bead (provided by manufacturer) vs measured fluorescence intensity PE-A was plotted based on data of four standard beads (*filled circles*). The site density of CD8 on T cells was calculated by comparing the fluorescence intensity of the sample (*open square*) with the calibration curve after subtracting negative control fluorescence intensity.

3.3.2 T Cell activation analysis

A mouse T lymphocyte activation antibody cocktail (BD) was used to identify activated T lymphocytes by direct immunofluorescent staining with flow cytometric analysis. In short, 1×10^5 naïve OTI T cells and 1×10^7 million pMHC coated or plain RBCs were mixed and pelleted by centrifugation $\times 200g$ for 5 minutes, and incubated at 37 ^{0}C for 12

hours. After centrifugation and decanting the supernatant, the cell pellet was resuspended in 300 μl RBC lysis buffer (eBioscience) and incubated at room temperature for 5 minutes to lyse the RBC, then 700 ml PBS was added to the tube to stop the reaction. The remaining T cells were centrifuged and washed by FACS buffer for three times, and resuspended in 200 μl FACS buffer for antibody staining. The T cells were further stained by 20 ml antibody cocktail (a mixture of PE-conjugated anti-CD69 (clone H1.2F3), PE-Cy7 conjugated anti-CD25 (clone PC61) and APC conjugated anti-CD3 (clone 145-2C11) antibodies) or isotype control cocktail. The activation of T cell was analyzed on a BD LSR flow cytometry (BD).

3.3.3 T cell intracellular staining

One million T cells were resuspended in 100 μl modified FACS buffer (PBS/5% FCS/0.02% NaN_3), and the Fab of anti-CD8α mAb (clone 53.6.7 or CT-CD8) was added to the T cells at a specific concentration (50μg/ml or 10μg/ml) and incubated for 30 minutes at 4 ^{0}C. After wash, the cell pellet was resuspended in 100 μl 2% PFA/PBS (4% paraformaldehyde in PBS) solution and incubated for 10 minutes in dark at room temperature. Then the cells were incubated with first antibody (anti-PY394 or anti-PY505) in the SAP (HBSS/0.1% saponin/0.05% NaN_3/5% FBS) buffer at the concentration of 10 μg/ml for 30 minutes in dark at room temperature. After repeat wash, the cells were continuously staining with fluorescence labeled secondary goat-anti-mouse antibody. After wash, the T cells were resuspended in 0.5ml modified FACS buffer and analyzed immediately at flow cytometry (add additional fixative if stored).

3.4. Micropipette adhesion frequency assay

3.4.1 Two dimensional kinetics measurement

2D kinetics of MHC-CD8 (or TCR) interactions were measured using a micropipette adhesion frequency assay modified from that described previously (74, 75). Briefly, a pMHC-coated RBC and a T cell were aspirated by two apposing micropipettes with respective diameters of 1.5 and 3 μm in isotonic chamber medium (L-15/5mM HEPES/1% BSA). Adhesion between the RBC and the T cell was staged by placing the cells into controlled contact via micromanipulation (Fig. 3.2). The presence of adhesion at the end of a given contact period was detected mechanically by observing microscopically the deflection of the soft RBC membrane upon retracting it away from the T cell. Such detection was reliable and unambiguous in >90% of the tests, as clearly observable membrane deflections could be generated by a force as low as 2 pN at the RBC apex. This approach-contact-retraction cycle was repeated 50 times to calculate an adhesion frequency, P_a, at that contact duration, t. For each pMHC, >30 pairs of cells were used to obtain several P_a vs. t curves that correspond to different CD8 (or TCR) and pMHC densities, m_r and m_l. Each binding curve was fitted using nonlinear regression to the following probabilistic kinetic model for single-step monovalent receptor-ligand interaction (74, 75),

$$P_a = 1 - \exp\{-m_r m_l A_c K_a^0 [1 - \exp(-k_r^0 t)]\}, \tag{3.1}$$

To estimate a pair of parameters: a zero-force reverse-rate, k_r^0, and an effective binding affinity, $A_c K_a^0$, where A_c is the contact area (which was kept constant in all experiments). Means and standard errors of k_r^0 and $A_c K_a^0$ were calculated from their individual values

estimated from different P_a vs. t curves corresponding to different m_r and m_l for each pMHC.

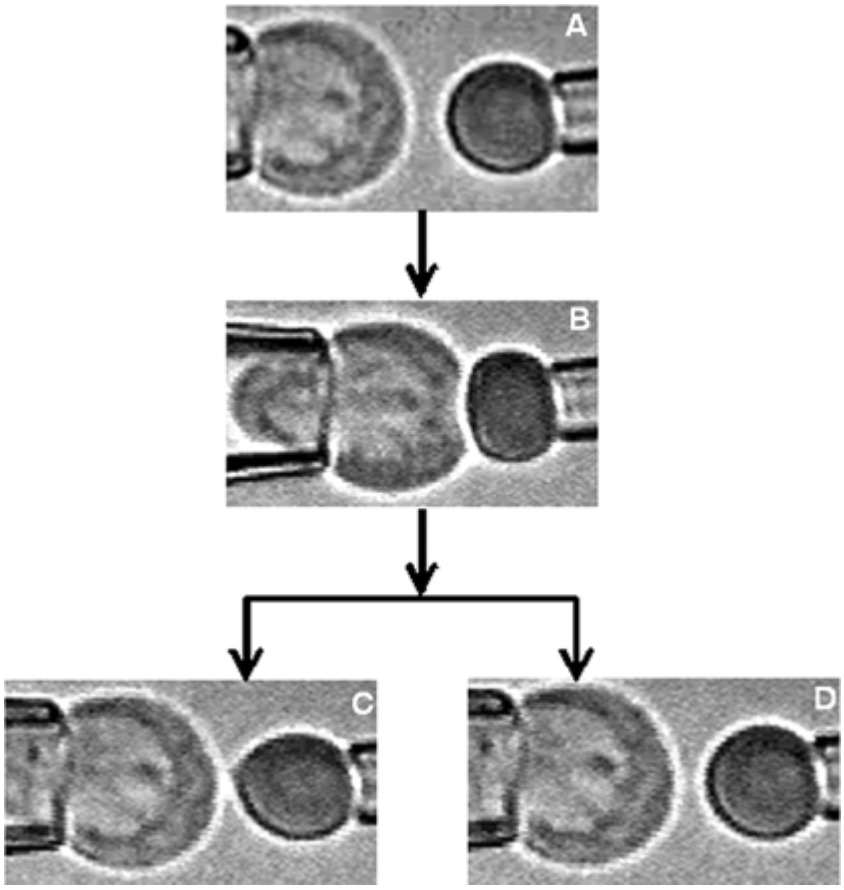

Figure 3.2 Micropipette adhesion frequency assay. A micropipette-aspirated T cell (*A*, *left*) was driven by a piezoelectric translator to make a controlled contact with a RBC coated with pMHC held stationary by another pipette (*B*, *right*). At the end of the contact period, the computer-driven translator retracted the pipette to the starting position. An adhesion, if present, would result in elongation of the RBC upon its retraction, enabling visual detection of the adhesion (*C*). The RBC membrane would retract away from the T cell surface smoothly if there was no adhesion (*D*).

Two variant forms of Eq. 3.1 were used in data analysis. The first form is a log transformation of Eq. 3.1 at $t \to \infty$,

$$\ln[1 - P_a(\infty)]^{-1} = A_c K_a^0 \cdot m_r m_l , \tag{3.2}$$

which predicts that the transformed adhesion frequency, $\ln[1 - P_a(\infty)]^{-1}$, is proportional to the product of the CD8 (or TCR) and pMHC densities, $m_r m_l$, with the effective binding affinity, $A_c K_a^0$, as the constant of proportionality. The second form is to normalize the adhesion frequency by dividing the molecular site densities after the log transformation, but keep the time dependence:

$$\ln(1 - P_a)^{-1} / m_r m_l = A_c K_a^0 [1 - \exp(-k_r^0 t)] . \tag{3.3}$$

Applying the log transformation and normalization according to Eq. 3.3 is predicted to collapse a family of P_a vs. t curves corresponding to different m_r and m_l into a single curve, provided that they correspond to the same set of kinetic reverse-rate and effective affinity.

3.4.2 Dose curve and EC_{50} analysis

The adhesion frequency, P_a were measured at that site density of agonist pMHC OVA, m_{OVA}. For each condition, >30 pairs of cells were used to obtain a P_a vs. m_{OVA} curve that correspond to a single OVA pMHC or a combination of OVA pMHC and other pMHCs. Each binding curve was fitted using a one phase exponential model,

$$P_a = P_{\max}(1 - e^{-km_{OVA}}) , \tag{3.4}$$

To estimate a pair of parameters: P_{max} ($0 \leq P_{max} \leq 1$), the maximum plateau of adhesion and k, the dose index of each binding. When P_a equals half of P_{max},

$$m_{OVA}(EC_{50}) = \frac{\ln 2}{k} \tag{3.5}$$

where EC_{50} is the half maximal effective concentration.

3.4.3 Running frequency analysis

At any specific contact duration t:

$$P(i) = 1 - \exp[- < n_1(i) - < n_2 >],$$

where i is the test cycle, and $< n >= m_r m_l A_c K_a^0 (1 - k_r^0 t)$

$< n_1 >$, decay portion of receptor on T cell surface,

$< n_2 >$, constant portion of receptor on T cell surface,

Then transform to:

$$P(i) = 1 - \exp\{-m_r \exp(i \cdot d) m_l A_c K_a^0 [1 - \exp(-k_r^0 t)] - < n_2 >\}$$

where "*d*" is decay rate and "*i*" is the test cycle

Transform to

$$P(i) = 1 - \exp\{-a \cdot \exp(-i \cdot d) - < n_2 >\}, \qquad (3.6)$$

where $a = m_r m_l A_c K_a^o [1 - \exp(-k_r^o \cdot t)]$ is a constant at any specific contact duration *t*.

Fitting data to get *a*, *d* and $< n_2 >$

Then can extrapolate to get "$P_a\ (t)$" without decay, decay factor "*d*" and basal level binding "$P(t) = 1 - \exp\{- < n_2(t) >\}$".

CHAPTER 4

MEASURE THE RESTING STATE KINETICS OF MHC-CD8 INTERACTION AT CELL MEMBRANE

4.1 Introduction

CD8 is a glycoprotein initially discovered as a cell surface marker distinguishing cytotoxic T cells from helper T cells in mice (12), and along with TCR and CD3, is part of the surface molecular assembly involved in antigen recognition (64). As a coreceptor, CD8 associates with the Src family kinase $p56^{lck}$ (Lck), which can phosphorylate CD3ζ and initiate T cell activation. CD8 also serves as an adhesion molecule to bind MHC to promote and stabilize the interaction of MHC with TCR (12, 78-84), which recognizes the specific peptide complexed with MHC (pMHC) (11, 44). This dual function provides an opportunity, but does not necessarily set a requirement, for TCR-MHC and MHC-CD8 interactions to affect each other. However, it is controversial whether coreceptor CD8 and TCR bind pMHC cooperatively or independently (78, 80, 82, 85-88).

On the T cell surface, CD8 is expressed as either a homodimer CD8αα or a heterodimer CD8αβ linked by a disulphide bond (12, 79, 85). The α and β chains are encoded by two closely related genes (89) and share ~20% amino acid sequence homology (12). CD8αβ is expressed primarily on peripheral αβ T cells whereas CD8αα is expressed broadly on αβ T cells, γδ T cells, natural killer cells, and dendritic cells (12, 79, 90). CD8αβ has been shown to be a more potent coreceptor than CD8αα in helping the TCR recognize antigen (12, 79, 91-93), yet the reason for this is unclear (12, 79, 89, 90, 92, 93). One possibility is that CD8αβ may have a higher affinity for MHC than CD8αα. Only cell surface CD8αβ, but not CD8αα or soluble CD8αβ, has been found to

significantly increase the avidity of TCR-MHC binding (79). Furthermore, inconsistent results have been obtained using cell adhesion (94), surface plasmon resonance (SPR) (95-98), and MHC tetramer staining assays (89).

During thymocyte development, positive and negative selection ensures generation of a repertoire of self MHC-restricted and self peptide-tolerant T cells; the trimolecular interaction of TCR, pMHC, and CD8 plays a critical role in determining the fate of a developing thymocyte. The kinetic properties of CD8 binding to polymorphic MHC may serve as determinants in the selection process (99-101), just like the kinetic properties of TCR binding to pMHC are determinants of T cell recognition (44).

Although several studies have used SPR to measure MHC-CD8 binding kinetics, these measurements may not account for all interaction characteristics of CD8 on the T cell membrane. The cell membrane provides an important environment for molecular assembly and interactions (10). Many cell surface molecules have to be assembled or linked to other membrane molecules/structures in order to carry out their functions fully. For example, TCR$\alpha\beta$ is complexed with CD3 signaling module (CD3$\delta\varepsilon$, CD3$\gamma\varepsilon$, CD3$\zeta\zeta$) via its transmembrane domain (9). For the CD8 molecule in particular, the larger α (than β) chain connects CD8 to the signaling kinase Lck through its cytoplasmic domain (12, 79). The β chain promotes constitutive association of CD8 with TCR/CD3 via its shorter cytoplasmic tail (79) and mediates CD8 partitioning in membrane rafts (79, 89). Recombinant molecules purified for SPR studies lack the linkage to the cell membrane, which precludes their interactions with other molecules on cell surface and intracellular structures such as signaling molecules that may regulate binding. For this reason, interactions between molecules respectively anchored on two apposing cell membranes

can be biologically different from and more relevant to molecular recognition than those in solution using purified molecules.

As a first step towards characterizing the 2D molecular interactions between T cells and APCs, we used a micropipette adhesion frequency assay (74) to measure the TCR-independent 2D kinetics of CD8 on the T cell membrane interacting with MHC coated on the surface of RBCs. Consistent with published SPR results, the 2D MHC-CD8 interaction was of very low affinity and depend on the MHC alleles but not on the peptide with which the MHC was complexed. The MHC-CD8 interaction was also indifferent to whether CD8 was composed of an $\alpha\alpha$ homodimer or an $\alpha\beta$ heterodimer. Surprisingly, the 2D affinity for the same MHC varied with T cells from different TCR transgenic mice on which the CD8 was expressed. These affinity differences were abolished by treatment with cholesterol oxidase to disrupt membrane rafts, which reduced MHC-CD8 binding affinity differentially in different T cells. These findings highlight the difference between 2D and 3D binding and emphasize the importance of directly measuring molecular interactions between T cells and APCs with 2D methods.

4.1 Results

4.1.1 Isolation of MHC-CD8 binding from the trimolecular TCR-MHC-CD8 interaction

Cytotoxic T cells express both TCR and CD8, which may bind different sites on the same or different pMHCs (71, 85, 91). A given TCR is capable of binding different peptides complexed with MHC of the same allele with different kinetic rates and affinities, which can differentially trigger T cell activation (11, 44). To isolate MHC-CD8

binding from trimolecular TCR-MHC-CD8 interactions, an anti-TCR Vα2 mAb (B20.1) was used to block TCR-MHC binding. Also, an anti-CD8α blocking mAb (CT-CD8a) was used to confirm that, apart from a low level background, the measured binding was predominately due to specific MHC-CD8 interaction. T cells expressing a monoclonal TCR from transgenic mice were pre-incubated with 50 μg/ml of anti-TCR Vα2 or 10 μg/ml of anti-CD8α for 30 min at 4 ^{o}C and micropipette assays were performed in the continuous presence of the same concentrations of mAbs. In this study, TCR-independent, MHC-CD8 specific interactions were isolated for the three types of T cells (OTI, P14 and F5) used and for all pMHCs tested, including the peptides listed in Tables I and II bound to either H-2K^{b} or H-2D^{b} MHC alleles. Some of the results are exemplified in Fig. 4.1 using H-2K^{b} complexed with three peptides with various properties for OTI T cells --- VSV (null), R4 (antagonist), and OVA (agonist) (44, 71).

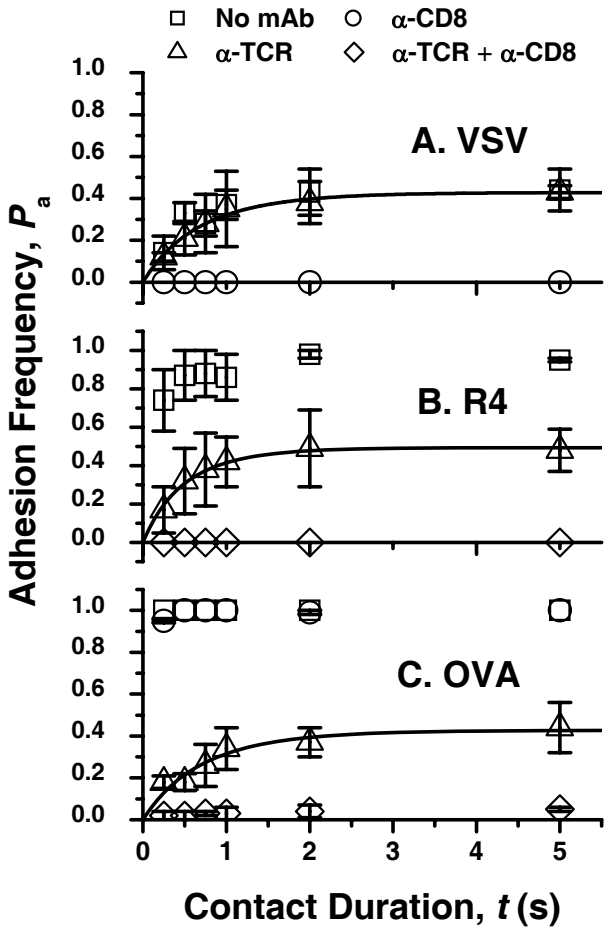

Figure 4.1 Isolation of MHC-CD8 binding from TCR-MHC-CD8 interaction. Plots of adhesion frequency vs contact duration measured using T cells from OTI TCR transgenic mice interacting with RBCs coated with H-2K^b MHC complexed with null peptide VSV (*A*), antagonist peptide R4 (*B*) and agonist peptide OVA (*C*) in the absence (□) or presence of blocking mAb(s) against TCR (Δ), CD8 (○), or both (◊). Data (*points*) were presented as mean ± SEM (or single value) of 1–5 pairs of T cells and RBCs each making 50 contacts to observe the frequency of adhesion. Using independently measured CD8 (m_r) and MHC (m_l) site densities, Equation 3.1 was fit (*curves*) to the anti-TCR Vα2 blocked data set (Δ) to estimate a pair of kinetic parameters, a reverse-rate k_r^0 and a 2D effective binding affinity $A_cK_a^0$.

For the null peptide VSV (Fig. 4.1A), micropipette adhesion tests in the absence of antibody yielded an adhesion frequency that increased with contact duration initially then reached a steady state (□). Addition of the anti-CD8α mAb completely abolished binding at all contact durations tested (○), suggesting that the measured adhesion between T cells and RBCs was solely mediated by the specific MHC-CD8 interaction. This was further supported by the lack of effect of the anti-TCR Vα2 mAb which yielded a binding curve (Δ) indistinguishable from that without antibody (□). Similar results were obtained for another null peptide K4 (data not shown). The inability to detect TCR binding indicated that OTI TCR did not recognize the null peptides. This agreed with results from other assays including SPR measurement (11, 44), synapse formation, and fluorescence resonance energy transfer (FRET) measurement (71). The results also indicated that anti-TCR Vα2 mAb did not sterically hinder MHC-CD8 interactions. Thus, binding of RBCs bearing MHC complexed with null peptides to T cells is measurable, TCR-independent, and MHC-CD8 specific. We also tested the effect of anti-TCR Vα2 mAb on binding between P14 T cells and RBCs coated with H-2K^b VSV pMHC and obtained similar results (data not shown). These data allowed us to use null pMHCs to measure the specific MHC-CD8 interaction in future experiments without using anti-TCR mAbs.

For antagonist peptide R4 (Fig. 4.1B), micropipette adhesion tests in the absence of antibody yielded much higher adhesion frequencies at all contact durations compared to VSV at equivalent site densities (□, compare Figs. 4.1A and 4.1B). These adhesions, especially those at contact durations >2 s, were also stronger, as it was more difficult to separate the RBC from the T cell. When the anti-TCR Vα2 mAb was added, however, the adhesion frequency dropped to levels that matched those mediated by the binding of

CD8 to VSV pMHC at corresponding contact durations (Δ, compare Figs. 4.1A with 4.1 B). Thus, there was a significant contribution from the TCR-MHC interaction to the measured adhesion binding when the antagonist R4 was used. This also ruled out the possibility that, when the peptide was VSV, the lack of blocking was due to problems with the anti-TCR Vα2 mAb (Fig. 4.1A). Addition of anti-TCR Vα2 and anti-CD8α mAbs to block both TCR and CD8 completely abrogated adhesion (◊), suggesting that binding in the presence of anti-TCR Vα2 alone (Δ) was mediated solely by specific MHC-CD8 interaction. Similar data were obtained for another antagonist V-OVA (data not shown). Thus, both TCR and CD8 bind MHC complexed with antagonist peptides R4 or V-OVA, and the specific MHC-CD8 interaction can be isolated by blocking the TCR-pMHC interaction using the anti-TCR Vα2 mAb.

For the agonist peptide OVA (Fig. 4.1C), micropipette adhesion tests in the absence of antibody yielded adhesion in every single test (i.e., 100% adhesion frequency) at all contact durations (□). These adhesions were even stronger than those mediated by R4 pMHC, as it was sometimes impossible to separate the RBC from the T cell, despite the fact that the pMHC densities on RBCs were matched for all three peptides (VSV, R4, and OVA). Also, addition of the anti-CD8α mAb alone did not lower the frequency of adhesions (○), although they appeared somewhat weaker. This indicates that OTI TCR interacted with agonist (OVA) pMHC much more strongly than antagonist (R4 or V-OVA) pMHC. When the anti-TCR Vα2 mAb was added, however, the adhesion frequency dropped to levels similar to those mediated by binding of CD8 to VSV-loaded MHC at corresponding contact durations (Δ, compare Figs. 4.1A and 4.1C). Again, addition of mAbs to block both TCR and CD8 completely abrogated adhesion (◊),

suggesting that binding in the presence of anti-TCR Vα2 alone (Δ) was mediated by specific MHC-CD8 interaction alone. Thus, both TCR and CD8 bind MHC complexed with agonist pMHC, and the specific MHC-CD8 interaction can be isolated by blocking the TCR-MHC interaction using the anti-TCR Vα2 mAb.

As an additional control, biotinylated RBCs not coated with pMHC were tested against T cells, which produced <2% adhesion regardless of the T cell specificity (data not shown). Thus, no adhesion molecules other than pMHC on RBCs and TCR and CD8 on T cells contribute to the adhesion frequencies measured with the micropipette adhesion assay.

To rule out the possibility that anti-TCR Vα2 mAb might cause changes in CD8 expression, we incubated OTI T cells with anti-TCR Vα2 mAb (50 μg/ml) in chamber medium (L-15/5mM Hepes/1% BSA) for 90 min, which was the time elapse of a typical micropipette experiment, then stained with PE-conjugated anti-CD8 mAbs in FACS buffer to quantify the expressions of CD8α and CD8β by flow cytometry. We also stained T cells not pre-incubated with anti-TCR Vα2 mAb with the same anti-CD8α and anti-CD8β mAbs as a control. CD8 expression was indistinguishable (data not shown), indicating that anti-TCR Vα2 mAb did not alter CD8 expression. It must be stressed that to detect the low affinity specific MHC-CD8 interaction, we had to use very high MHC site densities (~1000 sites/μm^2). In sharp contrast, ~10 sites/μm^2 of OVA pMHC were sufficient to produce a specific trimolecular TCR-MHC-CD8 binding comparable to the TCR-independent MHC-CD8 binding (data not shown).

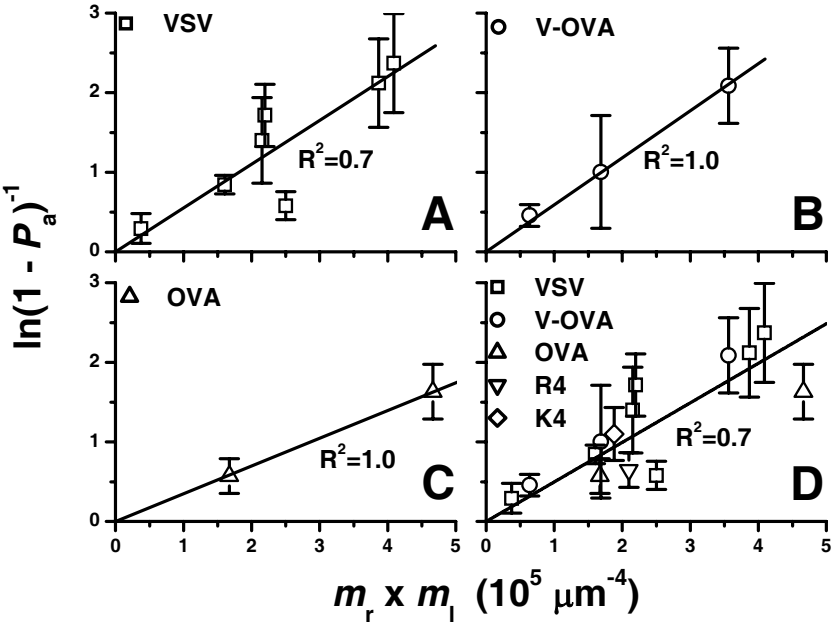

Figure 4.2 Effects of molecular site density on adhesion frequency. Adhesion frequency P_a was measured at 5 s contact duration from 2 to 7 pairs of T cells and RBCs (each making 50 contacts) per data point. P_a was transformed according to the left-hand side of Equation 3.2 by taking a natural log of the reciprocal of the frequency of no adhesion to yield $\ln(1 - P_a)^{-1}$, then plotted vs. the product of the CD8 and MHC site densities, $m_r m_l$, for H-2K^b MHC complexed with VSV (*A*), V-OVA (*B*), and OVA (*C*) peptides separately. The data from panels *A*–*C* were pooled in panel *D* on which data from two other peptides, R4 and K4, were also plotted. The error bars were computed from SEM of P_a according to the Gaussian error propagation law. A straight line with zero *y*-intercept was fit to data in each panel. The goodness-of-fit was indicated by the R^2 values.

4.1.2 Stoichiometry of the MHC-CD8 interaction

The density m_r of CD8 expressed on OTI T cells slightly varied from mouse to mouse. The density m_l of MHC coated on RBCs also varied depending on the coating conditions. How CD8 and MHC densities regulate the adhesion frequency P_a (through mass action) depends on the stoichiometry, or valency, of the MHC-CD8 interaction. To determine

this valency, we took the natural log of the reciprocal of the probability of no adhesion, $\ln(1 - P_a)^{-1}$, measured at 5 s contact duration and plotted it against the product of the site densities, $m_r m_l$, for several pMHC ligands (Fig. 4.2). The data in Fig. 4.1 show that MHC-CD8 binding had achieved steady-state at 5 s. Eq. 3.2 predicts that the $\ln[1 - P_a(\infty)]^{-1}$ vs. $m_r m_l$ plots should be linear with a zero *y*-intercept and a slope equal to the 2D effective binding affinity, $A_c K_a^0$, provided that CD8 binds pMHC monovalently. This prediction is supported by the data for CD8 on OTI T cells interacting with MHC complexed with the null peptide VSV coated on RBCs measured using seven $m_r m_l$ values (Fig. 4.2A). It is evident that the data points are evenly scattered around a straight line that passes through the origin. Eq. 3.2 is also supported by data from MHC complexed with different peptides, e.g., antagonist peptide V-OVA (Fig. 4.2B) and agonist peptide OVA (Fig. 4.2C), obtained using anti-TCR Vα2 blocking. The data from Fig. 4.2, A-C, are pooled in Fig. 4.2D along with additional data measured using the same MHC allele (H-2K^b) complexed with two other peptides, antagonist peptide R4 and null peptide K4. These data indicate that T cell CD8 forms monomeric bonds with MHC despite the fact that MHC was decorated on the RBC surface via biotin-streptavidin coupling, which might form dimers.

4.1.3 Evaluation of kinetic parameters for MHC-CD8 interactions

Having confirmed the 1:1 stoichiometry of MHC-CD8 interaction, Eq. 3.1 was fit to the TCR-independent, CD8-mediated binding data to evaluate the kinetic parameters, k_r^0 and $A_c K_a^0$, for various MHC-CD8 interactions studied in this work, as exemplified in Fig. 4.1. Table 4.1 summarizes the kinetic parameters so evaluated for OTI T cell CD8 interacting with H-2K^b MHC complexed with five peptides for each pair of CD8 and

pMHC densities tested (indicated). It is evident that, for each peptide, the kinetic parameters evaluated from individually fitting different P_a vs. t data sets agree well, despite the fact that they correspond to different m_r and m_l levels, as expected from the monovalency of the MHC-CD8 interaction, which also demonstrates reproducibility of our assay. To further test the reliability of these best-fit parameter values, the mean k_r^0 and $A_c K_a^0$ values were calculated and used, along with the corresponding m_r and m_l values measured from independent flow cytometry experiments, to predict each P_a vs. t data set, which shows excellent agreement, as exemplified in Fig. 4.3A for V-OVA.

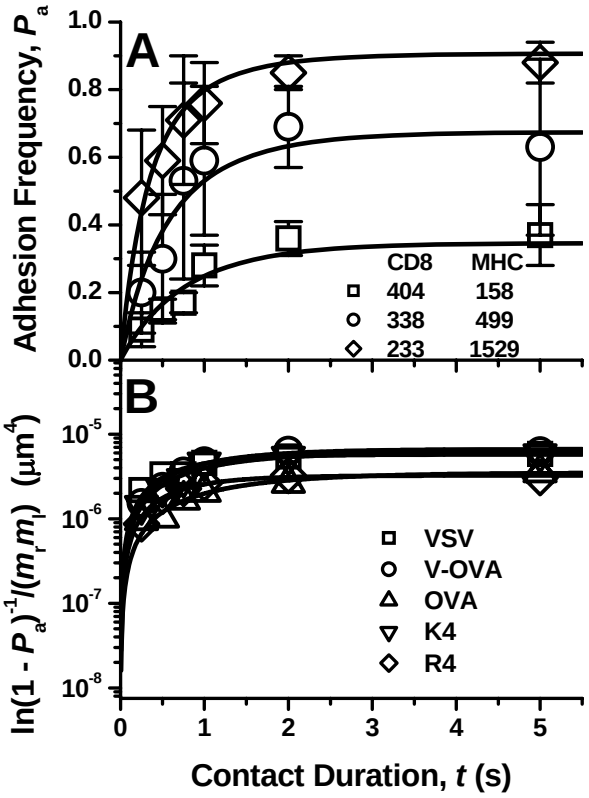

Figure 4.3 MHC-CD8 interaction is monovalent and peptide independent. *A*, Adhesion frequency was plotted against contact duration for each set of CD8 and V-OVA pMHC densities. Data (*points*) from three sets of site densities (indicated), each obtained from 15 to 29 pairs of OTI T cells and RBCs contacting 50 times each, were presented as mean ± SEM at each contact duration. Equation 3.1 was fit to each data set to

evaluate a pair of kinetic parameters, k_r^0 and $A_cK_a^0$, the values of which are summarized in Table I along with the site densities. The mean values of k_r^0 and $A_cK_a^0$ (see Table 4.1) were then used to predict theoretical binding curves for all three set of site densities (*curves*). The excellent agreement between experiment and theory supported the assumption on which Equation 3.1 was based, that the MHC-CD8 interaction is monovalent. *B*, Mean adhesion frequency data were transformed according to the left-hand side of Equation 3.3 and plotted vs. the contact duration (*points*). The right-hand side of Equation 3.3 predicts that binding curves so plotted would depend only on the k_r^0 and $A_cK_a^0$ values of the interactions involved.

TABLE 4.1

Kinetic Parameters for OTI TCR-independent, CD8-mediated Binding to H-2K^b MHC

H-2K^b pMHC	m_r (μm^2)	m_l (μm^2)	k_r^0(s^{-1})	$A_cK_a^0$(10^{-6} μm^4)
VSV	305	820	1.53 ± 0.37	2.32 ± 0.24
VSV	297	715	0.88 ± 0.48	5.72 ± 1.79
VSV	297	126	1.63 ± 1.01	8.06 ± 1.91
VSV	233	1661	1.58 ± 0.30	5.25 ± 0.55
VSV	326	1254	2.52 ± 0.61	5.53 ± 0.62
VSV	370	434	1.53 ± 0.24	5.10 ± 0.36
VSV	404	544	2.22 ± 0.24	7.20 ± 0.34
	Combined data		**1.53 ± 0.22**	**5.75 ± 0.31**
V-OVA	404	158	0.87 ± 0.18	7.74 ± 0.78
V-OVA	338	499	1.08 ± 0.34	6.90 ± 1.17
V-OVA	233	1529	2.00 ± 0.17	5.63 ± 0.48
	Combined data		**1.12 ± 0.15**	**6.66 ± 0.36**
OVA	281	1659	0.68 ± 0.14	3.58 ± 0.47
OVA	198	844	1.14 ± 0.25	3.33 ± 0.34
	Combined data		**0.83 ± 0.12**	**3.51 ± 0.22**
K4	290	648	1.04 ± 0.17	6.13 ± 0.52
R4	276	761	1.55 ± 0.15	3.25 ± 0.13

TABLE 4.2

Kinetic Parameters for OTI TCR-independent, CD8-mediated Binding to H-2D^b MHC

H-2D^b pMHC	m_r (μm^2)	m_l (μm^2)	k_r^0(s^{-1})	$A_cK_a^0$(10^{-7} μm^4)
gp33	233	1157	0.55 ± 0.17	7.81 ± 1.22
HIV gag	326	1713	0.55 ± 0.12	5.14 ± 0.60

4.1.4 MHC-CD8 interaction is peptide independent

Although differing in amino acid sequences and molecular weights, the five peptides listed in Table 4.1 were complexed with MHC of the same allele, H-2K^b. Co-crystal structures of pMHC:CD8 complexes show no contact between CD8 and the peptide (91) . However, it is still possible that a peptide could influence MHC-CD8 interaction should its binding induce a conformational change in the MHC that would alter the CD8 binding site. In Fig. 4.2D, the $\ln[1 - P_a(\infty)]^{-1}$ vs. $m_r m_l$ data from all five peptides appear to line up, suggesting that their binding affinities (equal to the slope of the line) have similar values. In Fig. 4.1, the TCR-independent, CD8-mediated P_a vs. t data (Δ) appear to have similar shapes and plateau levels regardless of the peptide used, indicating similar kinetic parameters. It can be seen from the binding affinities and reverse-rates listed in Table 4.1 that these are indeed comparable for all five H-2K^b pMHCs.

To visualize the peptide independence of the kinetic parameters for the TCR-independent, CD8-mediated binding to MHC, we make use of Eq. 3.3, which predicts that the $\ln(1 - P_a)^{-1}/m_r m_r$ vs. t data depend only on the kinetic parameters. Data for MHC complexed with all five different peptides were plotted in Fig. 4.3B (points). The collapse of data demonstrates graphically that these interactions have comparable kinetic parameters. Conversely, similar kinetic parameters predict similar $\ln(1 - P_a)^{-1}/m_r m_r$ vs. t curves, as shown by using the mean best-fit k_r^0 and $A_c K_a^0$ values for each peptide to plot the right-hand side of Eq. 3.3 (Fig. 4.3B, curves), which overlay regardless of the peptide as predicted.

To further test our hypothesis that the MHC-CD8 interaction is peptide independent, kinetic parameters were measured for OTI T cells interacting with RBCs

coated with H-2D^b MHC complexed with gp33 or HIV gag, which are null peptides not recognized by OTI TCR. As can be seen from Table II where data are listed, the corresponding $A_c K_a^0$ and k_r^0 values are very similar for the two peptides tested. Taken together, the data suggest that loading different peptides on MHC does not induce enough change in the CD8 binding site to affect the measured kinetic parameters of the MHC-CD8 interactions. In other words, the interactions between CD8 and pMHC are peptide-independent.

4.1.5 CD8 binds different MHC alleles with distinct kinetics

Using MHC tetramer staining and SPR experiment with purified molecules, Moody et al. found that CD8 bound H-2K^b MHC with higher avidity/affinity than H-2D^b MHC (98). Our 2D kinetic data support this finding. As shown in Fig. 4.4, CD8 from OTI T cells and P14 T cells respectively bound H-2K^b MHC with 7- and 20-fold higher 2D effective binding affinities than H-2D^b MHC, respectively (Fig. 4.4, A and B, left column). We were unable to measure kinetic parameters for F5 T cell CD8 interacting with H-2D^b MHC despite multiple attempts, because the affinity is too low to yield appreciable adhesion frequencies even at the highest MHC coating density we could achieve, which could measure affinity as low as ~10^{-8} μm^4. However, the interaction between F5 T cell CD8 and H-2K^b MHC was readily measurable, resulting in a 2D effective binding affinity of $A_c K_a^0 = 2.8\times10^{-6}$ μm^4 (Fig. 4.4C, left column). Thus, the affinity of F5 T cell CD8 for H-2K^b MHC was two orders of magnitude higher than that for H-2D^b MHC. The impact of MHC allele on the reverse-rate of CD8 dissociation is less clear. CD8 from OTI T cells dissociated 3-fold more rapidly from H-2K^b than H-2D^b MHC (Fig. 4.4A,

right column). By comparison CD8 from P14 T cells dissociated from H-2K^b and H-2D^b MHC with similar reverse-rates (Fig. 4.4B, right column).

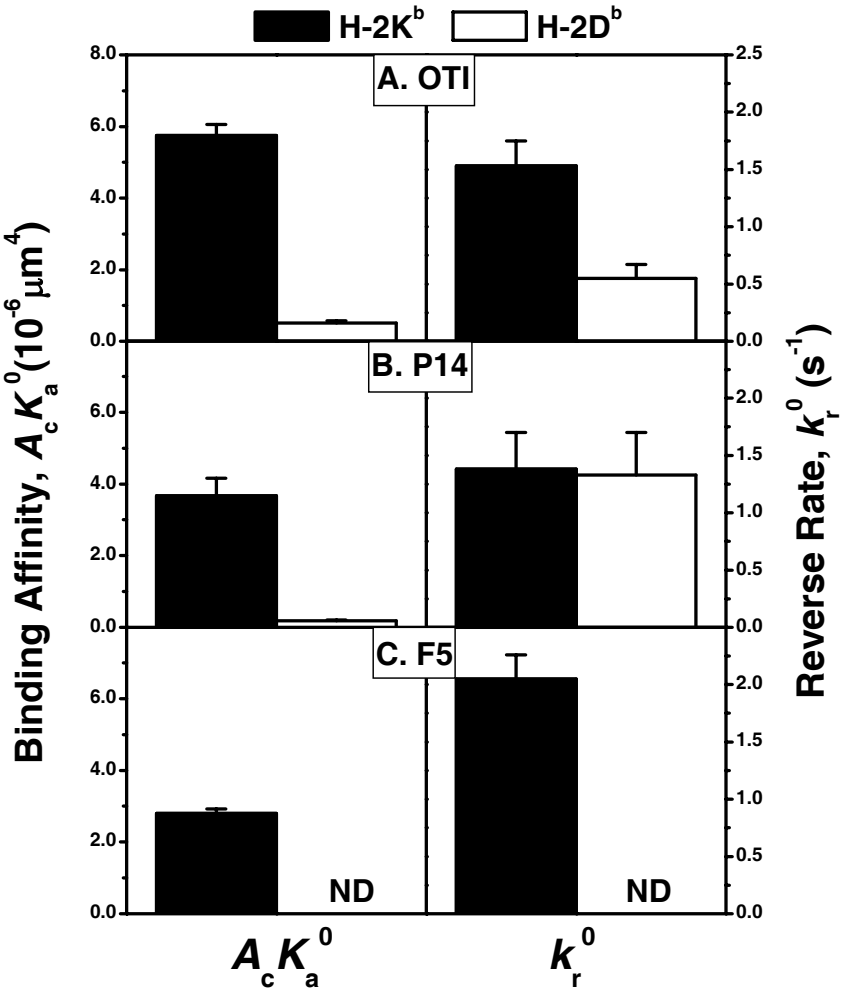

Figure 4.4 Dependence of MHC-CD8 binding on MHC alleles and T cell types. 2D effective binding affinity (*left column*) and kinetic reverse-rate (*right column*) of naive CTLs from three transgenic mice, OTI (*A*), P14 (*B*), and F5 (*C*), interacting with either H-2K^b (*solid bars*) or H-2D^b (*open bars*) were compared. Data were presented as mean ± SEM. ND = not detectable.

4.1.6 The same MHC allele binds CD8 from different T cells with different affinities

Unexpectedly, CD8 on T cells from different TCR transgenic mice was found to bind the same allelic pMHC with different affinities; the H-2K^b MHC binding affinity for CD8 on

OTI T cells was 50 and 100% more than those on P14 T cells and from F5 T cells, respectively (compare the three panels in Fig. 4.4, solid bars, left column). A similar trend was found for the H-2D^b MHC, which bound OTI T cell CD8 with an affinity 2- (compare panels A and B in Fig. 4.4, open bars, left column) and >10-fold more than those of P14 and F5 T cell CD8, respectively. To exclude the possibility that CD8 expression was changed by repeated touches with a pMHC coated RBC during the micropipette assay, OTI T cells were first incubated with 50 μg/ml anti-TCR Vα2 mAb for 30 min, mixed with OVA, R4 or VSV pMHC coated RBCs at a ratio of 1:100 in the presence of anti-TCR Vα2 mAb, pelleted the cells and incubated at room temperature for 10 min. After the RBCs were lysed with lysis buffer (eBioscience), the T cells were stained with anti-CD8α or β mAb to compare the CD8 expression levels. Flow cytometry data showed the CD8 expression level did not alter (Fig. 4.5A).

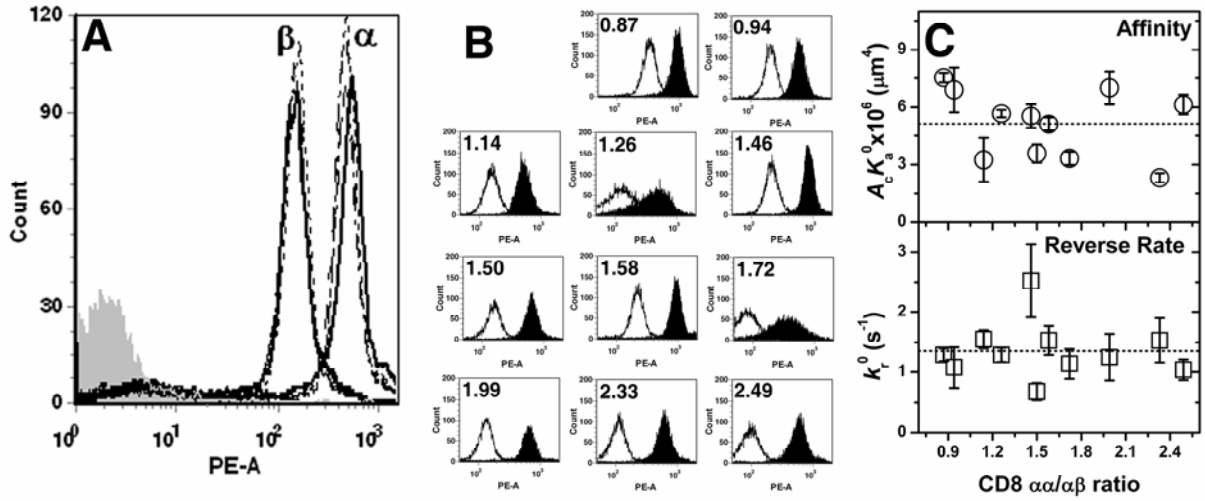

Figure 4.5 Lack of effect on CD8αα and CD8αβ expression. *A*, CD8α (α) and CD8β (β) expression levels on T cell were compared before interaction (*open histogram*) or after interaction with OVA (*dash histogram*), R4 (*dot histogram*) or VSV (*dash-dot histogram*) pMHC coated RBCs in the presence of anti-Vα2 mAb (50 μg/ml). Isotype control for nonspecific binding is shown as shaded histogram. Part of some

histograms are obscured due to overlapping. *B*, Flow cytometric analysis for the expression of CD8α (*filled histograms*) and CD8β (*open histograms*) on 11 batches of OTI T cells. The ratio value of CD8αα/CD8αβ was indicated on each small panel. *C*, 2D effective binding affinity ($A_cK_a^0$, *upper panel*) and kinetic reverse-rate (k_r^0, *lower panel*) measured using these 11 batches of OTI T cells were plotted against the CD8αα/CD8αβ ratio and compared with the average affinity or average reverse rate (*dash lines*). Data were presented as mean ± SEM.

CD8αβ is believed to be a more potent coreceptor than CD8αα. Therefore, we hypothesized that CD8αβ bound MHC better than CD8αα, and that CD8 expressed on OTI, P14, and F5 T cells with different CD8αα/CD8αβ ratios. However, flow cytometry results showed that the CD8αα/CD8αβ ratios were comparable for those three types of T cells (data not shown). To further test this hypothesis, we took advantage of the fact that the site densities of CD8αα and CD8αβ varied mildly among OTI T cells purified from different transgenic mice, with site density ratios of CD8αα/CD8αβ ranging from 0.9-2.5 (indicated in the upper-left corner of each panel in Fig. 4.5B). In the preceding section, we have shown that the MHC-CD8 binding affinity and reverse-rate are independent of the peptide. Here we plot the 2D effective binding affinity (Fig. 4.5C, upper panel) or reverse-rates (Fig. 4.5C, lower panel) measured using eleven batches of OTI T cells versus the CD8αα/CD8αβ ratio. It is evident that the two kinetic parameters $A_cK_a^0$ and k_r^0 measured from different batches of T cells scatter evenly around a horizontal line equal to their respective average values (dotted line in each panel of Fig. 4.5C), suggesting a lack of dependence on the CD8αα/CD8αβ ratio. These data indicate that the

difference in coreceptor potencies between CD8αα and CD8αβ in activating T cells does not manifest as difference in their binding kinetics for MHC.

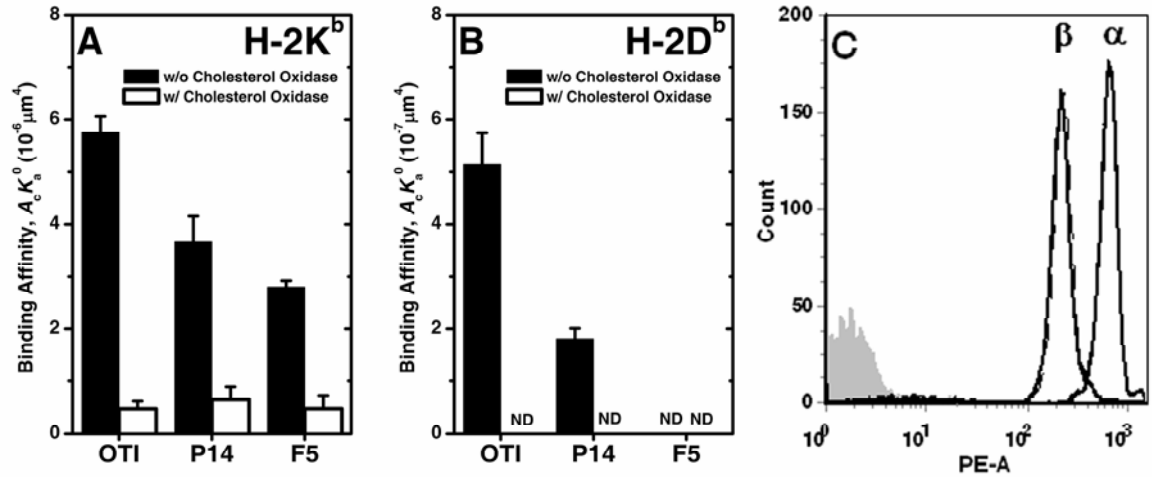

Figure 4.6 Reduction of MHC-CD8 affinity by cholesterol oxidase treatment. *A* and *B*, 2D binding affinities of H-2K^b (*A*) or H-2D^b (*B*) MHC for CD8 on three T cells with (*open bars*) or without (*solid bars*) cholesterol oxidase treatment. Data were presented as mean ± SEM. ND = not detectable. *C*, The CD8α and CD8β expression levels of F5 T cells treated with 1 U/ml cholesterol oxidase (*dash histogram*) were compared with untreated T cells (*open histogram*, which overlaps with the *dash histogram*). Isotype control for nonspecific binding is shown as shaded histogram.

TABLE 4.3

Binding affinities of MHC-CD8 w/(+) or w/o(-) cholesterol oxidase treatment

T cell	H-2Kb(-)	H-2Kb(+)	H-2Db(-)	H-2Db(+)
OTI (10^{-6} μm^4)	5.75 ± 0.31	0.47 ± 0.15	0.51 ± 0.06	ND
P14(10^{-6} μm^4)	3.67 ± 0.49	0.65 ± 0.24	0.18 ± 0.02	ND
F5(10^{-6} μm^4)	2.80 ± 0.12	0.48 ± 0.25	ND	ND

4.1.7 Disruption of membrane rafts differentially reduces affinity for MHC of CD8 from different T cells and abolishes the affinity differences

The micropipette frequency assay measured interactions between molecules anchored on the apposing membranes of a RBC and a T cell. These interactions can be impacted by the cell surface environment, as previously shown for membrane microtopology and

stiffness (102, 103). Another aspect of the membrane environment may be membrane rafts into which CD8 can partition (79). Membrane rafts, and/or the CD8 partitioning therein, could vary among the three transgenic T cells used in our study, thus altering the apparent MHC-CD8 affinity. To test this hypothesis, we measured 2D binding affinities after disrupting membrane rafts by incubating T cells with 1 U/ml of cholesterol oxidase (MP Biomedicals, Solon, OH) for 30 min (104, 105). Disruption of membrane rafts substantially reduced the MHC binding affinities for CD8 on all three T cells for both H-2K^b (Fig. 4.6A, compare the solid and open bars in each group, and Table 4.3) and H-2D^b (Fig. 4.6B, adhesion became undetectable after cholesterol oxidase treatment despite we used highest possible MHC site density, and Table 4.3) alleles. This was not due to a decrease in the CD8 expression by the cholesterol oxidase treatment, as flow cytometry measurement using OTI or F5 T cells with and without such treatment showed identical CD8 expression levels (Fig. 4.6C). Also, treating RBCs with cholesterol oxidase alone did not affect MHC-CD8 binding (data not shown). Remarkably, cholesterol oxidase treatment reduced the MHC-CD8 binding affinity by different amounts in different T cells: 12, 6, and 6-fold in OTI, P14, and F5 cells, respectively. Thus, the H-2K^b MHC binding affinities for CD8 on different T cells were similar after rafts disruption (Fig. 4.6A, compare the three open bars). These results suggested that partitioning of CD8 in membrane rafts differentially enhanced its MHC binding affinity in the three T cells tested. The enhancement was abolished after the membrane rafts were disrupted, resulting in comparable CD8-MHC binding affinities regardless of the T cell specificity.

4.2 Discussion

The present work represents a first step towards dissecting the 2D molecular interactions between T cells and APCs, which involve a number of molecular players, including TCR, coreceptors, adhesion molecules, and costimulatory molecules. Some molecules provide physical linkages to bridge the two cell membranes and form junctional structures, while others deliver signals upon antigen recognition; Some interactions take place between binding partners respectively residing on apposing membranes of the T cell and the APC, while others occur between molecules both residing on the same membrane. Kinetic rates and binding affinity are important determinants for these molecular interactions, for such parameters are believed to correlate with T cell activation. Most published work employed SPR for kinetic measurement, which uses purified molecules that have been isolated from their native T cell surface environment (11, 44, 78, 79, 96-98, 106, 107). Some studies use MHC tetramer or MHC-Ig dimeric molecules to stain T cells (37, 81, 82, 89, 98, 108-111), but still measure 3D kinetic parameters. A few experiments measured 2D binding by a simple cell adhesion assay (71, 94, 112). However, this assay lacks sufficient temporal resolution to measure the kinetics of MHC-CD8 interactions. A different method has been used to measure 2D affinity, which visualizes bond formation between a receptor-expressing cell and a glass-supported lipid bilayer reconstituted with fluorescently-labeled, lipid-anchored, freely mobile ligands (14, 19, 20). At physiological receptor and ligand densities, thousands of bonds are typically formed in a time scale of ~10 min, which is a large enough number of bonds and sufficiently long time to smoothen the self-assembled contact area. By comparison, the micropipette method detects binding in seconds on a rough T cell surface full of microvilli. These differences

probably underlie the orders of magnitude of differences in the 2D affinities measured by the supported bilayer method and the micropipette method (41). Moreover, it required extension for this method to be used for measuring 2D kinetics(113). Our paper reports the first 2D kinetic measurements using T cell CD8 to interact with pMHC presented on the membrane of RBCs. The measured effective binding affinities of TCR-independent MHC-CD8 interactions are much lower than those of selectin-ligand interactions (75, 114) and the high affinity integrin-ligand interactions (115) but are similar to the IgG binding affinities of the low affinity Fcγ receptors CD16b (116) and CD32a (117).

There are two known receptors on the surface of cytotoxic T cells for MHC: TCR and CD8. Multiple lines of evidence suggest that CD8 facilitates or enhances TCR to recognize antigen and initiate T cell activation, and it was shown after abolishing the CD8 binding by making a mutation on the α3 domain of MHC, not only the tetramer staining efficiency for T cell was reduced, but the T cell activation was dramatically diminished (110). However, the detail mechanisms of cooperation between CD8 and TCR are not yet clear (12). One hypothesis proposes that binding of one molecule (CD8 or TCR) holds MHC to an optimal configuration, thereby accelerating the association of the other molecule (TCR or CD8) to MHC (80, 87). An alternative but related hypothesis proposes that binding of the second molecule (CD8 or TCR) to MHC stabilizes the interaction between the first molecule (TCR or CD8) and MHC, thereby decelerating the dissociation of both molecules from MHC (81, 97). These hypotheses imply cooperation between TCR and CD8 at the level of MHC binding. Although SPR experiments did not find significant difference in the binding of solution MHC to immobilized TCR in the presence or absence of solution CD4/8 (78, 106), these negative data cannot rule out the

possibility of cooperation when both TCR and CD8 reside on the same T cell membrane. The data in Fig. 4.1 show that inhibiting the TCR-MHC interaction by a blocking mAb does not result in detectable change in the kinetics of MHC binding to CD8 at a resting state. In other words, TCR-MHC and MHC-CD8 interactions appear to be independent at the level of adhesion measured by the present assay and the adhesion levels mediated by these two interactions are additive rather than synergistic, which provides a partial answer to the question of cooperation.

Co-crystal structures of both human and mouse pMHC: CD8 complexes reveal that CD8 mainly binds to the invariant α3 domain of the heavy chain and to the β2-microglobulin subunit of MHC (85, 91). By comparison, co-crystal structures of TCR: pMHC complexes reveal that TCR interacts with the α1 and α2 domains of the heavy chain of MHC where the peptide cleft is located (64, 118). Thus, TCR and CD8 bind to spatially separated sites on MHC. Crystallographic studies also reveal little structural differences in MHC complexed with different peptides (64, 118). It is therefore not surprising to find that the kinetic parameters of the TCR-independent, CD8-mediated MHC binding are peptide independent (Figs. 4.1, 4.2D and 4.3B, Tables 4.1 and 4.2). Indeed, this conclusion has been supported by previous studies using SPR measurement (97) and the cell adhesion assay (71). Thus, unlike the TCR-MHC interaction, MHC-CD8 interaction is independent on the peptide potency in triggering T cell activation.

By comparison, different MHC alleles, such as H-2K^b and H-2D^b, may have sufficient structural differences to impact their CD8 binding kinetics (98, 107). In support of this hypothesis, we found that CD8 bound H-2K^b to have a much a higher affinity than H-2D^b for the three types of T cells tested (Fig. 4.4). This is consistent with previous SPR

measurements, which found that binding of CD8 to H-2K^b MHC was at least 2-fold better than H-2D^b (98). Similar results were obtained for HLA-CD8 interactions in a human system, where CD8αα bound differently to different alleles of HLA with subtle conformational differences in α3 domain (107). The agreement of the present results with previous observations obtained using MHC tetramers, CD8 transfectants, and SPR supports the validity of the micropipette assay as applied to the T cells.

Co-crystal structures of human CD8αα:HLA-A2 (85) and mouse CD8αα:H-2K^b (91) complexes show that CD8αα primarily binds the α3 domain of MHC asymmetrically in an antibody-like fashion. The first α subunit interacts with MHC α3 and β2-microglobulin domains, which comprises of >70% of the contact surface. The second α subunit engages less and interacts only with the MHC α3 domain (85, 91). Although no crystal structure of MHC:CD8αβ complex has been published yet, such structure has been modeled by replacing either CD8α subunit of CD8αα with a CD8β subunit (90). Based on the model, Chang et al. proposed that, although CD8αβ could bind MHC with two distinct orientations, the primary binding site was still the α3 domain of MHC and the basic interaction mode was the same as that of CD8αα (90). By comparison, Devine et al. suggested that only the CD8α subunit could make a major contact with MHC class I (119). Nevertheless, both CD8αα and CD8αβ interact with MHC and promote TCR-MHC recognition (64), yet CD8αβ is two orders of magnitude more efficient as a coreceptor than CD8αα (93). However, it is controversial as to whether the different coreceptor efficiencies correspond to different MHC-CD8 binding. Sun et al. found that CD8αα and CD8αβ mediated similar levels of cell-cell adhesion

(94). Similarly, SPR measurement found that CD8αα and CD8αβ had similar 3D affinities for H-2K^b MHC (95, 96, 98). By comparison, MHC tetramer staining experiment found that CD8αβ mediated greater interactions with MHC than CD8αα, although this discrepancy might come from either the CD8 expressing transgenic mice or the H-2D^k MHC used (89). Our data suggest that the different coreceptor functions of CD8αα and CD8αβ are not due to their different 2D binding for MHC as they bind the same MHC allele with comparable 2D affinities and off-rates (Fig. 4.5).

Surprisingly, we found that CD8 expressed on different T cells bound the same MHC allele with different affinities (Fig. 4.4), and cholesterol oxidase treatment differentially reduced these affinities in different T cells. Remarkably, the 2D MHC-CD8 binding affinities became comparable for cholesterol oxidase treated T cells. These data are consistent with the hypothesis that partitioning of CD8 into membrane rafts differentially enhances its 2D binding affinity for MHC depending on the rafts in a particular type of T cells. Further studies are required to fully test this hypothesis and understand its implications to the regulation of MHC-CD8 interaction.

CHAPTER 5

INVESTIGATE THE ROLE OF CD8 IN HELPING THE TCR'S ANTIGEN RECOGNITION

5.1 Introduction

It has been well known that the co-receptor CD8 plays a critical role in helping TCR recognition of antigenic pMHC presented on the APC surface. Most of the studies use SPR, multimer staining or functional assays to address the importance of CD8 (12, 78, 82, 90, 92, 97, 98, 120). Those assays are usually lacking either of physiological similarity, temporal resolution, or detection sensitivity in addressing the function of CD8 in binding of pMHC. For example, SPR usually measures the 3D binding properties and kinetics of TCR or CD8 using purified proteins which are isolated from the cell membrane of either CTL or APC. Those purified molecules are physically prevented the cooperation, signaling and communication from the adjacent membrane molecules or the intracellular signaling kinases, thereby the measured data may not represent the real function and activity of the molecule in physiology condition (41). Although multimer staining is an important tool in studying the T cell immunology, it has its own pitfalls. Because it is usually very difficult to detect any effective binding using soluble monomeric pMHC, in order to achieve enough binding efficiency and amplify the binding signal for detection, multimers are structurally assembled by several pMHCs into one complex such as dimer or tetramer. Such structural modification may change the binding mode and behavior of the TCR-pMHC or CD8-MHC interaction, and more importantly, may affect the coordination of TCR and CD8 in the binding process. Meanwhile, the multimer staining is still measuring the 3D kinetics in soluble condition.

However, the pMHC is anchored on the APC surface in physiology condition. More and more evidences have suggested the importance of the 2D environment to the receptor-ligand interaction (14, 41). Also, the multimer staining is lacking of good temporal resolution and detection sensitivity. It usually measures the interaction in minute level and requires high binding affinity of the pMHC/TCR interaction. As to the functional assays, they usually measure the downstream responses of the CTLs, such as cytotoxicity, proliferation or cytokine release. Those results usually can be affected by many factors and only can indirectly reveal the function of the studied molecules.

Recently, it was identified that the cognate pMHC bearing RBC binding to F5 CTLs displays a two-step binding curve using a 2D micropipette adhesion assay (121). In this chapter, we continued the previous study using an OTI CTL system. We further characterized the molecular mechanism of the two-step binding. We also extended our study to the coordination and communication between TCR and CD8 on the live CTL surface. Our data stressed the fast kinetics of TCR-pMHC interaction, the active signaling between TCR and CD8 and the critical role of CD8 in the antigen recognition of the T cell.

5.2 Results

5.2.1 The fast kinetics of agonist pMHC-TCR interaction and the CD8 dependent two-step binding.

In order to mimic the physiological trimolecular interaction of TCR-pMHC-CD8 on the cell membrane, we used the real live naive OTI CTLs. we then constructed artificial APCs by coating human RBCs with the monomeric biotinylated agonist OVA pMHCs onto its surface via specific streptavidin-biotin interaction. The RBC can serve as

an ultra-sensitive interaction detector. Meanwhile, in order to individually study the TCR-pMHC interaction and specifically investigate the role of CD8 in the recognition process, an anti-CD8 blocking mAb (CT-CD8a) and an CD-8 null H-2K^b mutant which does not bind to CD8, were used in our study. Using the micropipette adhesion assay we tested the binding properties of how the OVA pMHC bind to TCR and CD8 on the cell membrane.

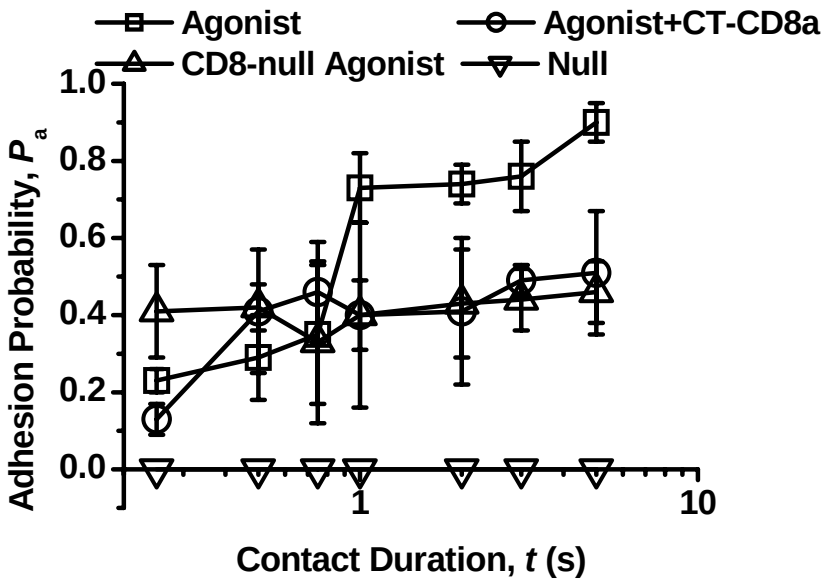

Figure 5.1 The fast kinetics of pMHC-TCR interaction and the CD8 dependent two-step binding for agonist pMHC. Plots of adhesion probability (P_a) vs. contact duration (t) measured using OTI CTLs interacting with RBCs coated with WT H-2K^b MHC complexed with agonist OVA peptide in the absence (□) or presence of blocking mAb (CT-CD8a) against CD8 (○),CD8-null H-2K^b MHC complexed with agonist OVA peptide (Δ), and WT H-2K^b MHC complexed with null peptide VSV (∇). Data (*points*) were presented as mean ± SEM (or single value) of 1–5 pairs of T cells and RBCs each making 50 contacts to observe the probability of adhesion.

Considering the complexity of the trimolecular TCR-pMHC-CD8 interaction, in order simplify the binding scenario and separate the TCR-pMHC interaction from the

trimolecular one, we firstly studied the individual TCR-pMHC interaction by using a CD8-null pMHC complexed with OVA agonist (Fig. 5.1, Δ) or blocking the CD8-pMHC interaction of WT pMHC with an anti-CD8 mAb (CT-CD8a) (Fig. 5.1, ○). The binding (Fig. 5.1, Δ or ○) reached equilibrium in very short time (< 0.25s), indicated that the TCR-pMHC interaction of agonist posses a very quick association and dissociation rates (>2 s^{-1}). The 2D dissociation rate is at least one order higher than that of reported 3D value (0.02 s^{-1}) using SPR measurement (44). Although due to the geometry difference, we could not directly compare the association rate or the affinity between 2D and 3D measurements. However, our 2D measurement still indicated that the agonist TCR-pMHC interaction has a very high affinity. By comparison, the 2D TCR-pMHC affinity for agonist OVA is more than one order higher than the reported value of 2D CD8-MHC interaction at resting state (38). Also, the data and curve overlapping between those of CD8-null pMHC (Fig. 5.1, Δ) and CD8 blocking (Fig. 5.1, ○) conferred us confidence on the accuracy of measurements.

Next we investigated the role of CD8 in helping the TCR recognition of agonist pMHC. Similar to previous studied observed in F5 CTL's system (121), with the participation of CD8, the trimolecular interaction of TCR-pMHC-CD8 displayed a sigmoid shape two-step binding curve (Fig. 5.1, □), and the switch from first-step to second-step was around one second contact duration. Before one second, the binding probability increased very slightly and reached a first plateau very soon. At around one second, the adhesion probability suddenly jumped to a higher level binding, and it reached a second plateau very quick as well, indicated that the interaction reached a second equilibrium.

Coincidently, this first-step binding overlapped with the TCR-pMHC binding curve pretty well (Fig. 5.1, compare the □ with Δ or ○ before one second contact duration). It was known that the CD8-pMHC interaction at resting state has a very low affinity compared with the TCR-pMHC for agonist. As demonstrated on Figure 5.1, there was no any detectable binding for null pMHC (Fig. 5.1,∇), which had same coating site density as the agonist (Fig. 5.1, □) and only could be bound by CD8 but not TCR (38, 44). So, the data suggested that the first-step binding is mediated by TCR-pMHC interaction. More important, after one second duration, the second-step binding only occurred for WT agonist pMHC (Fig. 5.1, □), but not for the CD8-null agonist pMHC (Fig. 5.1, Δ) and the WT agonist pMHC treated with anti-CD8 mAb (Fig. 5.1, ○) which had excluded CD8-MHC interaction. The data indicated that the second-step binding is triggered by agonist TCR-pMHC interaction and mediated by CD8-MHC interaction.

5.2.2 Directly triggering the second-step binding using an anti-CD8 mAb 53-6.7.

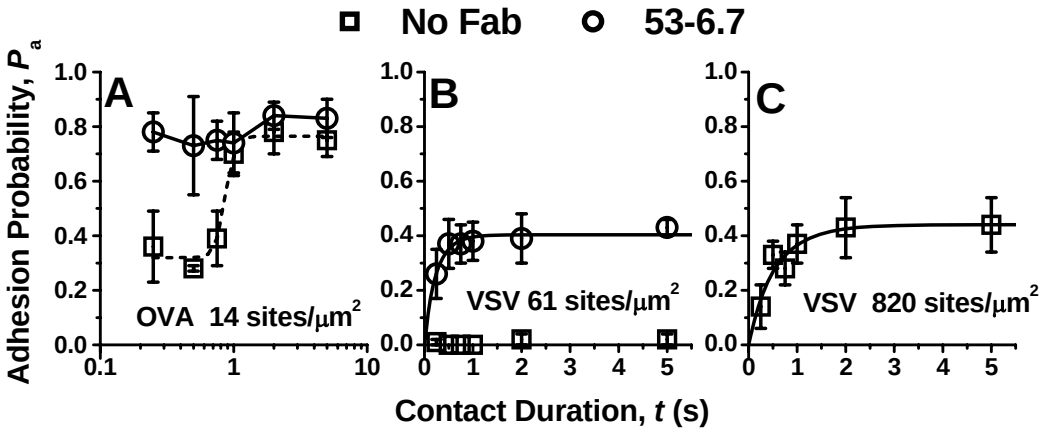

Figure 5.2 Anti-CD8 mAb 53-6.7 enhances binding between pMHC coated RBCs and OTI CTLs. Plots of adhesion probability (P_a) vs. contact duration (t) measured using OTI CTLs interacting with RBCs coated with H-2K^b MHC complexed with agonist peptide OVA (A) and null peptide VSV (B and C) in the

absence (□) or presence (○) of activating Fab (53-6.7). The coating densities of pMHC on RBC surface are labeled. Data (*points*) were presented as mean ±SEM of 2–5 pairs of CTLs and RBCs each making 50 contacts to observe the probability of adhesion.

The important role of CD8 has been well recognized. However, it is not clear whether the CD8 have multiple affinity states in binding to pMHC. It has been reported that one anti-TCR antibody can trigger the affinity up-regulation of CD8 on activated CTLs (122), but this antibody does not work for naïve CTLs (Personal Communication with Dr. Matthew Mescher). Also, it was reported that the some anti-CD8 antibodies can significantly augment the tetramer staining efficiency (82), and one of those antibodies 53-6.7 was found to enhance the binding between OTI CTLs and pMHC coated RBCs in micropipette assay (Fig. 5.2). For agonist OVA pMHC, after adding the 53-6.7 mAb, the binding probability bypassed the initial first-step plateau and directly reached the second-step binding (Fig. 5.2A, compare □ with ○). Similarly, this 53-6.7 mAb could enhance the binding for the null VSV pMHC (Fig. 5.2B, compare □ with ○), which cannot be recognized by OTI TCR. By calculation we found that the binding affinity increased ~10 folds after adding the anti-CD8 mAb for null VSV pMHC (Compare Fig. 5.2 B with C). Coincidently, the affinity difference between the first-step binding and second-step binding for agonist OVA pMHC (Fig. 5.2A) is also ~10 folds. The data suggested that the 53-6.6 mAb can have similar but not necessary same function as TCR to trigger CD8 to reach a higher binding state. Also, the results suggested that the CD8 might be able to have multiple affinity states which can be triggered either by TCR-pMHC interaction or by the anti-CD8 mAb binding. The epitope mapping of the 53-6.7 mAb also indicated that the existence of different CD8 conformations (123).

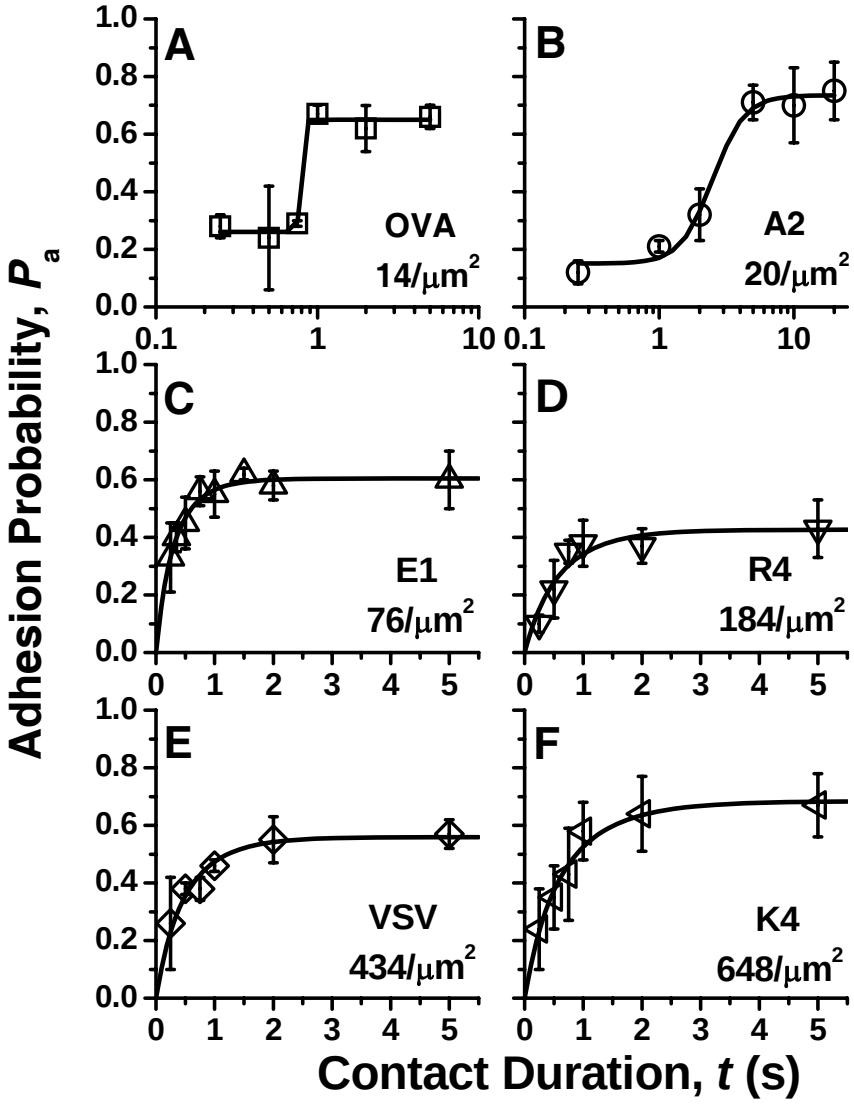

Figure 5.3 The binding characteristics of different pMHCs. The plots of adhesion probability (P_a) vs. contact duration (t) measured using OTI CTLs interacting with RBCs coated with WT H-2K^b MHC complexed with agonist peptides OVA (A) and A2 (B), antagonist peptides E1 (C) and R4 (D), and null peptides VSV (E) and K4 (F). The coating densities of pMHC on RBC surface are labeled. Data (*points*) were presented as mean ±SEM of 2–5 pairs of CTLs and RBCs each making 50 contacts to observe the probability of adhesion.

5.2.3 The peptide dependence of two-step binding

It is known that different pMHCs bind to TCR with different kinetics and affinity. Next we tested how the binding of TCR-pMHC affects the CD8-pMHC interaction for different pMHCs. Since we have observed that the TCR-pMHC interaction of agonist can efficiently trigger the CD8 dependent second-step binding, it is interesting to know whether the interaction of TCR with other pMHCs can have similar or different function affecting the CD8-pMHC binding. We chose six types of pMHCs to test, including two agonists OVA (Fig 5.3 A) and A2 (Fig 5.3 B), two antagonists E1 (Fig 5.3 C) and R4 (Fig 5.3 D), and two nulls VSV (Fig 5.3 E) and K4 (Fig 5.3 F).

Similar to the OVA, the A2 is also an agonist. The A2 pMHC also displayed a two-step binding curve as the OVA did (Fig. 5.3 A and B). However, the difference was that the switch time of A2 from first-step to second-step was distinct from that of OVA, i.e., the A2 switch time was ~3s, which was three times longer than that of OVA. Also, the switch time of A2 was not sharp and clear as that of OVA, and the switch process was relative slower and smoother compared with that of OVA.

For antagonists E1 and R4, and nulls VSV and K4, we failed to observe any two-step binding curve (Fig. 5.3 C, D, E &F). All of those four pMHCs exhibited typical monovalent receptor-ligand binding curves as reported in many receptor-ligand interactions (38, 74, 75, 115, 117). It is known that the binding affinity of those four pMHCs was significant lower than those of agonist OVA and A2 (44, 71). The affinity difference also was demonstrated in our 2D micropipette assay (Fig. 5.3). The binding affinity of each pMHC could be directly calculated using a mathematical transformation. Simply speaking, at same equilibrium adhesion probability, the binding affinity of each

pMHC is reversely proportional with its site density. As shown in figure 5.3, with similar equilibrium binding probability for all pMHCs, the site densities of pMHC was continuously increasing from OVA to K4 (Fig. 5.3 A-F). The data suggested that the binding affinity is OVA≈A2>E1>R4>VSV≈K4 if we ranked them from high to low. Our results actually correlated well with the published 3D SPR measurements (44, 71).

In short, the above data suggests that the binding kinetics and affinity of pMHC-TCR interaction is the key in determining whether to trigger the CD8 dependent second-step binding. The data also indicates that the peptide discrimination in adaptive immune response occurs in the TCR-pMHC mediated first-step binding, and is amplified in the CD8 dependent second-step binding.

5.2.4 The two-step binding requires signaling between TCR and CD8.

TCR and CD8 are not only receptors that recognize their corresponding ligands, but are signaling molecules that transmit signals to stimulate CTLs. It is known that the TCR/CD3 complex composed of six chains: the TCR αβ heterodimer is responsible for the ligand recognition, while the CD3 polypeptides (γε, δε, ζζ) are signaling modules whose cytoplasmic domains are phosphorylate by Src kinases in the early stages of activation (1, 9). Meanwhile, the extracellular domain of CD8 binds to invariant domain of pMHC (85, 91), and its cytoplasmic domain associates with Lck kinase or LAT adaptor molecule to trigger downstream signaling (89, 124). It is highly possible that the two-step binding is signaling involved, and we therefore designed a series of experiments to test the hypothesis based on known T cell signaling pathways from literatures.

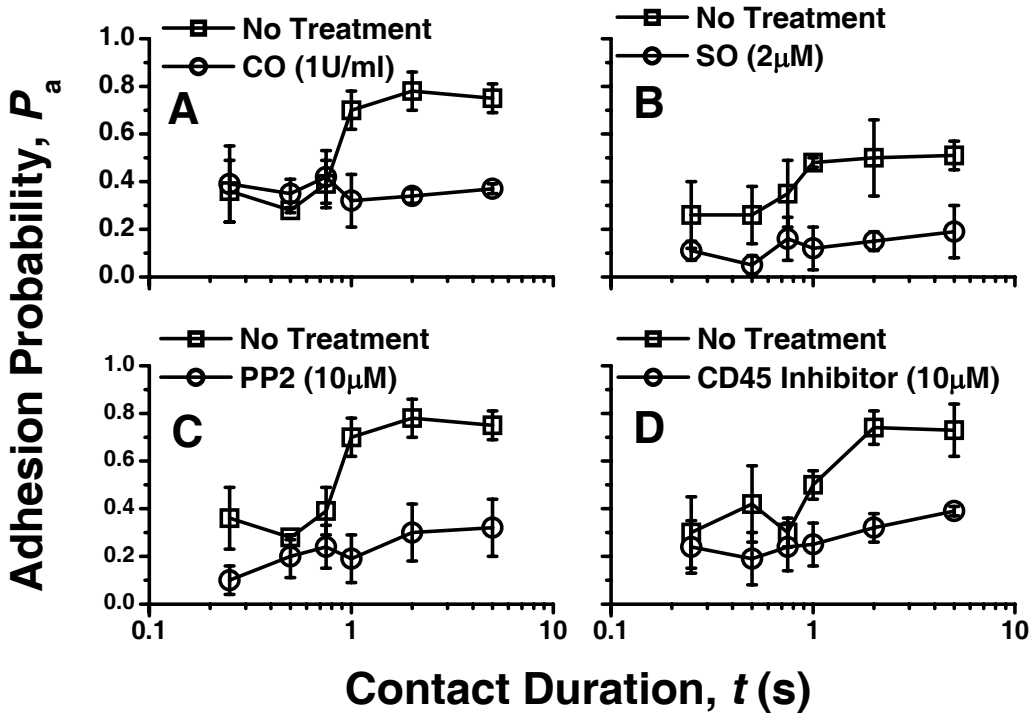

Figure 5.4 The effects of signaling inhibitors on two-step binding. The plots of adhesion probability (P_a) vs. contact duration (t) measured using OTI CTLs interacting with RBCs coated with agonist pMHC in the absence (□),) or presence (○) of cholesterol oxidase (CO) (A) , sodium orthovanadate (SO) (B), PP2 (C) and CD45 inhibitor (D). Data (*points*) were presented as mean ±SEM of 2–5 pairs of CTLs and RBCs each making 50 contacts to observe the probability of adhesion.

First of all, lipid rafts is the platform for the molecular signaling at the T cell membrane (34) and the integrity of raft is a prerequisite for efficient TCR signal transduction (125). Here we tested whether the integrity of the lipid rafts is required for occurrence of the two-step curve. Lipid rafts were disrupted by using the cholesterol oxidase (1U/ml), which converts cholesterol to cholestenone. Consistent with previous observation in F5 T cell system (121), we found that the TCR-induced and CD8-dependent two-step binding curve no longer existed, and it was reduced to the first-step

binding level (Fig. 5.4A, compare □ with ○). The data reinforced the important role of lipid rafts in CTL recognition of antigen and indicated that the two-step binding needs an integral lipid environment where is the place for active T cell signal transduction.

In order to further test whether the signaling is involved, we used sodium orthovanadate (SO) to check the signaling through the regulation of protein phosphorylation, which is one of the most important and common signaling pathways in CTLs. SO is an inhibitor of protein tyrosine phosphatases (PTP), alkaline phosphatases and a number of ATPases, most likely acting as a phosphate analogue. SO (Na_3VO_4) contains the tetrahedral VO_4^{3-}, which binds irreversibly to the active sites of most PTP, thereby preserves the phosphorylation of proteins by inhibiting endogenous phosphatases present in the cell. After incubating the SO with OTI CTLs for 30 minutes, the micropipette binding assay clearly showed that the first-step of binding was slightly decreased, and more pronounced, the second-step binding was fully inhibited (Fig. 5.4B, compare □ with ○). The data demonstrated that the two-step binding involves signaling, and it depends on the protein dephosphorylations by phosphatases.

Recent evidence has implicated at least three cytoplasmic protein tyrosine kinases (PTKs), Lck, Fyn, and ZAP-70, that are involved in the initiation of TCR signal transduction (126). It has been reported that the TCR-coupled Src family PTKs Lck and Fyn on lipid rafts plays a critical role in CTLs signaling (27). CD8α chain can associate with Lck and CD8β chain mediates the coupling of CD8/Lck with TCR/CD3 partition into the lipid rafts, thereby activating Lck to phosphorylate CD3 and initiate T cell activation (79). We therefore employed the PP2 (4-amino-5-(4-chloro-phenyl)-7-(*t*-butyl) pyrazolo [3, 4-*d*] pyrimidine) to determine the possible involvement of tyrosine

phosphorylation in the modulation of Src family PTK's activity. PP2 is a potent and selective inhibitor of Src family PTKs for Lck and Fyn but only weakly inhibits ZAP-70 (127). PP2 showed similar effect as that of anti-CD8 blocking mAb in inhibition of binding, as the CD8 dependent second-step binding was fully suppressed (Fig. 5.4C). The data again demonstrated that the TCR induced and CD8-dependent second-step is signaling involved and more specifically, it relies on the Src family kinase such as Lck and Fyn.

The PTP CD45 is one of the most abundant glycoproteins expressed on CTLs and it plays a pivotal role in antigen-stimulated proliferation of T lymphocytes and in thymic development (24). CD45 serves as both positive and negative signaling elements by dephosphorylating regulatory phosphorylated tyrosine (PY) residues on Src family PTKs, Lck and Fyn, which have been implicated as physiological substrates of CD45 (23, 128). Lck seems to be the major contributor (27). The dual activity of CD45, both enabling and downregulating Lck activity, has been elegantly demonstrated in vivo (25). Using PTK inhibitor PP2 we have demonstrated the importance of the PTKs Lck and Fyn in mediating the two-step binding. After treating with the PTP CD45 inhibitor (N-(9,10-Dioxo-9,10-dihydro-phenanthren-2-yl)-2,2-dimethyl-propionamide) to prevent the dephosphorylation of PTKs such as Lck for OTI CTLs (129), it was found that the second-step binding was effectively inhibited (Fig. 5.4D). The data stressed the important role of PTP CD45 in the TCR recognition and signaling and indicated that the signaling through CD45 is required for triggering the second-step binding.

Taken together, the data clearly showed that the TCR-induced and CD8-dependent two-step binding involves signaling between TCR and CD8. The data

suggested that TCR binding to antigenic pMHC can elicit a signal which leads to a CD8-dependent second-step binding in the process of antigen recognition. This signaling requires the unperturbed lipid rafts, the Src family PTKs and the PTP CD45.

5.2.5 The memory effects caused by signaling

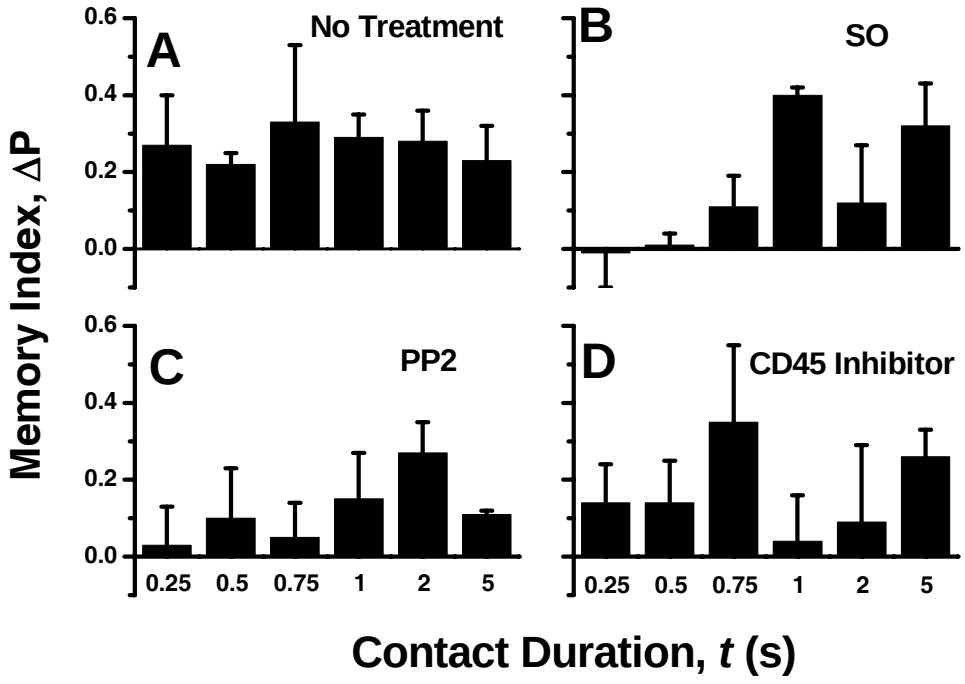

Figure 5.5 The effects of signaling inhibitors on adhesion memory. The calculated adhesion memory index in the absence of inhibitor (A), or the presence of SO (B), PP2 (C) and CD45 inhibitor are plotted at six contact durations (0.25~5 second). Data (*points*) were presented as mean ±SEM. (Analyzing program provided by Zarnitsyna (130))

The data have shown that the two-step binding is signaling dependent. Besides the readout from the direct observation on the adhesion probability, we also identified the signaling information using adhesion memory analysis (130). The adhesion memory index Δp are calculated using the published method (130) to analyze the adhesion scores

of a sequence of fifty adhesion testes for each pair of cells at different experimental conditions. The memory index Δp represents the ability of a system to remember the result of the previous adhesion test, as evidenced by a change in the likelihood of the outcome in the subsequent adhesion test. It has been identified all three theoretically possible scenarios in nature: no memory (Δp=0), positive memory (Δp>0), and negative memory (Δp<0). One of the most possible reasons for the generation of memory is signaling. Here we firstly demonstrated that the signaling can affect the adhesion memory in a T cell system. Without any treatment (Fig. 5.5A), it is clear that adhesion of agonist pMHC coated RBC interacting with OTI CTLs shows a strong memory phenomena because all the adhesion memory indexes Δp are positive and the values are >0.2 for all six contact durations (Fig. 5.5A). In sharp contrast, after adding the phosphatase inhibitor SO (Fig. 5.5B), the Src family kinase inhibitor PP2 (Fig. 5.5C) or the CD45 phosphatase inhibitor (Fig. 5.5D), the memory effects are reduced at different extents for different contact durations. The reduction is much more significant at short contact duration (contact duration t<1s) for all three inhibitors than those of long ones.

5.3 Discussion

It has been shown that TCR binds to different pMHCs with different kinetics/affinities using SPR measurements. TCR binds to agonist with a slower off-rate and/or higher affinity than those of antagonist and null (11, 44). Those data identify a positive correlation between the binding kinetics/affinity and peptide potency in activating the T cell and provides support for kinetic proofreading model of TCR discrimination. The critical role of co-receptor CD8 in antigen recognition has been reported in many publications. It was found that some anti-CD8 mAbs can inhibit pMHC

binding to T cell (82, 108, 109, 111, 131), and blocking the CD8 binding can prevent activation of T cell (81, 82, 108, 111, 131). Similar effect was observed using a MHC mutant lacking the CD8 binding site. The staining efficiency for CTLs of this mutant pMHC was greatly reduced, and its ability to activate the naïve CTLs was dramatically diminished compared with that of WT one (110). Similarly, the CD8 negative T cells bind to pMHC 10-100 times less than and lysed APC much poor than CD8 positive ones (131). How CD8 help TCR recognize antigen is an important issue that needs to be addressed.

In the SPR measurements, the class MHC-I agonist OVA pMHC binding to OTI TCR shows a very slow off-rate (0.020 s^{-1}) (44). A similar off-rate (0.061 s^{-1}) has been reported for a MHC-II Hb (64-76) agonist binding to 3.L2 TCR (11). These data fit well with the kinetics proofreading model which suggests that the potency of a pMHC is primarily determined by the off-rate of the TCR/pMHC interaction and the TCR/pMHC complex must sustain long enough to send a complete signal to fully activate a T cell. However, several exceptions were reported that slow off-rate does not necessarily result in better activation (45-47). In sharp contrast with SPR measurements, our 2D micropipette adhesion assay found that the TCR binds to agonist pMHC with a very fast off-rate (>2 s^{-1}) and the TCR-pMHC interaction reaches equilibrium in very short time (<0.25 s), which indicates a fast on-rate as well. The discrepancy between the published SPR data and our 2D micropipette results can be explained from below two aspects. Firstly, those two measurements are physical different. The SPR is referred to as 3D measurement and the micropipette as 2D measurement (41). For SPR measurement, there is one molecule in the fluid phase, and the receptor and ligand encounter each other by

diffusion and/or flow of soluble molecule in a volume, the concentration has a unit of M, and the 3D binding affinity is measured in M^{-1}. By comparison, for micropipette assay, both receptor and ligand are anchored on the cell membrane and they only can diffuse along the membrane, their surface site densities have a unit of m^{-2}, and the 2D binding affinity is measured in m^2. More importantly, the receptor and ligand only can meet each other by bringing two interacting cells together because membranes separated by a distance greater than the molecular size would physically preclude binding (41). It has been demonstrated that the molecular length and orientation (75) as well as cell surface roughness and stiffness can significantly affect 2D (but not 3D) affinity (102, 103). Although the off-rate k_r has the same unit (in s^{-1}) for 2D and 3D interaction, only in the 2D (but not 3D) case can k_r be regulated by force applied to the molecular bonds—they would be disrupted by the separation of the cells (41). Secondly, the SPR measurements use the soluble molecules or recombinant proteins which are purified from cell membrane. These molecules lose their linkage to the cell membrane, communication to signaling kinases or adaptor molecules inside of the cell, and the cooperation of adjacent molecules on the cell membrane. Therefore the measured kinetics might not represent the actual values in physiology condition. In contrast, our 2D micropipette assay is more physiology relevant though we also used an artificial APC by coating the RBC with the pMHC in order to simplify the system. The fast on- and off-rates suggest the CTLs can quickly scan the APC surface and response to antigen efficiently.

The most striking discovery is that the binding between agonist coated RBCs and OTI CTLs shows a two-step binding (Fig. 5.1, □). Because blocking the CD8-MHC interaction by either adding blocking anti-CD8 mAb or using CD8-null pMHC will

abolish the second-step binding. The data suggests that the first-step binding is mediated by TCR, while the second-binding is the contribution of CD8. Although the SPR experiments did not find any significant difference in the interaction of soluble pMHC to immobilized TCR in the presence or absence of soluble CD4/8 co-receptor (78, 106), the negative data cannot rule out the possibility of cooperation when both TCR and CD8 reside on the same T cell membrane. Actually, our 2D micropipette data clearly indicate the cooperation and signaling between TCR and CD8 on the surface of live T cells. When the TCR is blocked by an anti-TCR blocking mAb, not only the first-step binding mediated by TCR-pMHC is inhibited, but the second-step CD8 dependent binding is completely abolished (data not shown). There is no second-step binding anymore even though there is still CD8-MHC interaction, which cannot be detected at such a low pMHC site density (38). Also, only the agonist, but not the null pMHC coated RBCs can elicit second-step CD8-dependnent binding to OTI CTLs (Fig. 5.1, compare the □ with ▽). The reason is that although CD8 has same binding site to MHC for both agonist and null pMHCs, the OTI TCR only recognize agonist but not the null pMHC. So an appropriate TCR-pMHC interaction is the prerequisite of triggering CD8-dependent second-step binding. An interesting question is naturally raised: How the two-step binding come from? More explicit, how the TCR-pMHC interaction affects the CD8-pMHC binding?

There are several alternative ways to explain the two-step binding. The most straightforward one would be that the TCR-pMHC interaction activates the CD8 to a higher affinity state for binding to pMHC compared with a resting state MHC-CD8 interaction (38). Actually, the activation of CD8 by treating the activated CTLs with an

anti-TCR β antibody has been reported by Mescher et al. (122).The difference between their finding and our discovery is that we use the naïve OTI CTLs, and more important, we detect the CD8 activation if it is in a more physiological condition without using any artificial antibody to trigger. Another alternative but more complicated interpretation of two-step binding is that though the CD8-MHC interaction is fairly weak but it generates an activation signal to boost the TCR-pMHC binding to reach a higher level. The third possibility is that the TCR aggregation or cluster triggered by CD8, thereby the overall avidity increasing to cause the second-step binding. The most obvious obstacle of the explanation is that the TCR clustering or aggregation must be accomplished in one second and in a CD8 dependent way.

We firstly tested whether the CD8 has multiple binding affinity states. It has been reported one anti-CD8 mAb 53-6.7 can significantly enhance the pMHC multimer staining efficiency to CTLs (82). We also found this mAb can significantly enhance the binding between pMHC coated RBCs and OTI CTLs in 2D micropipette assay. More interestingly, this mAb can bypass the TCR-pMHC triggering and directly induce the binding to the second-step (Fig. 5.2A). This mAb also can enhance the binding of null pMHC coated RBC to OTI CTLs (Fig. 5.2B). Because the TCR cannot recognize null pMHC, it is normally to explain the enhancement of binding by the CD8 activation induced by mAb. Two papers also suggested that this mAbs stabilizes a higher affinity CD8 conformation using antibody epitope mapping and multimer staining (18, 123).

Let's go back to the T cell discrimination of pMHCs. It is commonly accepted that the discrimination is based on the difference of peptides. Previous studies (11, 44) and our data have shown that the TCR-pMHC interaction has different kinetics and/or

affinity for different pMHCs. However, one puzzle still exists: how the T cell can transmit and amplify those subtle kinetic differences into distinct discrimination signals so the CTLs can accurately decide whether it should be activated or not. There are many models have been proposed to explain the mechanism and the kinetic proofreading model is the most wildly accepted one (42). Our data showed that the two-step binding is peptide dependent, i.e., only the agonist, but not the antagonist and null, can trigger the two-step binding. This discovery partially answers the question of signal amplification in T cell discrimination of peptide: The TCR engagement provides the initial detection signal, while the CD8 contributes the discrimination via a signaling amplification pathway. Further study is needed to fully understand the significance the dependence of two-step binding on peptide.

The data have demonstrated a requirement of signaling for two-step binding, i.e., disrupting the lipid rafts and inhibition of PTPs and PTKs abolish the two-step binding. Activation of T cells through the TCR represents an alteration in the dynamic equilibrium between PTPs and PTKs (25), which was also indicated in the micropipette adhesion assay data using the kinase inhibitors. Mobilization of PTP CD45 and dephorsphorylation of Lck by CD45 are the perquisites for PTKs Lck and Fyn activation and subsequent phosphorylation of the CD3 complex (25). Blocking the PTPs by a universal inhibitor SO or a specific CD45 inhibitor abolished the second-step binding. The TCR-pMHC binding triggers the exposure of CD3 docking sites (50), and the concomitant binding of CD8 to the same pMHC can amplifies the lipid raft coalescence (36, 132) and brings associated PTKs such as Lck to TCR (133, 134), thereby phosphorylating ZAP-70 and triggering

downstream signaling. Consistently, inhibition the Src family PTKs Lck and Fyn by PP2 blocks the second-step binding.

The signaling of T cell has also been revealed by a memory analysis of adhesion scores. In the absence or presence of signaling inhibitors, the adhesion memory indexes showed distinct values, especially at short contact duration (<1s). It has been shown that the second-step binding appears at ~ 1s, and all three inhibitors can efficiently prevent the triggering of the second-step binding (Fig. 5.4). The correlation suggested that the fast TCR-pMHC interaction can generate a signaling in the initial short contact duration (<1s) leading to the second-step CD8 mediated binding. However, after 1s duration, the memory of the adhesion increased (Fig. 5.5 B, C or D). The reason is not clear. A potential explanation could be that the TCR-pMHC interaction might elicit several signaling events, those inhibitors only could selectively block some of those quick events which can leading to second step-binding, or longer contact duration can generate stronger signaling to bypass the blocked signaling pathways. Clearly, the mechanism and the application of those memory effects need further investigations. Nevertheless, the memory analysis provides us a new approach to recheck our adhesion data. It allows us to draw more information from a simple binary adhesion tests, and provides us another eye to look into the nature of T cell signaling and recognition.

Taken together, many data have emphasized the importance role of CD8 in helping TCR recognition. However, several studies have shown that the MHC-CD8 binding is very weak (38, 98) and is negligible if compared with TCR-MHC interaction (78). These apparently contradictory findings indicate that CD8 binding to MHC might be activated through the TCR-pMHC interaction and the results reported here suggest

that is the case. Possible mechanisms by which TCR signaling activate CTL binding mediated by CD8 include: rapid up-regulation of surface CD8 expression level (less likely in one second-time scale), signaling induced TCR or CD8 microclustering, CD8 and TCR association, or conversion of CD8, TCR or both from a low-affinity to a high-affinity conformation state through a series dephorsphorylation and phorsphorylation signaling steps. These possibilities are not mutually exclusive and more than one could contribute to the generation of two-step binding.

CHAPTER 6

FURTHER CHARACTERIZE THE CROSSTALK BETWEEN TCR AND CD8

6.1 Introduction

CTLs specifically recognize antigen presented on APC surface via their special sensor TCRs, whose highly variable complementarity-determining regions interact with the α1 and α2 peptide-binding platform of the pMHC complex (55, 64). Meanwhile, the co-receptors CD8 bind to the invariant α3 domain of MHC (85, 91). Many publications have suggested that the TCR and CD8 cooperate together in the recognition of antigenic pMHC and triggering of the T cell activation. However, how TCR and CD8 communicate and coordinate during the recognition process, remains unclear.

The TCR/CD3 complex consists of six different polypeptides (α, β, γ, δ, ε, and ζ) (Fig. 2.1). After the heterodimeric αβ TCR bind to the pMHC ligand, the recognition is translated into intracellular signal events by other polypeptides in the complex. One of first reported signaling event is the phosphorylation of CD3ζζ chain, which contains six ITAMs. The CD8 is a glycoprotein marker expressed on the surface of CTLs. The cytoplasmic tail of CD8α can associate with the Src tyrosine kinase Lck to trigger signaling (12, 135), while the CD8β plays a role in organizing TCR within lipid rafts (79, 136). CD8 can function as an adhesion molecule by binding MHC to stabilize the TCR/pMHC interaction, or serve as a co-receptor by associating with Lck or LAT to trigger the downstream signaling cascade that results in T cell activation (12, 79, 136).

It has been shown that CD8 plays a critical role in helping TCR recognizes antigen pMHC presented on the APC surface. The blockade of CD8 binding to MHC by

either mutating the CD8 binding epitope or abrogating the CD8 expression on CTLs, will lead to the pMHC binding efficiency decrease and T cell activation diminish (110, 131). Interestingly, it was found that some anti-CD8 antibodies can greatly inhibit CTLs binding to pMHC and prevent the CTL activation (81, 82, 108, 111, 131), while some other anti-CD8 antibodies can significantly enhance pMHC binding (82, 111) and promote CTL activation (111).

In the previous chapter, we have identified that the generation of two-step binding requires signaling between TCR and CD8. Here we used two anti-CD8 mAbs CT-CD8a and 53-6.7 to further characterize the crosstalk between TCR and CD8. According to the literature report, the CT-CD8a mAb epitope locates in residues of CD8α chain that contact MHC, while 53-6.7 mAb epitope locates on the D–E loop of CD8α chain (123). Using a 2D micropipette adhesion assay, we confirmed the previous observation that the CT-CD8a and 53.6.7 mAbs can either inhibit or enhance the pMHC binding to T cells (18, 82). The results validated our measurements and conferred us the confidence to further characterize the crosstalk between TCR and CD8 by using these two anti-CD8 mAbs. We also used two types of MHC molecules, WT H-2K^b MHC or CD8-null H-2K^b MHC chimera to complex with four types of peptides: OVA (agonist), G4 (weak agonist), E1 (Antagonist) or VSV (null) respectively. The CD8-null H-2K^b MHC chimera is constructed by replacing the mouse α3 domain of K^b molecule with a human HLA one. Because the CD8 binding site is located on α3 domain (85, 91), this mutation structurally abolishes the CD8 binding.

Because the readout of our micropipette assay is binding, we systematically investigated how the TCR and CD8 affecting each other in the binding of pMHCs. The

crosstalk between TCR and CD8 was revealed from the view of either inhibition or enhancement of binding. These data implied a tight cooperation between TCR and CD8 in the antigen recognition.

6.2 Results

6.2.1. Characterize the crosstalk of TCR and CD8 from the inhibition of binding

In the previous chapter, we have identified the two-step binding curve between OTI CTLs and RBCs coated with agonist pMHC. The data suggested that triggering the second-step binding requires the signaling between TCR and CD8. To better characterize the communication between TCR and CD8 in the process of binding to pMHC, we further tested whether blocking the TCR binding could affect CD8 binding to pMHC. Meanwhile, we investigated whether the CD8 binding could interfere with the TCR-pMHC interaction.

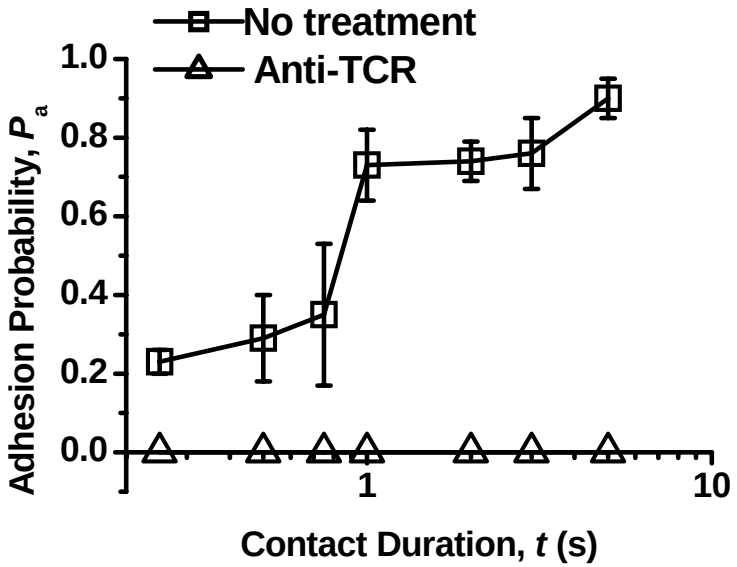

Figure 6.1 The anti-TCR mAb completely abolishes the two-step binding. Plots of adhesion probability (P_a) vs. contact duration (t) measured using OTI CTLs interacting with RBCs coated with WT H-2K^b

complexed with agonist OVA in the absence (□) or presence of anti-TCR mAb (Δ). Data (*points*) were presented as mean ± SEM of 2–5 pairs of T cells and RBCs each making 50 contacts to observe the probability of adhesion.

6.2.1.1 Blocking TCR-pMHC interaction abolishes CD8 mediated second-step binding

In the chapter 5, we have shown that the binding between an OTI CTL and an OVA pMHC coated RBCs displays a two-step binding curve (Fig. 6.1, □). The first-step binding is the mediated by TCR, while the second-step binding is the contribution of CD8. However, after adding the anti-TCR mAb to block the TCR-pMHC interaction, not only the TCR mediated first-step binding was abolished, but the CD8 mediated second-step was disappeared (Fig. 6.1, Δ). The data demonstrated that blocking the TCR-pMHC interaction can affect the CD8-pMHC binding and indicated the crosstalk between TCR and CD8.

6.2.1.2 The CT-CD8 mAb binding to CD8 can affect TCR-pMHC interaction

We found that an inhibitory mAb CT-CD8a binding to CD8 could affect the TCR-pMHC interaction for weak ligands. According to published 3D SPR measurement, a weak ligand G4 pMHCs bound to TCR with moderate affinity (10 μM) (71). Similarly, in our micropipette assay, the binding between OTI CTLs and RBCs coated with G4 CD8-null pMHCs could be readily detected at suitable site density (Fig 6.2). Because the CD8-null pMHC does not have CD8 binding site, so the binding was mediated by the specific TCR-pMHC interaction (Fig 6.2, □). Unexpected, treating OTI CTLs with inhibitory mAb CT-CD8a abolished the binding between OTI CTLs and RBCs coated with the G4 CD8-null pMHC (Fig. 6.2, ○). The puzzle was why the anti-CD8 mAb

binding to CD8 could block the TCR-pMHC interaction for CD8-null pMHC. According to the epitope mapping, the CT-CD8a mAb occupies the CD8 binding epitope to the MHC molecule (123). One possibility is the steric hindrance caused by this mAb. However, the data in the chapter 5 suggested it was less likely the case, because the same inhibitory mAb did not sterically prevent the OVA WT pMHC interacting with TCR (Fig. 5.1A, ○). Meanwhile, the Fab of the CT-CD8a showed similar effects as the whole antibody (data not shown). Because the CD8-null pMHC completely abrogates the pMHC-CD8 interaction but keeping the TCR-pMHC binding, it was clear that the CT-CD8a mAb does not only block the pMHC-CD8 interaction, but also affects the TCR-pMHC interaction in a peptide dependent manner.

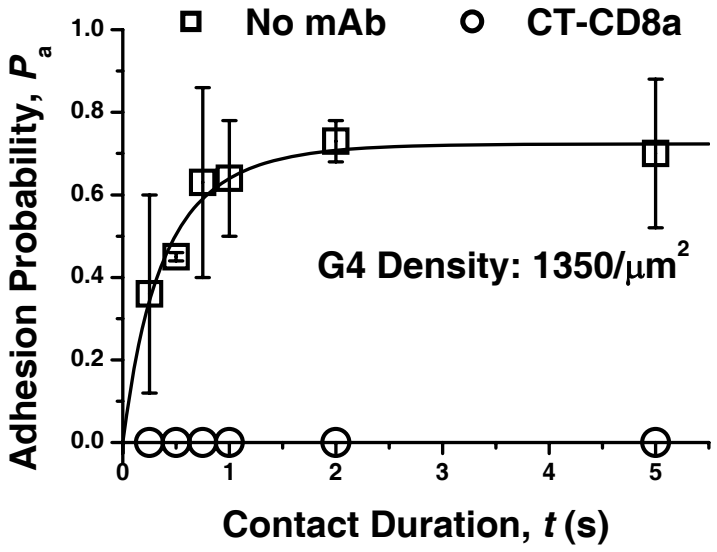

Figure 6.2 The inhibitory CT-CD8 mAb blocks the adhesion between CD8-null pMHC coated RBCs and OTI CTLs. Plots of adhesion probability (P_a) vs. contact duration (t) measured using OTI CTLs interacting with RBCs coated with CD8-null H-2K^b-HLA chimera complexed with weak agonist G4 in the absence (□) or presence of inhibitory CT-CD8a mAb (○). Data (*points*) were presented as mean ± SEM of 2–5 pairs of T cells and RBCs each making 50 contacts to observe the probability of adhesion.

6.2.2. Study the crosstalk from enhancement of binding

In the chapter 5, we have shown that the TCR-pMHC interaction of agonist pMHC could trigger the CD8 activation, therefore it bound to the same pMHC with much higher affinity. The data actually demonstrated the crosstalk of TCR and CD8: the TCR engagement enhanced the CD8 binding to pMHC. We also identified that one anti-CD8 mAb 53-6.7 could significantly enhance the binding between OTI CTLs and RBCs coated with pMHC. We therefore designed a series of experiments to further dissect the crosstalk between TCR and CD8 by taking the advantage of this 53-6.7 mAb.

6.2.2.1 CD8 directly mediates the enhancement of binding induced by 53-6.7

Since we have identified the enhancing role of the 53-6.7 in the binding between OTI CTLs and pMHC coated RBCs in chapter 5, it was important to understand whether the CD8 directly mediates the enhancing binding induced by this 53-6.7 mAb. To better characterize the CD8 binding in the presence of anti-CD8 mAb, we used the CD8-null pMHC complexed with either OVA agonist or VSV null peptide. For the CD8-null OVA pMHC, it bound to the OTI CTLs fairly well. Importantly, the binding of CD8-null OVA pMHC coated RBCs to OTI CTLs was not influenced by adding activating 53-6.7 mAb (Fig. 6.3A, compare □ with Δ). Similar data was obtained for a CD8-null VSV pMHC (Fig. 6.3B). The data suggested the 53-6.7 mAb no longer can enhance pMHC binding to OTI CTLs in the absence of CD8. In other words, the enhanced binding triggered by 53-6.7 is directly mediated by CD8. These data emphasized a critical role of CD8 in the recognition of pMHC and clearly suggested that the CD8 directly mediates the binding of pMHC. The results were consistent with the tetramer staining data obtained by swell group (18). It was clear that the anti-CD8 mAbs can apply a direct effect on the CD8

binding, an interesting question was naturally raised, whether the augment effects induced by the 53-6.7 mAb are TCR dependent?

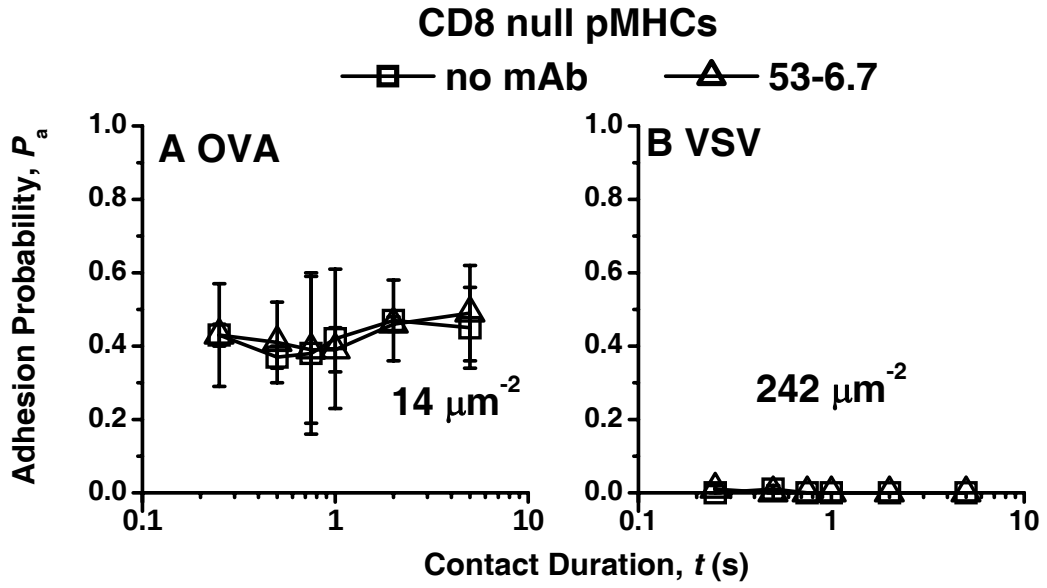

Figure 6.3 The binding characteristics of CD8-null pMHC. Plots of adhesion probability (P_a) vs. contact duration (t) measured using OTI CTLs interacting with RBCs coated with CD8-null H-2K^b-HLA chimera complexed with agonist OVA (A) and null peptide VSV (B) in the absence (□) or presence of activating 53-6.7 mAb (Δ). The site densities of pMHC were labeled. Data (*points*) were presented as mean ± SEM (or single value) of 1–5 pairs of T cells and RBCs each making 50 contacts to observe the probability of adhesion.

6.2.2.2 The enhanced binding induced by anti-CD8 53-6.7 mAb is TCR dependent

It has been shown that the inhibitory CT-CD8a mAb can affect the binding of pMHC to TCR. We further designed three experiments to test whether there is an indirect role of TCR in affecting the function of activating 53-6.7 mAb in augmenting binding. We firstly tested whether the enhanced binding caused by activating 53-6.7 mAb is TCR dependent. After blocking the TCR-pMHC interaction using an anti-TCR mAb, it was

found that the activating 53-6.7 mAb failed to enhance the binding no matter the WT MHC was complexed with agonist OVA or null VSV (Fig. 6.4 A and B). Pretreatment with anti-TCR mAb did not alter the level of the CD8 on the T cell surface (data not shown).The data showed the importance of TCR in regulating the enhanced binding induced by the activating 53-6.7 mAb. The data also indicated that the OTI TCR must recognize its restricted H-2Kb MHC in order to accomplish the recognition of antigen. This was actually similar with the scenario of the T cell positive selection: The TCR must recognize self-restricted MHC in order to complete its development program (2).

Secondly, we used H-2D^b pMHCs to further test whether the enhanced binding induced by 53-6.7 mAb is TCR dependent. Because the OTI TCR is H-2K^b restricted, it can not recognize the H-2D^b pMHC. However, the D^b MHC keeps the CD8 binding site. According to previous study (38), the binding affinity of D^b pMHC to CD8 is much lower than that of K^b, so we coated D^b pMHC with very high site density (>1000/μm^2) on the RBC surface to guarantee the micropipette can detect appreciable binding. However, no matter whether the activating 53-6.7 mAb was present or not, we did not find any significant binding difference between OTI CTLs and RBC coated with D^b MHC complexed with P14 or NP34 peptide (Fig. 6.4 C and D).

To completely rule out the potential interference of TCR to the interaction of CD8-MHC, we used a hybridoma (71) which only expresses CD8$\alpha\beta$ but not TCR molecule to further test the role of the activating 53-6-.7 mAb. The expression of CD8 and TCR were also checked by flow cytometry using corresponding anti-CD8 and anti-TCR fluorescence labeled mAbs, and the results confirmed that the hybridoma is CD8 positive and OTI TCR negative (data not shown). Using the RBC coated with H-2K^b

pMHC and the CD8 hybridoma, we firstly confirmed that the binding between MHC and CD8 was specific. The CD8 hybridoma did not bind to a biotinylated RBC (data not shown), and we could easily detect binding when the same batch of biotinylated RBC were coated with H-2K^b pMHC complexed with VSV peptide. Moreover, the binding could be specifically blocked by adding the inhibitory CT-CD8a mAb (Fig. 6.4E, compare the filled bar with open bar). After confirmation of the binding specificity of CD8-MHC interaction on the hybridoma, we tested the role of activating 53-6.7 mAb to the CD8 without the interference of TCR. The results showed that there was no obvious binding difference before and after adding the activating 53-6.7 mAb (compare Fig 6.4F, compare the □ with ○). Interestingly, the CD8-MHC binding affinity on hybridoma was 30 folds higher than that on OTI CTLs, although both shared similar dissociation rates (1.37s^{-1} for hybridoma vs. 1.53s^{-1} for OTI (38)).The reason was not clear, and it could be the difference of surface environment of cells, the glycosylation extent or post-expression decoration of the CD8 molecule. However, the antibody 53-6.7 lost its enhancing function without the presence of TCR on the hybridoma surface.

Taken together, these data clearly suggested that the TCR played a critical role in mediating the binding enhancement induced by activating 53-6.7 mAb. Importantly, the CD8 activation was not an independent event, but accompanied with the TCR involvement. In other words, it indicated that the CD8 and TCR bind to the pMHC synergistically rather than independently at such specific scenario. An important hint was that the activating 53-6.7 mAb not only triggered CD8 activation, but revealed a crosstalk between CD8 and TCR. So, there must be a communication existing between TCR and CD8: molecular signaling.

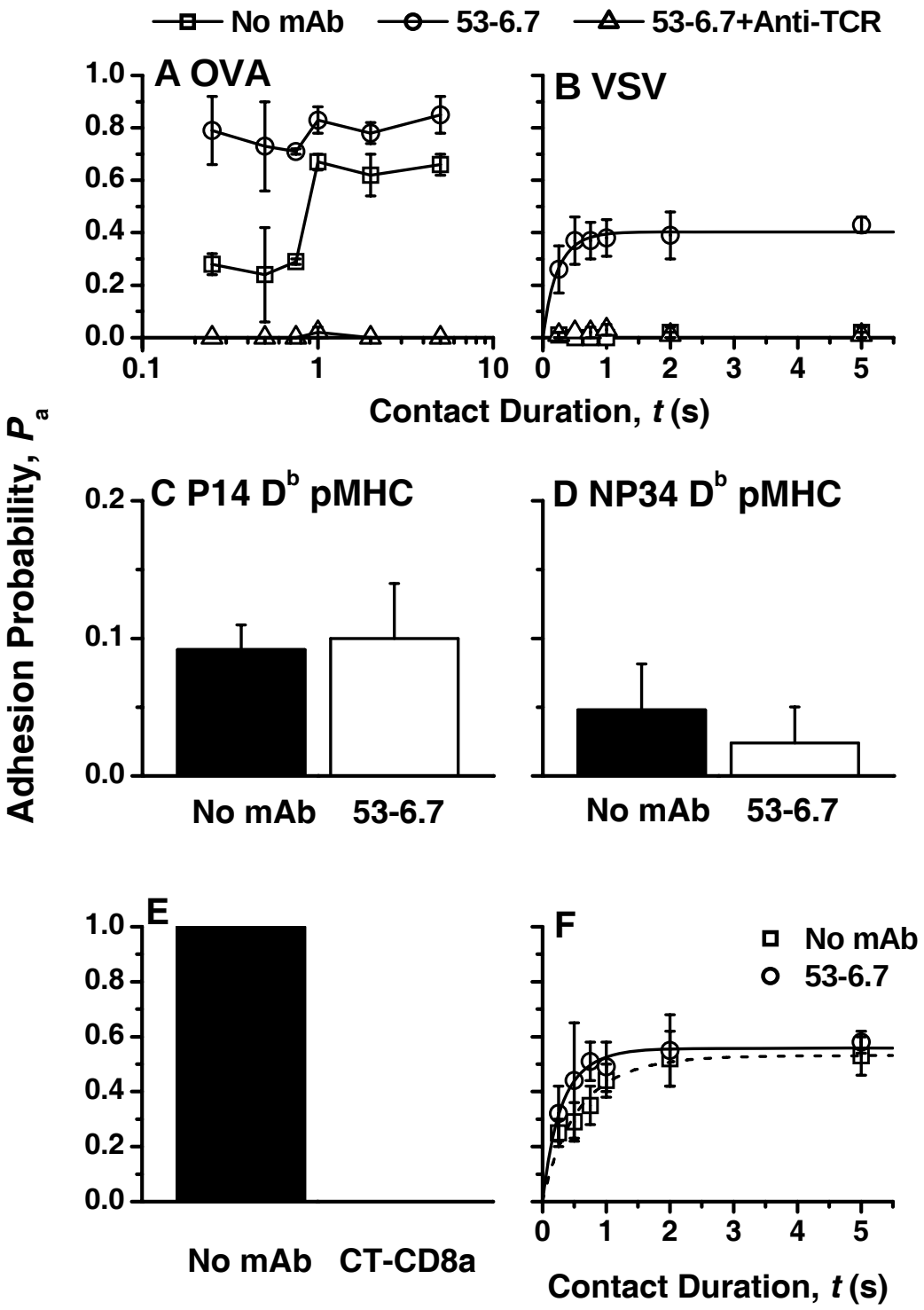
No mAb
53-6.7
53-6.7+Anti-TCR
A OVA
B VSV
Adhesion Probability, P_a
Contact Duration, t (s)
C P14 D^b pMHC
D NP34 D^b pMHC
No mAb
53-6.7
E
No mAb
CT-CD8a
F
No mAb
53-6.7
Contact Duration, t (s)

Figure 6.4 The activating 53-6.7 mAb enhanced binding is TCR dependent. A & B. Plots of adhesion probability (P_a) vs. contact duration (t) measured using OTI CTLs interacting with RBCs coated with WT H-2K^b MHC complexed with agonist OVA (A) or null peptide VSV (B) in the absence (□) or presence of activating 53-6.7 mAb (○) or 53-6.7 mAb and anti-TCR mAb (Δ). **C & D**. The adhesion probability (P_a) at contact duration $t=5s$ measured using OTI CTLs interacting with RBCs coated with WT H-2D^b MHC complexed with P14 (C) or NP34 peptide (D) in the absence (solid bar) or presence of activating 53-6.7 mAb (open bar). **E.** The adhesion probability (P_a) at contact duration $t=5s$ measured using CD8αβ expressing hybridoma interacting with RBCs coated with WT H-2K^b MHC complexed with null peptide VSV in the absence (solid bar) or presence of inhibitory CT-CD8a mAb (open bar, undetectable). **F.** Plots of adhesion probability (P_a) vs. contact duration (t) measured using CD8αβ expressing hybridoma interacting with RBCs coated with WT H-2K^b MHC complexed with null peptide VSV in the absence (□) or presence of activating 53-6.7 mAb (○). Data were presented as mean ± SEM of 2–5 pairs of T cells and RBCs each making 50 contacts to observe the probability of adhesion.

6.2.2.3 The binding enhancement induced by 53-6.7 requires signaling

Co-receptor CD4 or CD8 can physically associate with TCR (137, 138), and co-receptor and TCR association can be induced by antigen ligation or the anti-TCR stimulation (139, 140). Also, the coupling of TCR/CD3 with CD8/Lck via the partition of lipid rafts efficiently triggers the intracellular signaling to activate the T cell. It was reported that the CD8 antibodies can trigger TCR signaling by phosphorylating the LAT and CD3ζ (111). We have observed that the anti-CD8 mAbs could either inhibit or enhance the binding between CTLs and pMHC coated RBCs. Next, it is interesting and important to find out whether there is signaling between TCR and CD8 induced by these anti-CD8 mAbs, and if so, which signaling molecule (s) is (are) involved?

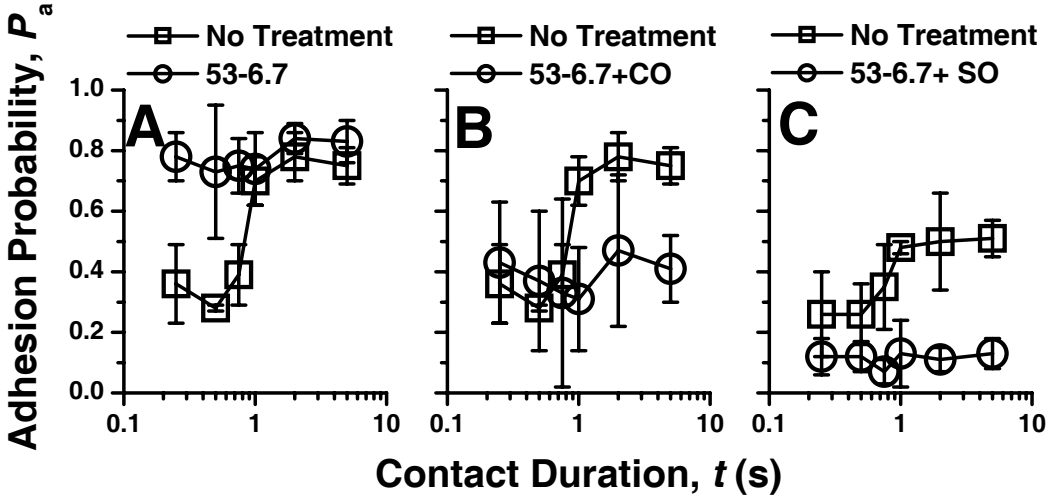

Figure 6.5 Disruption of lipid rafts or inhibition of phosphatases disables the function of activating 53-6.7 mAb in enhancing binding. Plots of adhesion probability (P_a) vs. contact duration (t) measured using OTI CTLs interacting with RBCs coated with WT H-2K^b MHC complexed with agonist OVA peptide. **A**. In the absence (□) or presence of activating 53-6.7 mAb (○). **B**. In the absence (□) or presence of activating 53-6.7 mAb and CO (1U/ml). **C**. In the absence (□) or presence of activating 53-6.7 mAb and SO (2μM). Data (*points*) were presented as mean ± SEM of 2–5 pairs of OTI CTLs and RBCs each making 50 contacts to observe the probability of adhesion.

First of all, we tested whether there is signaling involved. It is well known that the lipid rafts serves as a platform for the molecular signaling at the T cell membrane (34). The TCR signal initiation machinery is pre-assembled and activated in a subset of membrane rafts (132). The integrity of raft is a prerequisite for efficient TCR signal transduction and disrupting lipid rafts will lead to the interruption of the earliest steps of T cell activation (125). Our micropipette binding assay also showed the importance of lipid rafts for the enhanced binding induced by the anit-CD8 activating 53-6.7 mAb. After disrupting the lipid rafts by using CO, not only the enhanced binding induced by

activating 53-6.7 mAb was abolished (Compare Fig. 6.5A ○ with Fig. 6.5B ○), but the CD8-dependent second-step binding was inhibited after one second contact duration (Fig 6.5B, compare ○ with □) .The data suggested that the activating 53-6.7 mAb could trigger signaling within the lipid rafts.

The TCR and CD8 signaling involves many phosphorylation and dephosphorylation steps, such as those of on Lck, ZAP-70 or ITAM of CD3. Here we used SO to inhibit the dephosphorylations of the OTI CTLs. Similar to the effects of CO, the SO efficiently disabled the function of the activating 53-6.7 mAb in enhancing the binding between OTI CTLs and OVA pMHC coated RBCs (Fig. 6.5C, compare □ with ○). The data indicated that the activating 53.6.7 might play its role by signaling through dephosphorylation.

It is known that the cytoplasm tail of CD8 can link with Lck kinase which is critical to the T cell signaling and activation (27, 57, 79, 141, 142). The activities of Lck are regulated via its C-terminal negative regulatory tyrosine (Y394). The unphosphorylated tyrosine site renders Lck in a so-called 'primed' state in normal condition. During TCR-pMHC interactions, Lck is recruited to the complex via its noncovalent association with CD8. Upon ligation or clustering of the CD8, the tyrosine (Y394) is phosphorylated and the Lck is activated. The active Lck is proximally positioned to phosphorylate ITAMs and ζ chains of TCR/CD3 signaling complex (27). Here, we use a phosphor- and site- specific mAb to detect the Y394 autophosphorylation on Lck as a measurement of Lck activation. We tested the Y394 phosphorylation after treating OTI CTLs with either the inhibitory or activating anti-CD8 Fab, which can rule out the potential Lck phosphorylation caused by crosslink of whole anti-CD8 antibodies.

OTI CTLs were incubated with either inhibitory or activating Fab for 30 minutes, fixed in 4% paraformaldehyde, intracellular stained with site specific antibody to pY394, and run flow cytometry to quantify the fluorescence intensity of the staining. The staining was specific (Fig. 6.6A, compare the first bar with other bars), and the Lck activation was significantly increased for the activating 53-6.7 Fab (Fig. 6.6A, third bar), but not for the inhibitory Fab (Fig. 6.6A, fourth bar) if compared with untreated control (Fig. 6.6A, second bar). The data showed that Y394 of Lck becomes autophosphorylated in response to activating mAb 53-6.7.

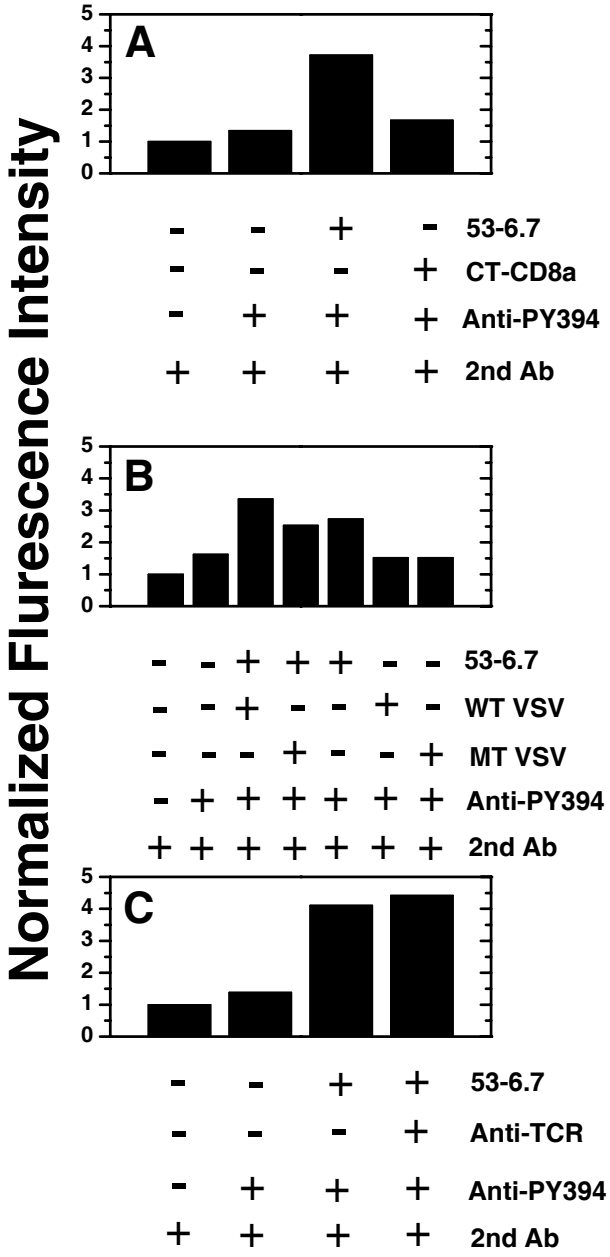

Figure 6.6 Intracellular staining of Lck tyrosine 394 phosphorylation. **A**. OTI CTLs were incubated with or without inhibitory CT-CD8a or activating 53-6.7 Fab; **B**. OTI CTLs were incubated with or without WT VSV or CD8-null VSV tetramer in absence or presence of activating 53-6.7 Fab; **C**. OTI CTLs were incubated with activating 53-6.7 Fab in the absence or presence of anti-TCR. Then all samples were incubated with or without specific anti-Y394 first mAb, and stained with fluorescence labeled second antibody for quantification of the phosphorylation of Y394.

Our data also emphasized the importance of CD8 engagement with pMHC to the phosphorylation of the Y394 on Lck. By using both the WT and CD8-null K^b tetramer complexed with VSV peptide, we investigated the effect of CD8 ligation to the phosphorylation of Y394 on Lck. OTI CTLs were incubated with either WT or CD8-null tetramer in the presence or absence of activating 53-6.7 Fab, after fixation and intracellular staining, the phosphorylation extent of Lck Y394 were quantified. In the presence of activating 53-6.7 Fab, it was clear shown that the WT tetramer which had the CD8 binding site further phosphorylated the Lck Y394 compared to the CD8-null tetramer (Fig. 6.6B, compare the third bar and fourth bar). However, adding additional CD8-null tetramer does not trigger more phosphorylation compared to the activating 53-6.7 Fab alone (Fig. 6.6B, compare the fourth bar and fifth bar). The data also indicated that the CD8 binding to pMHC is critical in generating intracellular signal. Without the presence of activating 53-6.7 Fab, because the VSV tetramer itself can barely bind to the OTI CTLs, the data did not show any significant difference among WT tetramer, CD8-null tetramer and untreated control (Fig. 6.6B, compare the second, sixth and seventh bar). This data suggests that the CD8 participation into the pMHC binding is critical to the intracellular signaling.

It has been observed that the anti-TCR antibody can fully block the enhanced binding triggered by activating 53-6.7 mAb (Fig. 6.4 A and B). Here we also checked whether the anti-TCR mAb could inhibit the Y394 phosphorylation on Lck induced by activating 53-6.7 Fab. OTI CTLs were incubated in cold with activating 53-6.7 Fab and/or anti-TCR antibody, after fixation and intracellular staining, it was found that adding additional anti-TCR did not alter Lck Y394 phosphorylation induced by activating

53-6.7 Fab (Fig. 6.8C, compare the third bar and fourth bar). Our data was consistent a report that the anti-TCR crosslink cannot trigger the Lck autophosphorylation of Y394 (143). Because treatment with anti-TCR mAb did not affected the CD8 expression (data not shown), it was more likely that the TCR was also participate into the binding of MHC induced by the activating 53-6.7 mAb, and the anti-TCR mAb thus physically blocked the binding. Another alternative possibility was that the anti-TCR might deliver another signal to change the TCR and CD8 binding states through other signaling molecule such as LAT. More investigations are needed to clarify the complexity of the data.

The results above, and those of Schott et al. (110) and Wooldridge et al. (111), suggested that the TCRs crosstalk with CD8 in recognition pMHCs. It is well established that cross-linking the TCR by anti-CD3 antibodies can generate an intracellular activation signal. We demonstrated that anti-CD8 mAbs were capable of communicate with the TCR indirectly, generating an intracellular activation signal through Lck phosphorylation. This result was in accordance with a previous study that showed that some anti-CD8 antibodies can trigger CTL activation as efficiently as anti-CD3 antibodies (144).

6.2.3 The enhancing or inhibitory role of anti-CD8 antibodies is reversely correlated with the peptide potency in activating T cells

After indentified the inhibitory and enhancing roles of these two anti-CD8 mAbs, we continuously characterized their function for four types of pMHCs with distinct potencies in activating T cells. In the absence of mAbs, as shown in fig. 6.7 and fig. 6.8, for all four pMHCs with appropriate pMHC site densities on the RBC surface, the specific bindings were measurable and peptide dependent. In describing order, the

agonist OVA, the weak agonist G4, the antagonist E1 and null VSV ligand bound strong, well, weak and negligible to the OTI CTLs respectively (Fig. 6.1 and 6.2, dotted lines). The results were correlated well with their biological potencies in activating the T cells (44, 71)

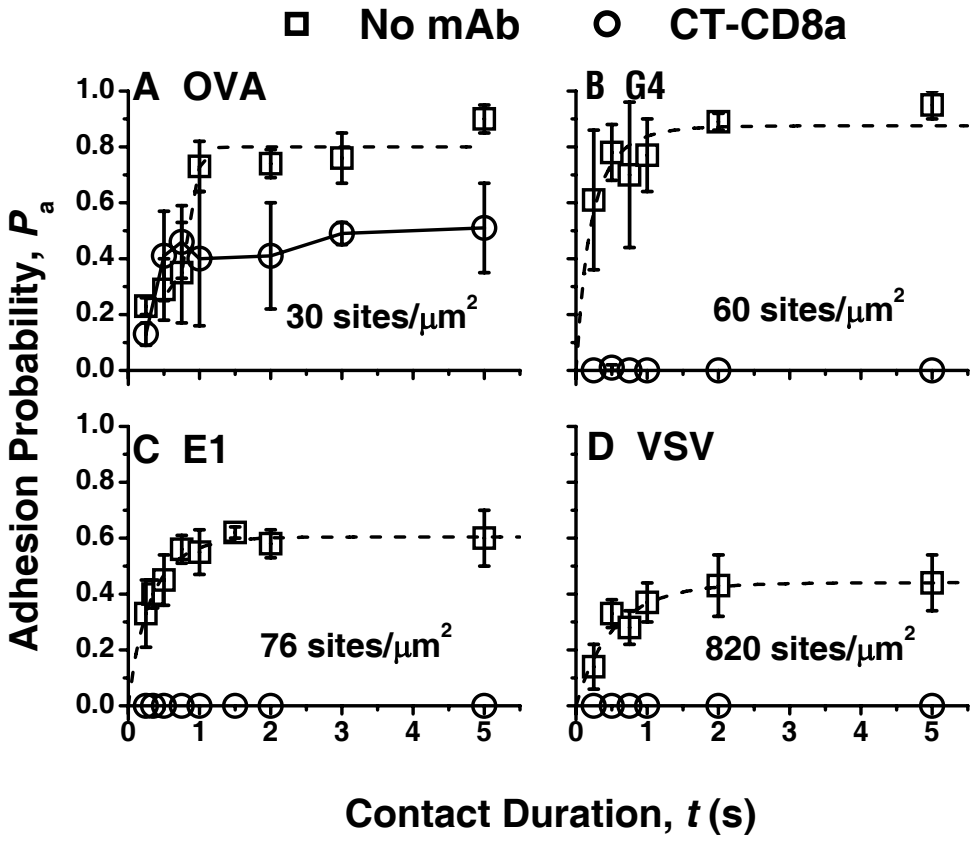

Figure 6.7 The effect of inhibitory anti-CD8 mAb (CT-CD8a) on the binding between pMHC coated RBC and OTI CTL. Plots of adhesion probability (P_a) vs. contact duration (t) measured using OTI CTLs interacting with RBCs coated with WT H-2K^b MHC complexed with agonist OVA (A), weak agonist G4 (B), antagonist E1 (C) and null peptide VSV (D) in the absence (□, linked by dotted line) or presence of inhibitory mAb (CT-CD8a) against CD8 (○, linked by solid line). The site density of each pMHC coated on the RBC surface is labeled on corresponding panel. Data (*points*) were presented as mean ± SEM (or single value) of 1–5 pairs of T cells and RBCs each making 50 contacts to observe the probability of adhesion.

We firstly tested the role of inhibitory CT-CD8a mAb. In the presence of CT-CD8a mAb, the binding between OTI CTLs and pMHC coated RBCs was significantly reduced for all four pMHCs (Fig. 6.7, compare □ with ○). The binding probability of agonist OVA dropped to ~half, while the bindings of weak agonist G4, antagonist E1 and null VSV were totally abolished (I also tested antagonist R4 and null K4 and obtained similar results). These data showed that the inhibitory mAb CT-CD8a significantly inhibited the binding of pMHC coated RBCs to OTI CTLs. Importantly, the inhibition was reversely correlated with the peptide potencies in activating the CTLs.

We then tested the role of the activating 53-6.7 mAb. In sharp contrast, in the presence of this activating mAb, the binding between OTI CTLs and pMHC coated RBCs was significantly enhanced for all pMHCs (Fig. 6.8, compare □ with ○). Also, the extent of increase was peptide dependent, and the rank was OVA<G4<E1<VSV. So, these data suggested that the enhancement caused by the activating 53-6.7 mAb was reversely correlated with the potencies of peptide in activating the CTLs.

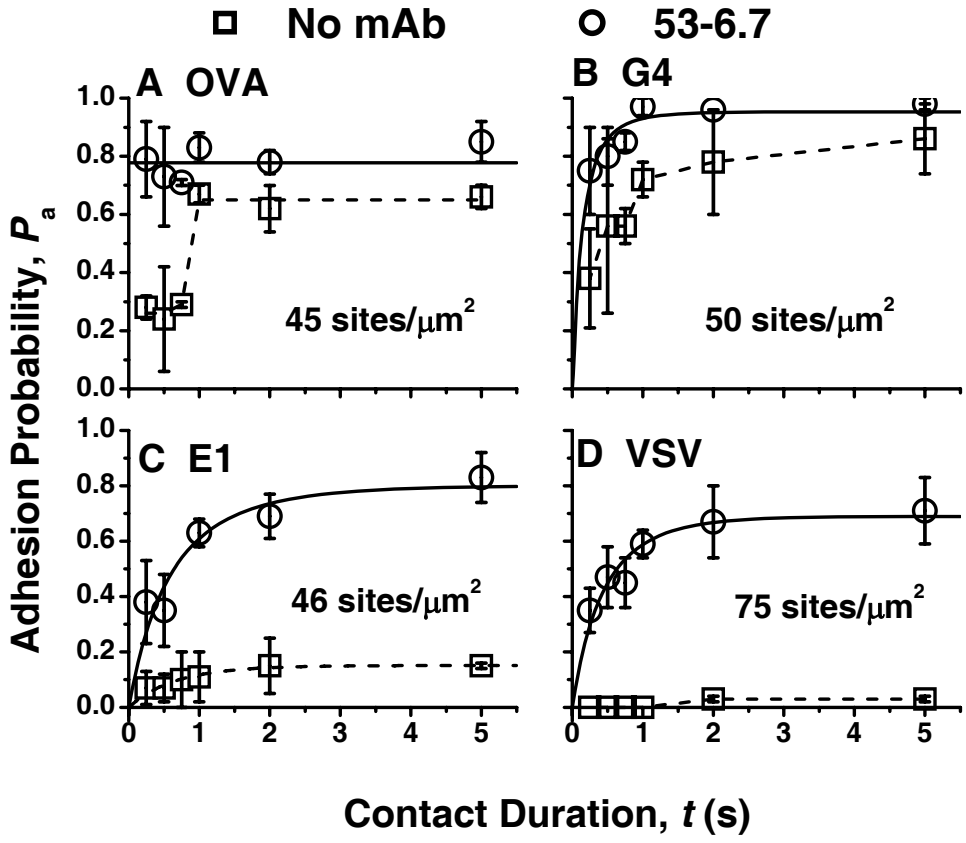

Figure 6.8 The effect of activating anti-CD8 mAb (53-6.7) on the binding between pMHC coated RBC and OTI CTL. Plots of adhesion probability (P_a) vs. contact duration (t) measured using OTI CTLs interacting with RBCs coated with WT H-2K^b MHC complexed with agonist OVA (A), weak agonist G4 (B), antagonist E1 (C) and null peptide VSV (D) in the absence (□, linked by dotted line) or presence of activating mAb (53-6.7) against CD8 (○, linked by solid line). The site density of each pMHC coated on the RBC surface is labeled on corresponding panel. Data (*points*) were presented as mean ± SEM (or single value) of 1–5 pairs of T cells and RBCs each making 50 contacts to observe the probability of adhesion.

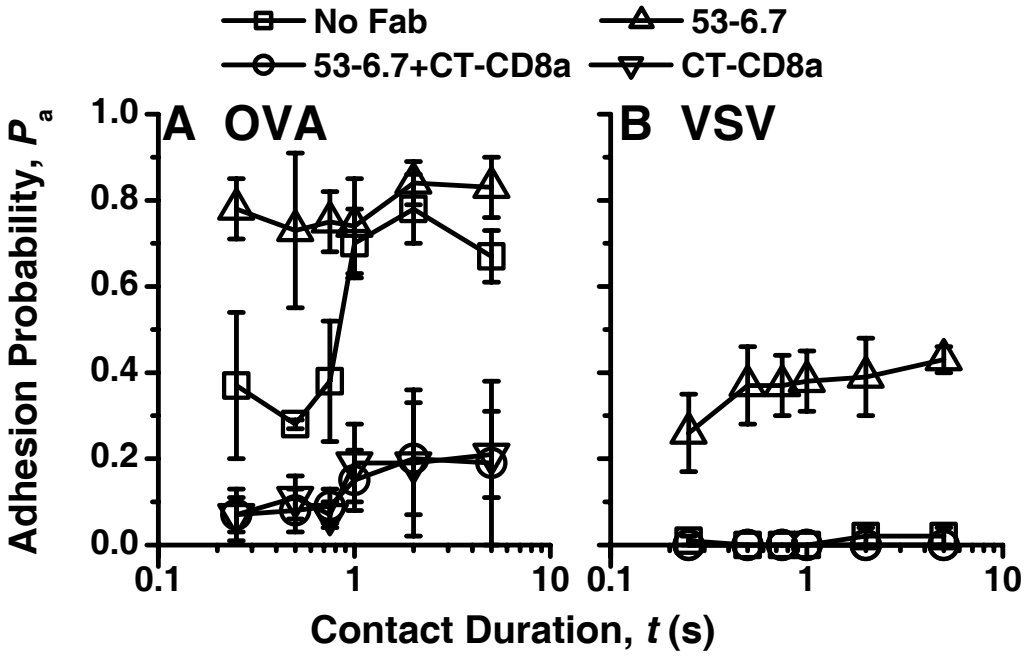

Figure 6.9 The function of inhibitory and activating Fabs. Plots of adhesion probability (P_a) vs. contact duration (t) measured using OTI CTLs interacting with RBCs coated with WT H-2K^b MHC complexed with agonist OVA (A) and null peptide VSV (B) in the absence (□) or presence of inhibitory CT-CD8a Fab (∇), activating 53-6.7 Fab (Δ), or both (○).Data (*points*) were presented as mean ± SEM (or single value) of 1–5 pairs of T cells and RBCs each making 50 contacts to observe the probability of adhesion.

To exclude the possibility of binding change caused by the crosslink of CD8, we used the Fabs of CT-CD8a and 53-6.7 mAbs and obtained similar results as those of whole mAbs (Fig.6.9). The data demonstrated that the enhancement or the inhibition of binding was not due to the crosslink of CD8 molecules. Actually, the effects of anti-CD8 antibodies in the pMHC binding to T cell have been identified and published, mainly using 3D tetramer staining measurement (18, 108, 111, 120). Our micropipette data correlated well with these published results. The excellent correlation not only validated our experimental method but also bridges the 2D and 3D measurements. Furthermore,

our micropipette adhesion assay provides a new aspect of the anti-CD8 mAbs in 2D condition with better sensitivity (in single molecular level) and higher temporal resolution (in second level).

6.3 Discussion

This study was designed to study the crosstalk between CD8 and TCR in binding of pMHC. Recent studies have shown that some anti-CD8 antibodies can either inhibit or enhance the binding of multimeric pMHC complexes to T cells (18, 81, 82, 108, 109, 111, 123, 145). As to the interpretation of the molecular mechanism, however, there are typically two different opinions. The Jameson group proposed that the inhibitory antibodies act to occlude MHC binding sites while the activating antibodies apply their effects by stabilizing higher affinity states of CD8 (18, 82, 123). They interpreted that blockade or enhancement of multimer binding induced by CD8 antibodies implied a direct participation of CD8 into the binding. In contrast, Sewell group augured that anti-CD8 antibodies exert their effects on T cell activation and pMHC binding rather than directly influencing CD8-MHC interaction, but changing the ability of the TCR to engage the multimer in an indirect way, and that CD8-MHC interactions per se were not required for multimer binding (108, 111, 145, 146). By taking the advantage of these anti-CD8 mAbs, we have therefore examined the role of the pMHC-CD8 interaction and studied the crosstalk between TCR and CD8 in binding of pMHC using a 2D micropipette assay, which is a more physiological relevant measurement compared with the 3D multimer staining. We also used a CD8-null pMHC chimera that abrogates CD8 binding site and a

hybridoma only expressing CD8 to facilitate our study of crosstalk between TCR and CD8.

According to our study, several key findings are that: 1) TCR and CD8 can affect each other in binding of pMHCs; 2) CD8 directly mediates the binding of pMHC in the presence of anti-CD8 antibodies; 3) The inhibitory or enhancing effects induced by anti-CD8 antibodies are not simply due to CD8 blocking or activation, they require the crosstalk between CD8 and TCR, 4) There is signaling between TCR and CD8 in the lipid rafts through phosphorylation and dephosphorylation. Anti-CD8 mAb 53-6.7 can generate a signal that leads to Lck Y394 phosphorylation, which is a sign of Lck activation; 5) Although CD8 plays a critical role in assisting the TCR-pMHC interaction, TCR can bind to pMHC in the absence of CD8. The CD8 requirement is peptide dependent. The inhibitory or enhancing role of anti-CD8 antibodies is reversely correlated with the peptide potency in activating T cells.

The central theme of this study is to dissect the crosstalk between TCR and CD8. Because our micropipette assay was design to measure the binding, we studied the crosstalk between TCR and CD8 from the view of either the inhibition or the enhancement of binding. We first checked the crosstalk from the inhibition of binding. In the chapter 5, we have indentified the two-step binding for agonist pMHC. Here we found that blocking the TCR-pMHC interaction could abolish CD8 mediated second-step binding. This observation was expected. Because we have known the CD8 mediated second-step binding was triggered by the first-step TCR-pMHC interaction, once the TCR binding was blocked, the CD8 activation no longer existed. The data demonstrated that the TCR engagement can affect the CD8-pMHC interaction. Meanwhile, we tested

whether the antibody binding to CD8 can indirectly affect the TCR-pMHC interaction. The results showed it was the case. Previous SPR measurements have demonstrated that the TCR binds to weak ligand G4 with moderate affinity (10 μM) (71). Our micropipette adhesion assay also demonstrated that the TCR can bind to the CD8-null MHC complexed with G4 peptide (Fig. 6.2, □). However, after adding the inhibitory CT-CD8a mAb, the TCR binding to the G4 CD8-null pMHC was abolished (Fig. 6.2, ○). Consistently, this inhibitory CT-CD8a mAb could completely block the binding of WT MHC complexed with weaker agonist G4 and antagonist E1 (Fig. 6.7B and C). One possibility is that the steric hindrance caused by the CT-CD8a mAb might physically block the TCR binding. However, we observed same blocking effects using Fab of CT-CD8a (data not shown). More important, the inhibitory CT-CD8a mAb only partially blocked the binding of agonist OVA pMHC (Fig. 6.7A), if there were any steric hindrance on TCR, it should block all pMHC binding, not just weak ligands. The data suggested that the anti-CD8 CT-CD8a antibody can have an indirect role on the TCR.

We then studied the crosstalk from the view of enhancement of binding. In the chapter 5, we have demonstrated that the TCR-pMHC interaction could activate CD8 to a higher binding state and then mediate a second-step binding. Meanwhile, the data showed the activation of CD8 requires the signaling between TCR and CD8. This was actually our initial motivation in charactering the crosstalk between TCR and CD8. We also identified that an activating 53-6.7 mAb can activate the CD8. In this chapter, our data demonstrated that the CD8 directly mediated the enhancement of binding induced by 53-6.7 mAb, because the binding of CD8-null pMHC chimera was not affected by the activating 53-6.7 mAb for both the agonist and null pMHCs. Consistently, the direct

participation of CD8 into pMHC binding has been demonstrated by Holman et al. by using CD8+ or CD8- T cells and CD8-null pMHC mutant (18). The antibody epitope mapping also indicated that the CD8 directly plays a role in mediating the binding change caused anti-CD8 antibodies (123). We then tested whether the 53-6.7 mAb triggered enhancement was TCR dependent, and we designed three sets of independent experiments to test this hypothesis. Firstly, it was found that blocking TCR-pMHC interaction using anti-TCR could completely disable the enhancing function of activating 53-6.7 mAb. Because this anti-TCR Vα2 mAb did not affect the CD8 expression (data not shown) and it did not sterically prevent the CD8-MHC binding (38), the data indicated the presence of TCR was necessary for the binding enhancement induced by activating 53-6.7 mAb. Secondly, the activating 53-6.7 mAb no longer could enhance binding when a D^b pMHC was used for OTI CTLs. Although the OTI TCR could not recognize D^b pMHC, however, the CD8 expressed on the OTI CTLs could still bind to the D^b MHC (38). If the activating 53-6.7 mAb played its role by simply maintaining a higher binding state of CD8 independent of TCR, it should bind to D^b MHC better due to the CD8 activation. Finally, the 53-6.7 mAb could not function to enhance binding if CD8 expressing hybridoma was used, which did not express TCR. The data again suggested the CD8 activation induced by 53-6.7 mAb is TCR dependent.

Taken together, by collecting data from both the inhibition and enhancement of binding, we demonstrated that the TCR and CD8 can affect each other in binding of pMHC. In other words, the TCR and CD8 have crosstalk in the antigen recognition process.

Since we indentified the crosstalk using binding assays, we further explored the signaling between TCR and CD8. It has been reported that the co-receptor CD8 can physically associate with TCR (137, 138). The association of CD8 and TCR can be induced by pMHC recognition or the anti-TCR stimulation (139, 140). Schott et al. confirmed that CD8 is associated with the TCR independently of the CD8 binding to pMHC (110). The Zamoyska group has shown that both the anti-CD8 and anti-TCR antibodies can induce the cocapping of CD8 and TCR (25). Yachi et al. observed ligand binding induced TCR-CD8 interaction using FRET technique (71). These observations suggested that the TCR and CD8 can form stable associations on the T cell surface. Also, the CD8 interaction with TCR/CD3 promotes its association with lipid rafts. Engagement of these TCR/CD3-CD8/Lck adducted by pMHC induces activation of Lck in rafts, which in turn phosphorylates CD3 and initiates T cell activation (79). The association of TCR, CD8 and signaling kinase on lipid rafts provide a great opportunity for TCR-CD8 communication. Our results further supported this possibility by showing that the disruption of the lipid rafts could abolish the enhancement of binding induced by 53-6.7 mAb. Disruption of lipid rafts could break the linkage or association of TCR and CD8, thereby physically preventing the communication between TCR and CD8. The data suggested there is signaling within the lipid rafts caused by anti-CD8 mAb. Also, inhibition the dephosphorylation of CTLs by adding SO efficiently blocked the enhancement of binding induced by 53-6.7 mAb. The importance of coreceptor in Y394 phosphorylation of Lck has been reported by Shaw group in a CD4 T cell system (143). Here, our intracellular staining data also demonstrated that the activating 53-6.7 mAb but not the inhibitory CT-CD8a mAb could trigger the Lck activation by phosphorylating the

Y394 in a CD8 T cell system. The data also demonstrated the important role of CD8 engagement onto pMHC in signaling. In the absence of the activating 53-6.7 Fab, both the WT and CD8-null tetramer complexed with VSV peptide could barely bind to OTI CTLs and the result was that we could not detect any increase of Lck phosphorylation after tetramer staining. However, in the presence of activating 53-6.7 Fab, the WT tetramer stained CTLs displayed a higher level of Lck phosphorylation than that of CD8-null tetramer due to the enhancement of CD8 binding.

Interestingly, our data indicated that the CD8 plays a critical role in pMHC interaction and the CD8 requirement is peptide dependent. The enhancing or inhibitory role of anti-CD8 antibodies is reversely correlated with the peptide potency in activating T cells. Although it was reported that the high affinity TCR-pMHC can bypass the aid of CD8 to activate the T cells (147) and Wooldridge et al. suggested that the CD8 is not critical for the pMHC tetramer staining (108), our data emphasized an important role of CD8 in the pMHC binding to T cell, which has been previously reported in many publications (12, 71, 80-82, 84, 109, 142). Our data indicated that the CD8 substantially enhances the binding efficiency, more important, the CD8 requirement is inversely correlated to the potency of peptide in activating the T cell. Similar conclusion has been reported by Sewell group using tetramer staining although their data lacking of good time resolution and detection sensitivity (47).

Actually, using the anti-CD8 antibodies, the Jameson group has identified the important role of CD8 in direct participation into the pMHC binding, while the Swell group stressed an indirect effect on TCR by signaling. The possible contradiction could either come from the distinct T cell systems or different anti-CD8 antibodies they used.

More importantly, both of them were too focusing on one specific either TCR or CD8 molecule, but neglecting the teamwork of them. The TCR and CD8 are physically associated and can actively communicate during antigen recognition, so each of them does not behave as a single molecule. Our study clearly indicated that both TCR and CD8 are important for the antigen recognition. The anti-CD8 antibodies are not only invaluable tools for determining which molecules are present on the surface of a given cell, but can serve as a tool to reveal the crosstalk between two adjacent molecules: TCR and CD8 in our case.

CHAPTER 7

STUDY THE DIVERSITY OF PEPTIDES AFFECTING THE ANTIGEN RECOGNITION

7.2 Introduction

During T cell development process, positive and negative selection ensures generation of a repertoire of self-MHC-restricted and self-peptide-tolerant T cells. A T cell is required to recognize self-pMHCs in order to survive in the positive selection. Meanwhile, this T cell cannot interact with self-pMHCs too well to trigger negative selection to eliminate itself. So, the T cell must recognize the self pMHCs with appropriate affinity to satisfy these two requirements. Meanwhile, a subset of altered peptide ligands (APLs) that inhibit T cell responses in the presence of the original stimulatory epitope are called antagonists. How the antagonist inhibits the T cell activation is matter of debate and the mechanism of TCR antagonism is not entirely clear (148, 149). It was found that some of the self pMHCs can also act as antagonist and trigger positive selection (149).

The self peptide may play a role in the antigen recognition process. At physiology condition, the concentration of antigenic peptide is usually very low compared with self peptides, so how to guarantee TCR can precisely and efficiently recognize such a small amount of antigenic peptides become an important issue to address. One interesting question is naturally raised: whether those confluent self-peptides play a role to help TCR recognize the low dose antigenic peptides?

Actually, the role of self pMHCs in the activation of T cell is in debate. Most of the literatures have reported that antigen-specific T cell responses can be enhanced by some nonstimulatory/self pMHC complexes (6, 88, 150). While some argued that the self pMHCs play a negligible role in TCR triggering (5, 151). Evan less papers addressed the recognition of antigenic pMHC in the presence of antagonists. In this chapter, we systemically tested the roles of nonstimulatory and antagonist peptides in the TCR recognition of antigenic pMHC. The relevant regulatory signaling was specifically investigated as well.

7.2 Results

7.2.1 Binding characteristics of different pMHCs.

The OTI TCR recognizes H-2K^b complexed with antigenic OVA. The agonist, antagonist and null peptide have been well defined for OTI TCR in which the sole variable is the peptide complexed to MHC molecule. The binding kinetics and affinities of these pMHCs with TCR have been well characterized using SPR measurements (44, 71). Also, in the physiology condition, some self peptides have no significant role while a few structurally homologous self-peptides can promote thymocyte positive selection (149). In the previous chapters, we have shown that the co-receptor CD8 plays a critical role in affecting the binding between OTI CTL and pMHC coated RBC. Here we systematically characterized the 2D binding curve for agonist OVA (Fig. 7.1A), antagonists E1 (Fig. 7.1B) and R4 (Fig. 7.1C), self peptides Mapk8 (Fig. 7.1C) and Stat3 (Fig. 7.1D), and null peptide VSV (Fig. 7.1E) in the presence of both TCR-pMHC and CD8-pMHC interactions.

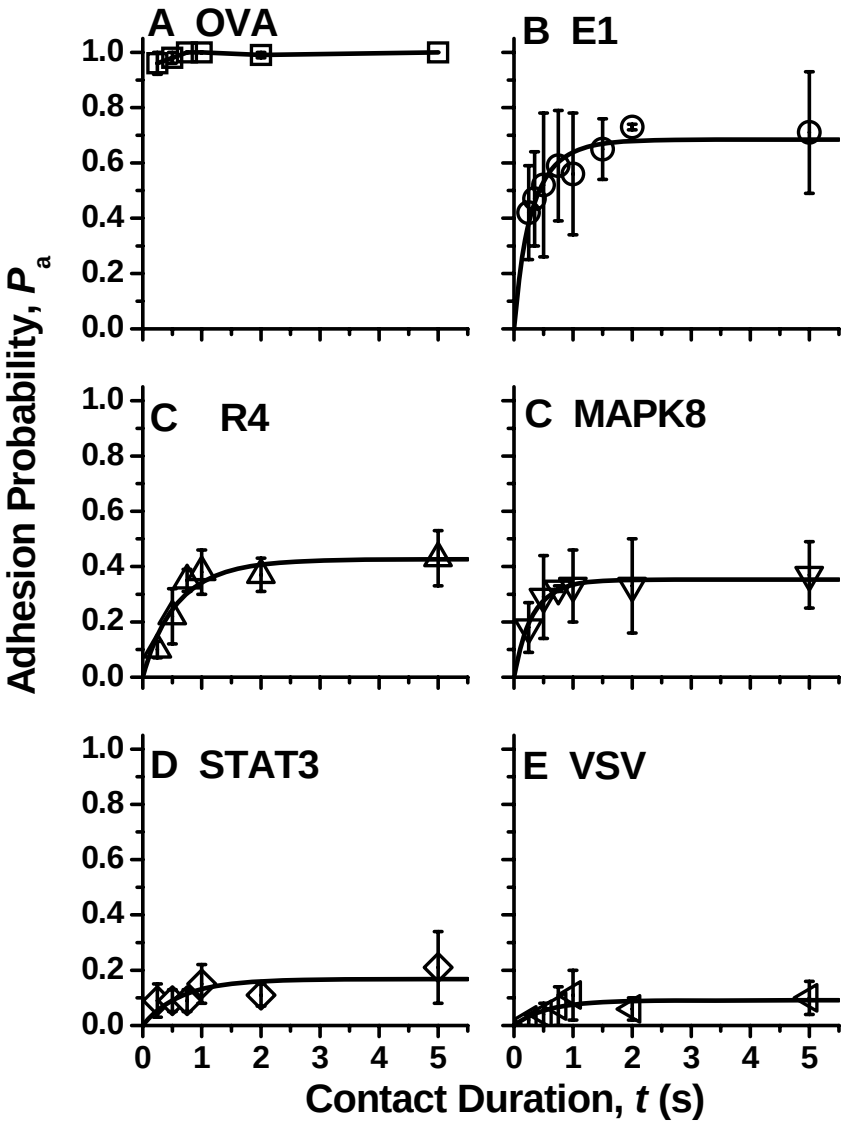

Figure 7.1 The 2D binding curves of different pMHCs. Plots of adhesion probability vs. contact duration measured using OTI CTLs interacting with RBCs coated with H-2K^b MHC complexed with agonist peptide OVA (A), antagonist peptides E1 (B) and R4 (C), self peptides Mapk3 (C) and Stat3 (D), and null peptide VSV (E). Data (*points*) were presented as mean ± SEM of 2–6 pairs of T cells and RBCs each making 50 contacts to observe the frequency of adhesion.

Table 7.1 The binding affinity/avidity of pMHCs to OTI CTLs

Peptide	$m_r A_c K_a^0 (\times 10^{-3}\ \mu m^4)$
OVA	82.98
E1	12.2
R4	3.02
Mapk8	1.97
Stat3	0.92
VSV	0.71

The data clearly showed that the binding spans ~0%−100% in adhesion probability depending on which peptide the MHC complexed. The sequence would be OVA>E1>R4>Mapk8>Stat3≥VSV if we ranked their affinity/avidity in binding of OTI CLTs. Because the adhesion probability of OVA pMHC has been pushed to ~100% while that of VSV pMHC could be barely detected with the same coating site density on RBC surface, in order to show the binding difference for each pMHC more accurately, we measured the binding of each pMHC at its suitable coating site density, and the binding affinity/avidities of the bindings were listed in table 7.1 for better comparison. Clearly, the agonist OVA binds best, the antagonists E1 and R4, and a positive selection self Mapk8 are in the mild, while a nonstimulatory self Stat3 and a null VSV have the lowest binding affinities/avidities. Our 2D affinity/avidity measurements correlated well with the outcome of peptide selection. It has been demonstrated that the OVA triggers the OTI T cell negative selection, while the E1, R4 and Mapk8 trigger the positive selection, and the Stat3 and VSV shows no function (44, 149). Our 2D measurements agreed well with the previous 3D SPR results (44). These data suggested that binding affinity/avidities plays a critical role in the peptide function in thymocyte selection and support the notion that some low efficacy ligands mediate positive selection.

7.2.2 Nonstimulatory peptides enhance antigen recognition

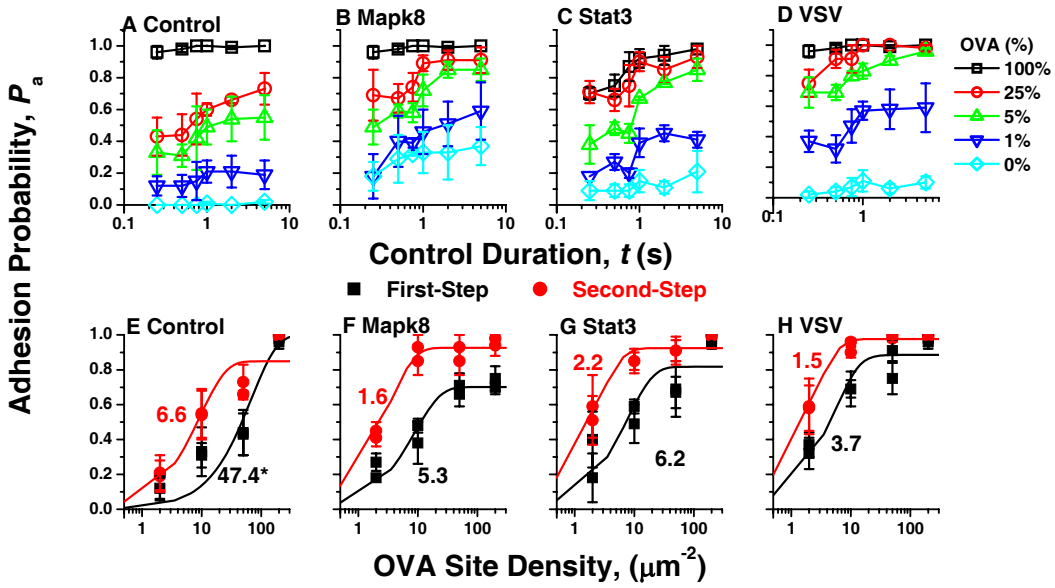

Figure 7.2 The nonstimulatory peptides enhance the antigen recognition of OTI CTLs. A-D: Plots of adhesion probability vs. contact duration measured using OTI CTLs interacting with RBCs coated with mixtures of pMHCs with different ratios (indicated by colors). **E-H**: Dose curves of first- (black) and second- (red) step binding vs. the site density of H-2K^b MHC-I complexed with OVA for each mixture. The MHC-I H-2K^b complexed with OVA was mixed with MHC-II I-A^b complexed with MOG (A&E), MHC-I H-2K^b complexed with Mapk8 (B&F), MHC-I H-2K^b complexed with Stat3 (C&G), or MHC-I H-2K^b complexed with VSV (D&H). **A-D**: The total MHC density on the RBC surface was kept as a constant ~200/μm^2. The percentages of H-2K^b MHC-I complexed with OVA in the mixture were labeled. Data (*points*) were presented as mean ± SEM of 2–6 pairs of T cells and RBCs each making 50 contacts to observe the probability of adhesion. **E-H**: The site densities of MHC-I H-2K^b complexed with OVA were calculated from the percentages for each pMHC mixture. The adhesion probabilities at 0.25s and 0.5s, and those of at 2s and 5s were assigned as first- and second- step binding probabilities for each corresponding OVA site density respectively. The dose curves were fitted using equation 3.4 and the values of EC_{50} of first- (black) and second- (red) step bindings were labeled for each mixture (E-H). (*) The P_{max} was pre-set as 1.

It has been reported that some nonstimulatory/self peptides can significantly enhance the TCR recognition of antigenic peptide (6, 88, 150). While some other publications had different opinions (5, 151). Here we used OTI CTL and H-2K^b pMHC plus different peptides to test whether that the nonstimulatory peptides play a role in affecting the TCR recognition efficiency.

In order to systematically study the function of nonstimulatory peptides, we used a biotinylated MHC-I H-2K^b or MHC-II I-A^b monomer which has been engineered a biotin tail at its C-terminal. Different peptides including agonist OVA, nonstimulatory peptides VSV and Stat3, or irrelevant peptide MOG have been pre-loaded to their corresponding MHC-I or MHC-II molecule to form pMHCs respectively and the loading efficiencies were greater than 95% for all peptides. The OTI TCR and CD8 do not recognize and bind to class II pMHC, so the MOG pMHC was served as a control. To test the function of nonstimulatory peptides, the OVA pMHC was mixed with MOG, VSV or Stat3 pMHC respectively and then coated to a biotinylated RBC surface by the streptavidin through a specific and irreversible streptavidin-biotin interaction. We titrated the OVA pMHC and varied the amount of control MOG, positive selection Mapk8, and nonstimulatory Stat3 or VSV pMHC so that the total amount of pMHCs on RBC coated with OVA pMHC plus control, positive selection or nonstimulatory pMHC were kept as a constant, but the percentages of OVA pMHC were precisely controlled (Fig. 7.2). We then plotted the adhesion probability as the function of contact duration *t* for the entire ratios of OVA pMHC spanning from 0% to 100%. Clearly, in the presence of positive selection or nonstimulatory pMHC, the adhesion probabilities were significant increased at each percentage for positive selection and nonstimulatory peptides compared with the

control (Fig. 7.2, compare the "control" with "Mapk3", "State3" or "VSV"). The enhancement was also revealed by the values of EC_{50} (Fig. 7.2, E-H), which is the concentration of an agonist produces 50% of the maximum possible response. By comparison, the EC_{50} value of control (E) was much higher than those of the positive selection (F) and nonstimulatory peptides (G-H) for both the first- and second- binding steps. Interestingly, although both nonstimulatory peptides enhanced the binding, the increased magnitude for each peptide was slightly different, i.e., the VSV aided better than Stat3. For the positive selection peptide Mapk8, although it indeed enhanced the binding probabilities, however, considering its high background binding, its role needs further studies.

7.2.3 Nonstimulatory peptide greatly enhances the antigen detection sensitivity

To better study the enhancive capability of nonstimulatory peptide and test the sensitivity of antigen recognition of T cell, we further titrated down the total pMHC site densities and chose a series of agonist percentages using the combination of agonist OVA and nonstimulatory peptide VSV. The data firstly verified that the nonstimulatory VSV pMHC can significantly enhance the ability of CTL in recognizing the antigenic OVA pMHC. Secondly, in the presence of VSV pMHC, the OTI CTL could efficiently detect a single antigenic OVA pMHC. As shown in figure 7.3, even the OVA pMHC percentage was titred down to 0.1% (Fig. 7.3A, total pMHC density 165 μm^{-2}) or 1% (Fig. 7.3B, total pMHC density 70 μm^{-2}) for RBC coated with lower pMHC site densities, we still could effectively detect the binding, although their standard error were relatively larger than those of higher percentages of OVA pMHC (Fig. 7.3 A and B). Considering the ~3μm^2 contact area between RBC and OTI CTL in our micropipette experiments, there

was only 0.5 (Fig. 7.3A) or 2 (Fig. 7.3B) OVA antigens inside of the contact area after a simple calculation. Thus the large standard errors of the adhesion probability were due to the extremely low site density of OVA pMHC, i.e., there was either none or a single OVA antigen inside of the contact area, therefore caused large standard errors in adhesion probabilities.

Clearly, the bindings between OTI CTLs and RBCs coated with mixture of OVA and VSV pMHCs also showed two-step binding (Fig. 7.3A and B). To better reveal the augment function of the nonstimulatory peptides on adhesion probability, we plotted the adhesion probability as the function of OVA site density for both steps (Fig. 7.3C and D). Therefore, any difference in the dose-response curves between the control (OVA alone) and the combination (mixture of OVA and nonstimulatory VSV pMHCs) was caused by the presence of the nonstimulatory VSV pMHC. Clearly, the adhesion probabilities were greatly enhanced in the presence of nonstimulatory peptide (compare Fig. 7.3C with 7.3 D). In the presence of excess nonstimulatory VSV peptide, only a very small amount of agonist peptides were needed to induce detectable adhesions and the TCR could easily detect a single antigenic OVA pMHC (Fig. 7.3C). It was much more sensitive than OVA pMHC alone (Fig. 7.3D). As exemplified by the EC_{50} values, which were 0.6 and 1.9, or 14.6 and 48.6 for the first- and second-step of bindings in the presence or absence of nonstimulatory peptide VSV respectively. By comparison, there was ~25-fold difference in EC_{50} values for both binding steps. In the absence of nonstimulatory peptides, much more antigenic pMHCs were required for recognition occurring.

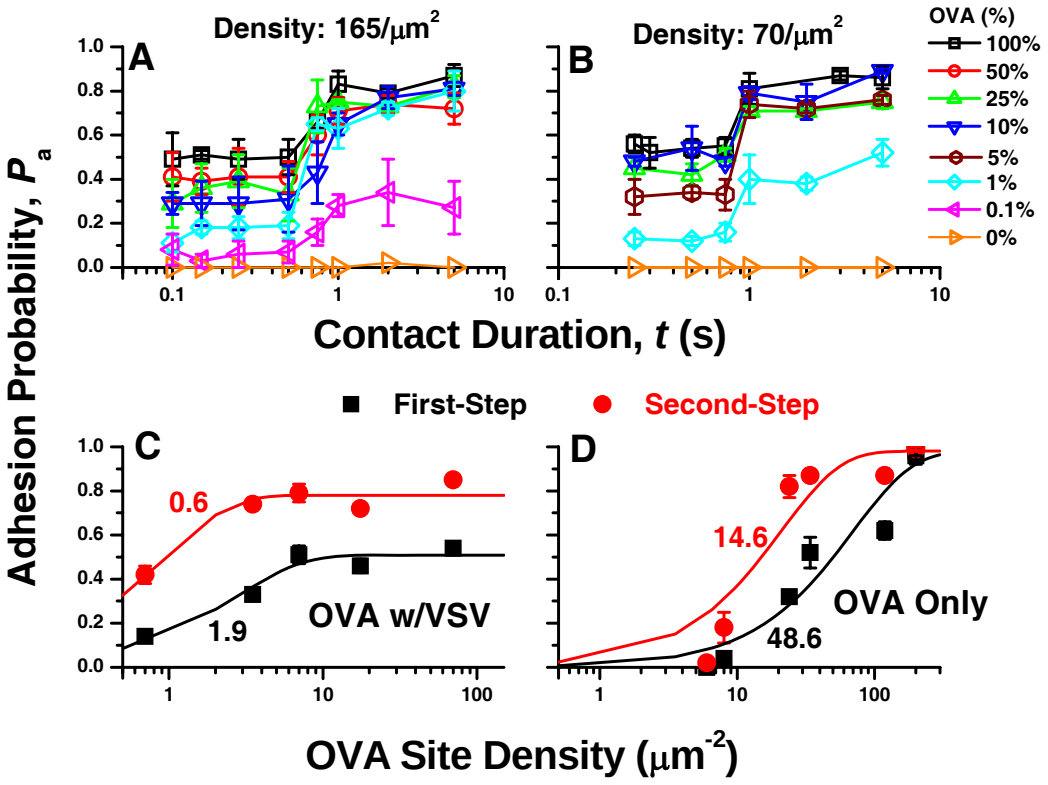

Figure 7.3 The presence of nonstimulatory peptide increases the antigen detection sensitivity of OTI CTLs. **A-B**: Plots of adhesion probability vs. contact duration measured using OTI CTLs interacting with RBCs coated with mixture of OVA and VSV pMHCs. The total MHC density on the RBC surface was ~165/μm^2 (A) or ~70/μm^2 (B). The percentages of OVA pMHC in the mixture were labeled. **C-D**: The dose curves of adhesion probability vs. OVA pMHC site density in the presence (C) or absence (D) of nonstimulatory VSV pMHC. The black and the red curves represented the first-step and second-step binding probabilities respectively. Data (*points*) were presented as mean ± SEM of 2–6 pairs of T cells and RBCs each making 50 contacts to observe the frequency of adhesion. The dose curves were fitted using equation 3.4 and the values of EC_{50} of first- (black) and second- (red) step bindings were labeled (C-D).

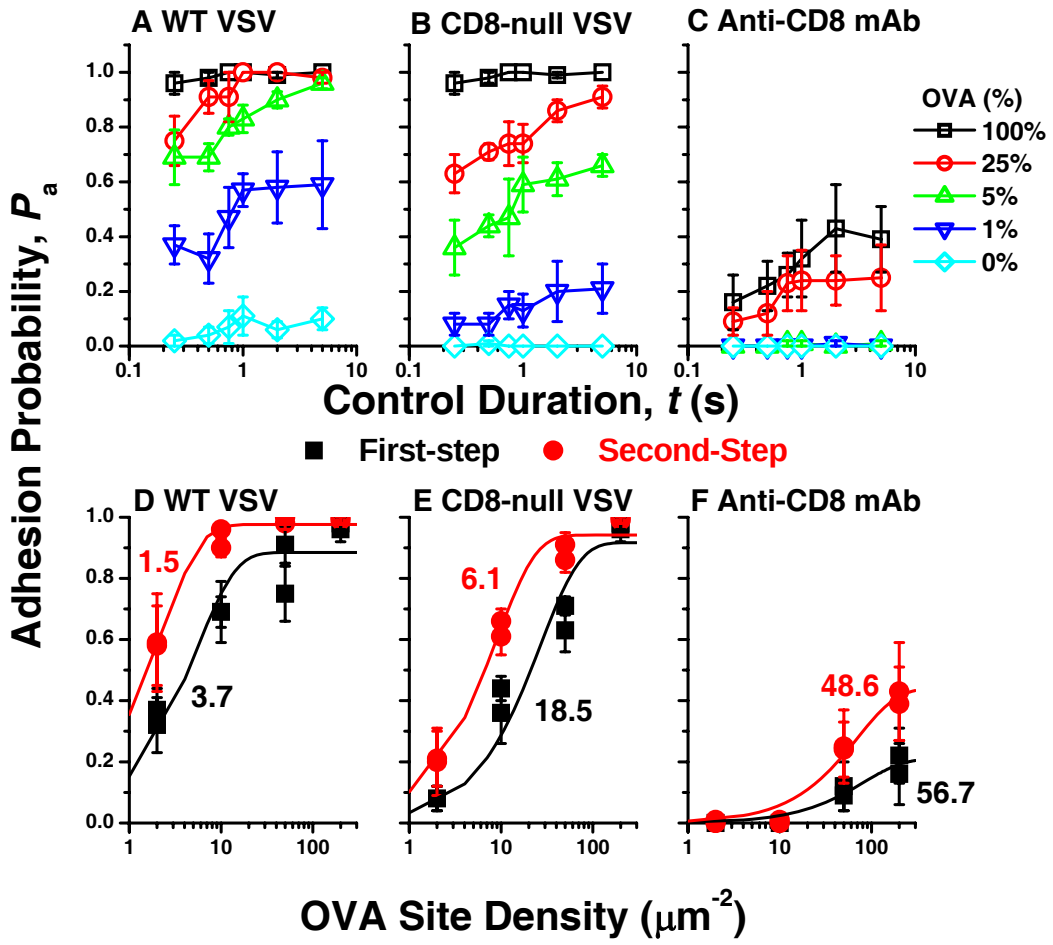

Figure 7.4 The role of CD8 in the enhancement of recognition. A-C: Plots of adhesion probability vs. contact duration measured using OTI CTLs interacting with RBCs coated with mixture of pMHCs with different ratios (indicated by colors). **D-F**: Dose curves of first- (black) and second- (red) step binding vs. site density of OVA pMHC for each mixture. The WT OVA pMHC was mixed with WT VSV pMHC in the absence (A&D) or presence of anti-CD8 mAb (C&F), or with CD8-null VSV pMHC (B&E). The total pMHC density on the RBC surface was ~200/μm^2. The percentages of OVA pMHC in the mixture were labeled. Data (*points*) were presented as mean ± SEM of 2–6 pairs of T cells and RBCs each making 50 contacts to observe the frequency of adhesion. The adhesion probabilities at 0.25s and 0.5s, and those of at 2s and 5s were assigned as first- and second- step binding probabilities for each corresponding OVA site density respectively. The dose curves were fitted using equation 3.4 and the values of EC_{50} of first- (black) and second- (red) step bindings were labeled (D-F).

7.2.4 Recognition enhancement is due to CD8 binding

With respect to the co-receptor CD8, many papers have shown that it plays a critical role in helping the CTL recognition of antigenic pMHC. In the previous chapters, we have shown that the CD8 mediates the second-step binding of agonist pMHC binding of OTI CTLs. Accordingly we found that blocking CD8 binding to MHC had a deleterious effect to the enhancement of binding caused by the nonstimulatory pMHCs. To discern the role of CD8 more precisely, we used a CD8-null H-2K^b chimera which abrogates the CD8-MHC interaction. Meanwhile, an anti-CD8 blocking mAb (clone CT-CD8a) was used to study the overall function of CD8 for the combination of antigenic and nonstimulatory peptides.

The RBCs were coated with the mixture of either OVA WT pMHC and VSV WT pMHC (Fig. 7.4A) or OVA WT pMHC and VSV CD8-null pMHC (Fig. 7.4B), and then we compared their bindings between these two RBCs to the OTI CTLs. It was found that the adhesion probabilities were significantly impaired if the VSV WT pMHC was replaced by the VSV CD8-null pMHC (compare Fig. 7.4A with 7.4B). We then blocked all the CD8-MHC interaction for the mixture of OVA WT pMHC and VSV WT pMHCs using an anti-CD8 blocking mAb (CT-CD8), the binding were further reduced for all the OVA pMHC percentages. Especially for those low percentages ($\leq$5%), the bindings were almost completely abolished in the presence of anti-CD8 blocking mAb (Fig. 7.4C).I also performed similar experiments using Stat3 nonstimulatory peptide, and obtained very similar results (data not shown). The importance of CD8 was also revealed by the dose curves and EC_{50} values (Fig. 7.4 D-F). Without the CD8-MHC binding for the CD8-null pMHC complexed with VSV nonstimulatory peptide, the EC_{50} values became

comparable to those of control (compare the EC_{50} between Fig. 7.2E and Fig. 7.4E), especially for those of second-step binding. In other words, the enhancement of recognition was due to CD8 binding to the nonstimulatory pMHC. The EC_{50} value also indicated a critical role of CD8 in helping the TCR recognition, after blocking all the MHC-CD8 interaction, the recognition was further suppressed.

7.2.5 The inhibitory role of antagonists in antigen recognition.

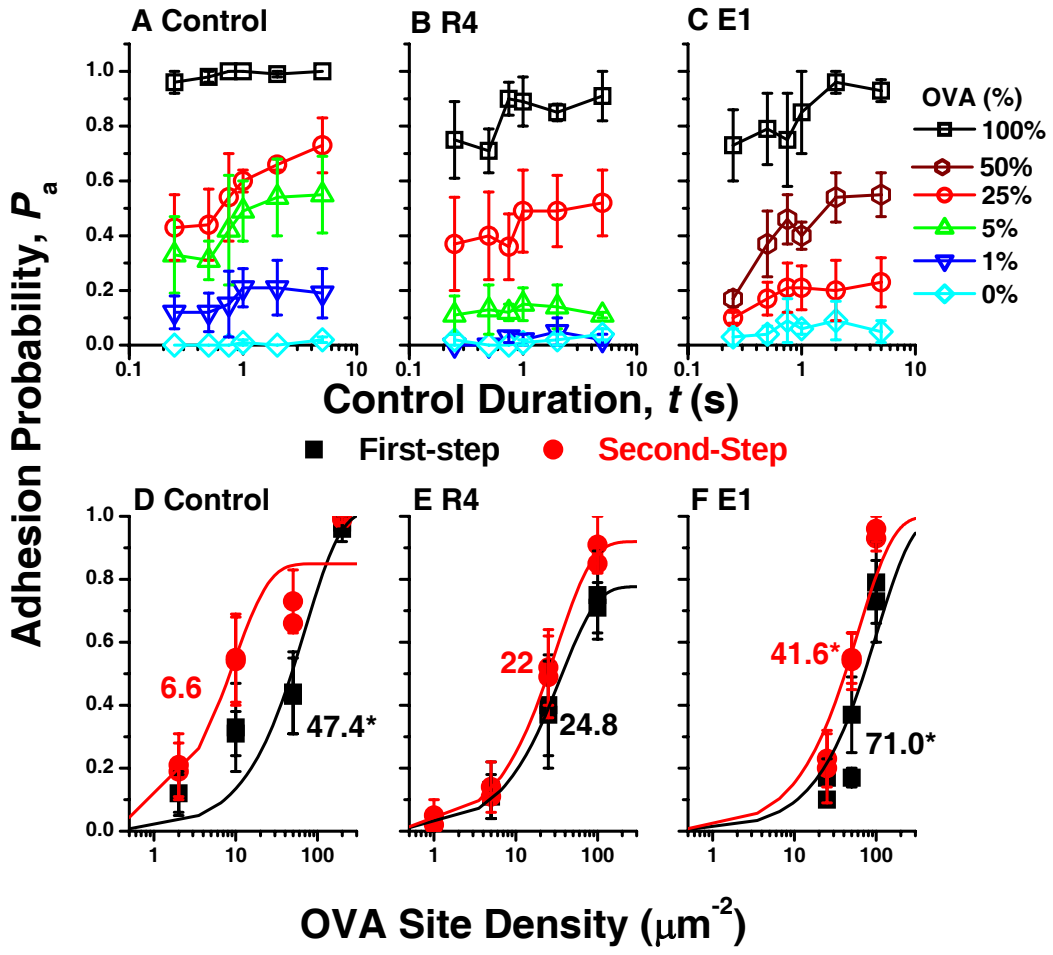

Figure 7.5 The inhibitory role of antagonist. A-C: Plots of adhesion probability vs. contact duration measured using OTI CTLs interacting with RBCs coated with mixtures of pMHCs with different ratios

(indicated by colors). **D-F**: Dose curves of first- (black) and second- (red) step binding vs. site density of H-2K^b MHC complexed with OVA for each mixture. The MHC-I H-2K^b complexed with OVA was mixed with MHC-II I-A^b complexed with MOG (A&D) , MHC-I H-2K^b complexed with R4 (B&E) or MHC-I H-2K^b complexed with E1 (C&F). The total MHC densities on the RBC surface were kept as either ~200/μm^2 for (A), or ~100/μm^2 for (B) and (C). The percentages of MHC-I H-2K^b complexed with OVA in the mixture were labeled. Data (*points*) were presented as mean ± SEM of 2–6 pairs of T cells and RBCs each making 50 contacts to observe the frequency of adhesion**.** The adhesion probabilities at 0.25s and 0.5s, and those of at 2s and 5s were assigned as first- and second- step binding probabilities for each corresponding OVA site density respectively. The dose curves were fitted using equation 3.4 and the values of EC_{50} of first- (black) and second- (red) step bindings were labeled (D-F). (*) The P_{max} was pre-set as 1.

According to the definition, an antagonist is a type of ligand that does not provoke a biological response itself upon binding to a receptor, but blocks or dampens agonist-mediated responses. For T cells, the signaling induced by agonist ligands can be severely impaired if antagonists are present. Although antagonists were discovered more than a decade ago, a molecular understanding of the inhibitory function remains elusive (148, 152-155). It was found that the antagonists can trigger positive selection (70), and some self peptides can serve as antagonists (149, 156). Here we used the combination of agonist with antagonist to study the biological function as well as molecular mechanism of antagonism.

Similar to previous experiments, the agonist (OVA) and antagonist (E1 or R4) pMHCs were mixed with different ratios while kept the total amount of pMHC on the RBC surface as a constant. In a sharp contrast with the enhancing role of nonstimulatory pMHCs (Fig. 7.2), the antagonist pMHCs significantly inhibited the binding probability of agonists (compare Fig. 7.2 and Fig 7.5). Especially in the high percentages of

antagonists (Fig. 7.5B OVA percentage≤5% or 7.5C OVA percentage≤25%), the binding of these mixed pMHCs are almost equivalent to those of antagonists alone (Fig. 7.5B and C). By comparison, although the EC_{50} values between control and antagonist (compare Fig. 7.5D with 7.5E or F) had comparable values for the first-step binding, they had more than 3-fold or 6-fold difference between control and R4 or E1 in the second-step binding respectively. The data indicated the second-step binding is critical for the antagonism occurring.

Also, we found that the inhibitory efficiency of E1 was more potent than that of R4 (compare the Fig. 7.5B with 7.5C, 25% OVA "○" for R4 and E1). The potency of inhibition could also be revealed by the EC50 values (compare Fig. 7.5 E with F). This result was consistent with the biological function analysis which showed that E1 is a better antagonist than R4 (70). Although many publications have shown the inhibitory role of antagonists by signaling or functional analysis (148, 152-154), our data was the first time to show that the antagonists actually play its role at the initial recognition stage.

7.2.6 The antagonist gradually shuts down the binding

Since we have indentified that the antagonist can inhibit the agonist binding, to find out how would be important. Another important finding was that the antagonist shuts down the binding between CTLs and RBC coated with mixtures of antagonist and agonist gradually. We have plotted the running frequency vs. the test cycle (Fig. 7.6) to check how the adhesion changes with the increase of test cycles.

Firstly, we tested how the percentages of antagonist affect the running frequency of the binding (Fig. 7.6A). If the RBC was purely coated with agonist OVA (Fig. 7.6A, "□") or antagonist E1 (Fig. 7.6A, "▽"), the running frequency reached equilibrium after

several test cycles and became a stable value. In sharp contrast, when the agonist OVA was mixed with antagonist E1, the running frequency was decreasing with the increase of test cycles (Fig. 7.6A, "○" and "Δ"). More importantly, the higher the percentage of the antagonist, the more decrease of the running frequency of binding (Fig. 7.6A, compare the "○" with "Δ"). We also tested another antagonist R4 and obtained similar results (data not shown).

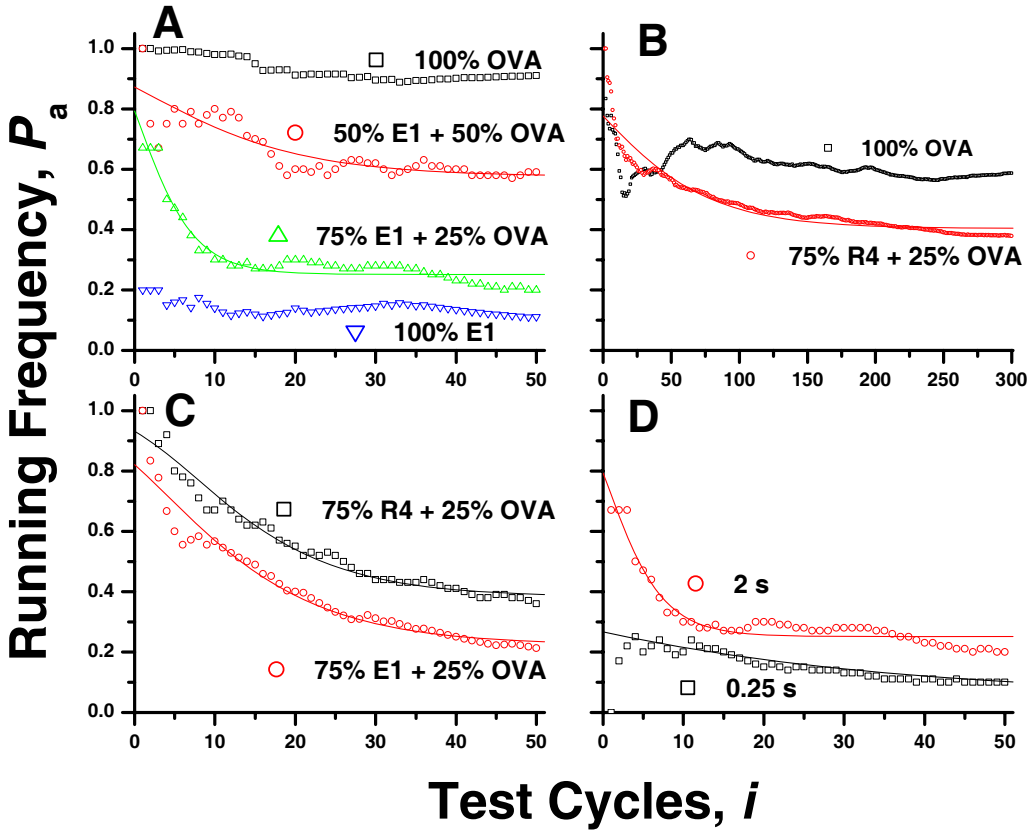

Figure 7.6 The presence of antagonist shuts down the binding of agonist. Plots of adhesion probability vs. test cycle measured using OTI CTLs interacting with RBCs coated with pMHCs E1, R4 and OVA or their mixtures. The inhibition dependence on: (A) Percentages of antagonist. The contact duration was 2s for all pMHC mixtures of OVA and E1. (B) Test cycles. The contact duration was 1s for OVA pMHC and mixture of OVA and R4 pMHCs. (C) Antagonists. The contact duration was 0.75s for the pMHC mixtures

of OVA and R4 or E1, (D) Contact durations. The percentage of E1 was 75% of the pMHC mixture for both contact durations. Data (*points*) were presented as mean ± SEM of 2–4 pairs of T cells and RBCs each making 50 or 300 contacts to observe the running frequency of adhesion. The SEMs were not presented due to the clarity of the figures. Equation 3.6 was fit (*curves*) to the mixture data sets to estimate and evaluate the inhibitory ability. The data were fitted using equation 3.6.

In order to further verify the reality of the decline of adhesion frequency caused by the presence of antagonist, we increased the test cycles from 50 to 300. Similarly, the decrease of running frequency was successfully repeated for the mixture of agonist OVA and antagonist R4 (Fig. 7.5B, "○"), while the running frequency of pure OVA agonist did not significantly change with the increase of test cycles (Fig. 7.5B, "□"). Another antagonist E1 was also tested and similar results were obtained (data not shown).

In third, we tested the potency of different antagonists in inhibiting the adhesion of agonist. Both E1 and R4 were mixed with OVA and coated to the RBC with same percentage 75% (Fig. 7.6C). We then observed the decreasing speed and magnitude of binding frequency for each antagonist. Also, equation 3.6 was used to evaluate the decline of the running frequency. Clearly, the presence of E1 made the running frequency drop quicker and larger than that of R4 (Fig. 7.6C, compare "○" with "□"). The evaluating parameters obtained from model fitting using equation 3.6 also supported the observation.

Finally, we tested how the contact duration affected the inhibitory function of antagonists. Using same batch of RBC coated with 75% E1 and 25% OVA, the running frequencies at 0.25 second and 2 second contact duration were plotted against the test cycles (Fig. 7.6D).Obviously, the longer the contact duration was, the better the

inhibitory effects would be (Fig. 7.6D, compare "○" with "□").The evaluating parameters obtained from the model fitting using equation 3.6 also supported the observation. We also tested another antagonist R4 and obtained similar results (data not shown).

7.2.7 The TCR and CD8 bind synergistically to same agonist pMHC.

Previously, the data have shown that the WT MHC complexed with OVA peptide displayed a two-step binding (Fig. 7.7A, "□") while the CD8-null MHC chimera complexed with OVA peptide showed a one-step binding (Fig. 7.7A, "○"). At same site density (~30/μm^2), the WT MHC complexed with VSV peptide only showed a background binding (Fig. 7.7A, "Δ") due to that the OTI TCR does not recognize VSV pMHC and the low binding affinity of resting state MHC-CD8 interaction. By using the binding characteristics of these pMHCs, we tested how the TCR and CD8 bind to pMHC.

There are typically two ways for TCR and CD8 binding to pMHC. The first is that both the TCR and CD8 bind synergistically to same pMHC, while the second is that the TCR and CD8 bind to different pMHCs separately. Since the WT OVA pMHC posses both the CD8 and TCR binding sites and shows a two-step binding, we therefore mixed the CD8-null OVA pMHC with WT VSV pMHC to test how the TCR and CD8 bind to pMHC(s), i.e., the CD8-null OVA pMHC only provides the TCR binding site while the WT VSV pMHC solely supplies the CD8 binding site. We have known that the resting state MHC-CD8 binding for VSV pMHC is undetectable at such a low site density (Fig. 7.5A "Δ" and 7.5B "◊"). If the combination also showed a two-step binding, and then it means that the TCR and CD8 bind to different pMHCs, otherwise the TCR and CD8 bind to same pMHC. As shown in figure 7.5B, no matter how we varied the ratios of CD8-null OVA MHC in the combination, the bindings only showed a one-step binding, so the data

suggested that the TCR and CD8 must bind synergistically to same pMHC in order to generate two-step binding and maximize the signal in activating the OTI CTLs. We also analyzed the EC_{50} value for the combination of CD8-null OVA pMHC, we found it increased ~ 7-fold compared to that of first-step binding of control which was lacking of the nonstimulatory VSV pMHC (compare Fig. 7.2E with Fig. 7.7C).

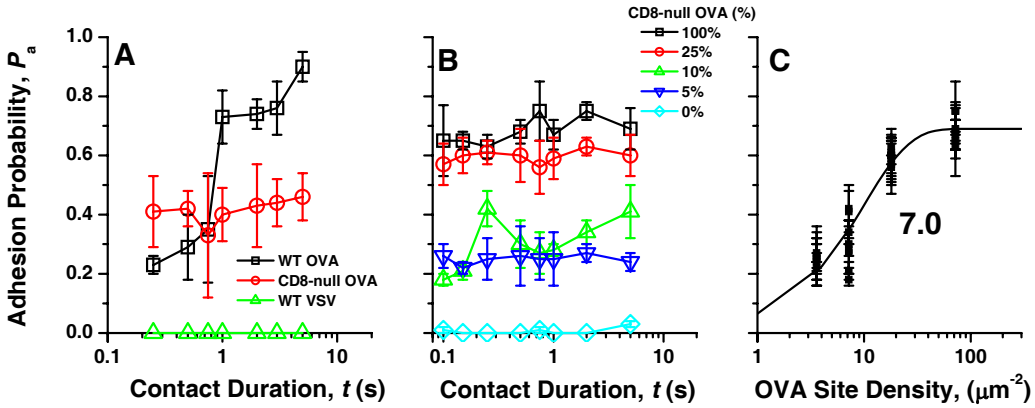

Figure 7.7 The TCR and CD8 bind synergistically to a same agonist pMHC. A. Plots of adhesion probability (P_a) vs. contact duration (t) measured using OTI CTLs interacting with RBCs coated with purely WT MHC complexed with OVA (□) or VSV peptide (Δ), or CD8-null MHC chimera complexed with OVA peptide (○). **B.** Plots of adhesion probability vs. contact duration measured using OTI CTLs interacting with RBCs coated with mixture of CD8-null MHC complexed with OVA peptide and WT MHC complexed with VSV peptide. The percentages of CD8-null MHC complexed with OVA were labeled. Data (*points*) were presented as mean ± SEM (or single value) of 2–5 pairs of T cells and RBCs each making 50 contacts to observe the probability of adhesion. **C.** Dose curves of one step binding vs. the site density of CD8-null H-$2K^b$ MHC complexed with OVA. The adhesion probabilities at all contact durations were assigned as one-step binding probabilities for each corresponding OVA site density. The dose curves were fitted using equation 3.4 and the values of EC_{50} was labeled.

7.3 Discussion

The TCR must recognize a few antigenic ligands in a vast excess of self-derived endogenous peptides. Recently, whether and how the endogenous peptides play a role in T cell recognition became a hot topic. Most of the publications supported the idea that some self nonstimulatory peptides can significantly enhance the T cell ability to recognize antigenic peptides for both CD4 and CD8 T cells (6, 88, 150). However, some other publications argued that the self peptides have a negligible role in the T cell recognition (5, 151). Most of these studies were using biological assays such as peptide accumulation, calcium flux, IL-2 production or CD69 expression to study the role of these self nonstimulatory peptides (5, 6, 88, 150, 151, 157), and the assessments were based on the functional outcomes of the T cells. However, few of them actually addressed how the T cell obtains the initial recognition signal from the molecular interaction among TCR, CD8 and pMHC in the presence of nonstimulatory peptide. Some of them indeed measured the interaction between CD8-TCR using FRET technique or the conjugation assays between T cells and (real or artificial) APCs (88, 150). However, those measurements were in the time scale of minute and were lacking of good temporal resolution and detection sensitivity. Here, by using a micropipette adhesion assay with second temporal resolution and single molecule detection sensitivity, we systematically studied the role of nonstimulatory peptide and the initial detection signal obtained by T cell in the antigen recognition.

Our results supported that the presence of nonstimulatory peptides can significantly enhance the T cell recognition capability. We found that the simultaneous

presence of nonstimulatory (Including exogenous and endogenous peptides) and agonist pMHC on the artificial APC (RBC in this study) enhanced naive OTI CTLs' responses. The simultaneous presence of nonstimulatory peptides greatly increased the binding between OTI CTLs and artificial APC, and the enhancement became more pronounced at the extremely low site density of agonist. With the participation of nonstimulatory peptides, the TCR could easily detect a single agonist pMHC at the time scale of 0.25 second contact duration. Thus, our micropipette data demonstrated that the presence of nonstimulatory peptides can enhance the T cell recognition efficiency.

Our results stressed the importance of CD8 in the enhancement of recognition. Blocking the CD8 binding to pMHC by mutation or antibody had a destructive effect on the T cell recognition. More specifically, blocking the CD8 binding of nonstimulatory pMHCs disabled their enhancing function (Fig. 7.4B), blocking the CD8 binding of agonist pMHCs abolished the second–step binding and decreased the stimulation signal (Fig. 7.7B), and of course blocking all the binding of CD8-MHC interaction deleterious diminished the T cell recognition (Fig. 7.4C). Our data were generally consistent with the published works (6, 150). The only difference was that Krogsgaard et al. found that the blocking of CD4 binding to the endogenous pMHC did not affect the enhancement. The reason might be the interaction of CD4-MHC is much weaker than that of the CD8-MHC. Actually, Yachi et al. found that the presence of nonstimulatory peptides greatly increased the CD8-TCR/CD3 interaction, especially between their cytoplasmic domains (88). The calcium flux measurements and conjugation experiments between T cell and artificial APC also demonstrated that the CD8 mediates the cooperation between noncognate and cognate pMHC in augmenting T cell response (150).

In a sharp contrast with the enhancing role of the nonstimulatory peptides, we found that antagonists can actually inhibit the T cell recognition. However, this finding is not surprising, a lot of previous functional studies have shown that the presence of antagonists can inhibit the T cell responses to the agonist peptide, and that's how the antagonist is named (148, 152-155). Meanwhile, the antagonists can trigger positive selection (70) and some self peptides with positive selection function can serve as antagonists (149, 156). As to the possibility whether there exist some self peptides that can inhibit the T cell recognition, still need more investigation.

Yachi et al. have demonstrated the dependence of nonstimulatory peptide-induced enhancement of antigen recognition on the differentiation status of the T cell. The enhancement is most pronounced in thymocytes, moderate in naive T cells, and mild in effector T cells (157). Then let us go back to the two publications that did not support the enhancing role of self peptides in T cell antigen recognition (5, 151). We noticed that Ma et al. actually used T cell blast, which might .affect the sensitivities of their measurements. For the paper of Sporri et al.(151), they did not load any specific exogenous nonstimulatory peptide to their APC, i.e., they used the self peptides generated by the APC itself. It has been reported some self peptides can serve as antagonists (149, 156), thereby neutralizing the enhancing role of the nonstimulatory peptides. Another important reason could be the timeline and sensitivities of their measurements. Both of them used biological functional assays to study the role of self peptides, which are usually measuring the down-stream outcomes of the T cells. After TCR recognizing the agonist pMHCs, the initial signal needs to be amplified through a series of signaling pathways to trigger the downstream functions. The difference between a weak and a

strong signal could be easily compensated by a non-linear amplification process which usually occurs in many biological systems. So the timeline and sensitivity of the measurements are two critical factors in determining their final results. The different time courses of nonstimulatory peptide contribution to antigen recognition also underline the developmental differences in the importance of nonstimulatory peptides in antigen recognition.

An obvious puzzle is that the T cell binds much poor to the RBC coated with the mixture of the antagonist and the agonist pMHCs than that of the nonstimulatory and the agonist pMHCs. According to the kinetic measurements, the antagonist (E1 and R4) pMHCs actually bind the T cell much better than the nonstimulatory (Stat3 and VSV) pMHCs (Fig. 7.1). Those data indicated that the agonist and antagonist compete, while the agonist and nonstimulatory peptide collaborate on the binding of the T cell. For the antagonist pMHCs, they can bind to both TCR and CD8, and their TCR-pMHC contribution is greater than or at least equivalent to that of CD8-pMHC (44, 78, 98). Although the affinity of TCR-pMHC interaction of antagonist is comparatively lower than that of agonist, the avidity can be compensated by increasing its site density, and thereby gradually excluding the agonist binding. It is exactly the case in our experiments as we gradually increased the percentages of antagonist in the mixture of agonist and antagonist. Because the agonist and antagonist compete for the same binding site: the TCR. With the increase of the antagonist and the decrease of the agonist on the local site densities, more and more TCR bind to the antagonist and then the readout binding frequency is more and more close to the pure antagonist (Fig. 7.2C R4 percentage≥5% or 7.2D E1 percentage≥25%). If antagonist is actually competing with agonist, then with the

increase of the antagonist affinity in binding to the TCR, the inhibitory role will be more potent. Our data have actually demonstrated that. As the data shown, the E1 bound better than the R4 (compare Fig. 7.1 B with C), and the inhibitory role of E1 was more potent than that of R4 (compare Fig. 7.5 B with C). While for the nonstimulatory pMHCs, the TCR-pMHC interaction does not (VSV) or negligibly (Stat3) exist (s) (Fig. 7.1 D&E), and the CD8-pMHC interaction is the dominant binding between T cell and pMHC bearing RBC. The SPR measurements (44) and our previous data (38) (and Fig. 6.4B) have shown the VSV pMHC does not bind to TCR. Repeatedly, the binding between OTI CTL and RBC coated with nonstimulatory pMHC were very weak compared with those of agonist and antagonist (Fig. 7.1). Since the nonstimulatory pMHCs do not or negligibly bind to TCR, they no longer can compete with agonist for the TCR even though their site densities are much higher than that of agonist. Meanwhile, the nonstimulatory pMHCs provide MHC-CD8 interaction to stabilize the conjugation between T cell and pMHC bearing RBC. At the same time, the interaction of MHC-CD8 recruits the CD8 and Lck to the conjugation and facilitates the CD8-TCR interaction (88). Our CD8 blocking data have demonstrated the indispensable role of CD8 in the enhancement of recognition caused by the nonstimulatory pMHCs (Fig. 7.4). So, the nonstimulatory and agonist pMHCs bind cooperatively to the T cells in a CD8 dependent way.

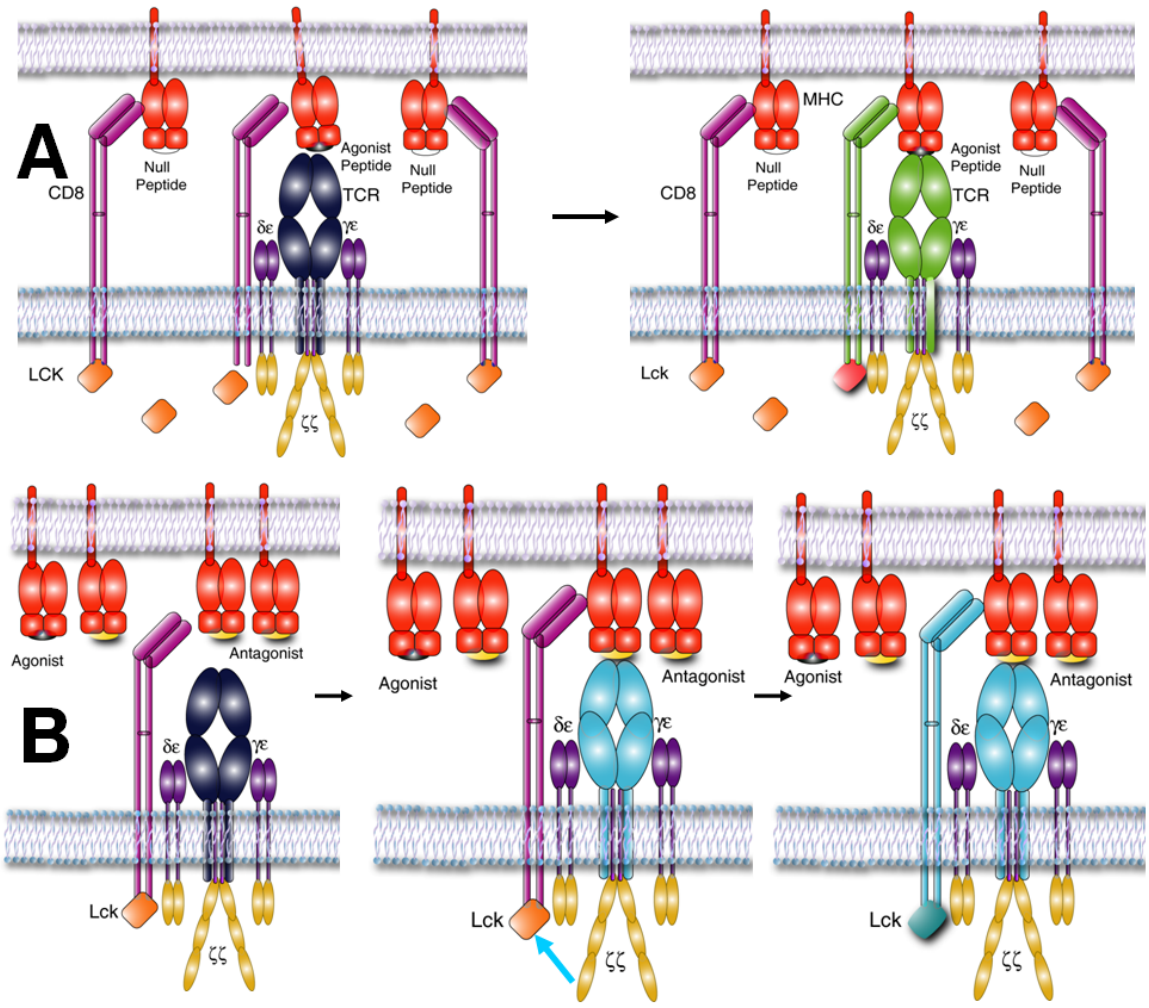

Figure 7.8 The amplification and competition model. A. Amplification. The null pMHC binding to the CD8 stabilizes the conjugation between T cell and APC and brings more Lck to the vicinity of TCR. Therefore the CD8 mediated second-step binding can be better triggered and the readout is the enhancement of recognition. **B**. Competition. The antagonist and agonist compete for a same TCR. The antagonist binding to TCR delivers a negative signal to gradually turn off the CD8 mediated second-step binding of agonist. Therefore the readout is the inhibition of binding.

In the classic model, TCR and CD8 bind to the same antigenic pMHC, with the cytoplasmic region of the CD8 providing Lck to phosphorylate CD3. Our data support this simple model. Using the combination of CD8-null MHC complexed with agonist

peptide and WT MHC complexed with nonstimulatory peptide, we have demonstrated that the TCR and CD8 actually bind synergistically to a same antigenic pMHC. However, that classical model explains neither how the nonstimulatory peptides enhance nor the antagonist peptides inhibit the antigen recognition. Gascoigne lab has shown that nonstimulatory peptides presented simultaneously with antigenic peptides increased the CD8-TCR interaction (88). Based on the data, we propose an "amplification and competition model" to explain the molecular mechanism of enhancement and inhibition caused by nonstimulatory and antagonist respectively (Fig. 7.8). The TCR-pMHC interaction provides the initial discrimination signal, while the CD8-pMHC binding serves as signal amplification machinery. In the presence of pure agonist or antagonist pMHC, the strong or weak TCR-pMHC interaction provides a positive or negative recognition signal which decides to either turn on or turn off the CD8 signaling amplification machinery through the TCR-CD8 interaction, and the corresponding readout is a two-step binding (Fig 5.3A) or a monovalent binding (5.3 C&D) in micropipette assay respectively. In the presence of both agonist and nonstimulatory pMHCs (Fig. 7.8A), the TCR binding to agonist pMHC provides an initial positive recognition signal. While the nonstimulatory CD8-pMHC interaction stabilizes the conjugation between T cell and APC and then facilitates the re-binding between TCR-pMHC for agonist, which has a very fast kinetics. Also, the CD8 binding to nonstimulatory pMHC brings much more Lck to vicinity of TCR that binds to the agonist pMHC, thereby greatly increasing the local concentration of Lck kinase to facilitate the communication between TCR and CD8. The overall effect is that the positive signal can be better amplified and the CD8 mediated second-step binding can be better triggered, so

the readout is the enhancement of recognition. In the presence of agonist and antagonist pMHCs (Fig. 7.8B), the agonist and antagonist compete for a same binding site: the TCR, with the increase binding of the antagonist, the overall recognition signal become negative and the CD8 amplification is gradually turned off, and the readout is the inhibition of recognition.

CHAPTER 8

CONCLUSION AND FUTURE RECOMMENDATION

The T cell recognition mechanism is a fundamental but unclear question in the immunology. The T cell recognition process involves the initial recognition of antigenic peptide, the signal transduction and amplification, and the activation of the T cell to eliminate the antigen. This process requires the molecular interaction among the TCR, CD8 and pMHCs, and the cooperation of accessory molecules on the cell surface, the communication and recruitment between surface molecules and intracellular kinases across the cell membrane, and the signaling transduction and regulation, gene translocation and transcription, and protein expression inside of the cell. In contrast to the clear understanding of intracellular events inside of the cell, the puzzle of how binding of pMHC initiates or triggers TCR signaling remains unclear.

Our project measured the TCR independent MHC-CD8 interaction, identified the TCR-pMHC triggered CD8-dependent two-step binding, characterized the crosstalk between CD8 and TCR, and studied the role of peptides affecting T cell recognition. These studies indeed provided valuable information and shed light to the understanding of the T cell recognition mechanism, however, the puzzle remains there. Our current project revealed that the complexities of recognition mainly are attributed to the trimolecular interaction among TCR, CD8 and MHC, the complexity of multichain TCR/CD3 structure, the diversity of peptides presented by MHCs on APCs, and the complicated environment where pMHC-TCR interaction takes place. To fully understand the T cell recognition mechanism, we need have a crystal clear picture regarding how the

initial recognition signal is obtained, how the initial signal is translated and amplified into a prolonged signal necessary for activation and how the activation signaling is controlled.

Current project used 2D micropipette adhesion assay to address the molecular interaction at the T cell membrane. This technique is very reliable for 2D binding affinity and kinetics measurements. It allows direct observation of the molecular interaction or bond formation on the cell membrane, so its measurement is more close to the physiological conditions. Another advantage of the micropipette assay is its measurement has a high temporal resolution (in second). However, the pitfall of the micropipette assay is obvious, because the readout is only the adhesion frequency. It omits a lot of important information in characterizing a molecular interaction, such as bond strength and lifetime, molecular conformation and extension and etc. A simple example is that an investigator cannot differentiate a TCR-pMHC bond from a CD8-pMHC one by this assay, although these two types of bonds are physically different. Another pitfall is the very low efficiency of this assay. The investigator needs repeat at least thousands of successful tests to obtain a stable binding curve, if you do not count the several-fold unsuccessful ones. To use the micropipette, an investigator needs a typical training for several weeks. All of those prevent the investigator obtain more information of an interaction, as well as its wild use and commercialization.

An evitable conclusion of every project is the additional recommendations and questions that arise from the findings. Regarding to better address the complex molecular interactions between T cell and APC, a more sophisticated technique called biomembrane force probe (BFP) could be an ideal candidate (158). BFP is a more advanced version of current micropipette. In addition to inherit all the advantages of current micropipette adhesion assay, it also can characterize the bond strength and life time, molecular

conformation and extension, on- and off-rates of a molecular interaction with a better temporal and spatial resolution. Using the BFP, the investigator can develop a lot of measurements to study the trimolecular interaction among the TCR, pMHC and CD8 on the cell membrane, thereby providing more details such as how the initial interaction occurs and how the CD8 and TCR affect each other or same neighborhood molecules upon pMHC binding.

The signaling is always occurs simultaneously and accompanies with the binding of pMHC to the T cell. So, anther important issue regarding the T cell recognition is to study the signaling. Most of the studied use traditional biochemical assays to address the T cell signaling such as measurements of cytokine secretion, calcium flux or protein phosphorylation. However, those assays usually were lacking of enough temporal and spatial resolution, therefore cannot faithfully reveal the real signaling process if you think of the interactions and signaling actually occur in second or subsecond time scale and involve different molecules in different locations of a live cell. Until recently, the Davis group successfully detected the phosphorylation of the LAT adaptor molecule in 4 seconds and calcium flux in 6-7 seconds by using a photoactivatable agonist peptide (159). Similarly, Wang et al. imaged and quantified the spatial-temporal activation of Src in live cells using a FRET-based Src indicator (160). Those kinds of new techniques can be incorporated into the BFP to measure such as the activation of Lck, the phosphorylation of the Zap-70, the calcium flux, or other kinase cascades inside of the cell as well as the concurrent binding characteristics of surface molecular interactions outside of the T cell upon binding of pMHCs in real time with high spatial and temporal resolution. Those studies will revolutionary advance the understanding of the T cell recognition mechanism.

REFERENCES

1. Davis, M. M., M. Krogsgaard, J. B. Huppa, C. Sumen, M. A. Purbhoo, D. J. Irvine, L. C. Wu, and L. Ehrlich. 2003. Dynamics of cell surface molecules during T cell recognition. *Annu Rev Biochem* 72:717-742.
2. Janeway, C. A., P. Travers, M. Walport, and J. D. Capra. 1999. *Immunobiology: The Immune System in Health and Disease* Elsevier Science Ltd/Garland publishing, New York, NY.
3. Davis, M. M., M. Krogsgaard, M. Huse, J. Huppa, B. F. Lillemeier, and Q. J. Li. 2007. T cells as a self-referential, sensory organ. *Annu Rev Immunol* 25:681-695.
4. Garcia, K. C., L. Teyton, and I. A. Wilson. 1999. Structural basis of T cell recognition. *Annu Rev Immunol* 17:369-397.
5. Ma, Z., K. A. Sharp, P. A. Janmey, and T. H. Finkel. 2008. Surface-anchored monomeric agonist pMHCs alone trigger TCR with high sensitivity. *PLoS Biol* 6:e43.
6. Krogsgaard, M., Q. J. Li, C. Sumen, J. B. Huppa, M. Huse, and M. M. Davis. 2005. Agonist/endogenous peptide-MHC heterodimers drive T cell activation and sensitivity. *Nature* 434:238-243.
7. Rudolph, M. G., R. L. Stanfield, and I. A. Wilson. 2006. How TCRs bind MHCs, peptides, and coreceptors. *Annu Rev Immunol* 24:419-466.
8. Gascoigne, N. R., T. Zal, and S. M. Alam. 2001. T-cell receptor binding kinetics in T-cell development and activation. *Expert Rev Mol Med* 2001:1-17.
9. Call, M. E., J. Pyrdol, M. Wiedmann, and K. W. Wucherpfennig. 2002. The organizing principle in the formation of the T cell receptor-CD3 complex. *Cell* 111:967-979.
10. Call, M. E., and K. W. Wucherpfennig. 2005. The T cell receptor: critical role of the membrane environment in receptor assembly and function. *Annu. Rev. Immunol.* 23:101-125.
11. Kersh, G. J., E. N. Kersh, D. H. Fremont, and P. M. Allen. 1998. High- and low-potency ligands with similar affinities for the TCR: the importance of kinetics in TCR signaling. *Immunity* 9:817-826.

12. Cole, D. K., and G. F. Gao. 2004. CD8: adhesion molecule, co-receptor and immuno-modulator. *Cell. Mol. Immunol.* 1:81-88.
13. Alegre, M. L., K. A. Frauwirth, and C. B. Thompson. 2001. T-cell regulation by CD28 and CTLA-4. *Nat Rev Immunol* 1:220-228.
14. Grakoui, A., S. K. Bromley, C. Sumen, M. M. Davis, A. S. Shaw, P. M. Allen, and M. L. Dustin. 1999. The immunological synapse: a molecular machine controlling T cell activation. *Science* 285:221-227.
15. Dustin, M. L. 1990. Two-way signalling through the LFA-1 lymphocyte adhesion receptor. *Bioessays* 12:421-427.
16. Dustin, M. L., and T. A. Springer. 1989. T-cell receptor cross-linking transiently stimulates adhesiveness through LFA-1. *Nature* 341:619-624.
17. Shamri, R., V. Grabovsky, J. M. Gauguet, S. Feigelson, E. Manevich, W. Kolanus, M. K. Robinson, D. E. Staunton, U. H. von Andrian, and R. Alon. 2005. Lymphocyte arrest requires instantaneous induction of an extended LFA-1 conformation mediated by endothelium-bound chemokines. *Nat Immunol* 6:497-506.
18. Holman, P. O., E. R. Walsh, and S. C. Jameson. 2005. Characterizing the impact of CD8 antibodies on class I MHC multimer binding. *J Immunol* 174:3986-3991.
19. Dustin, M. L. 1997. Adhesive bond dynamics in contacts between T lymphocytes and glass-supported planar bilayers reconstituted with the immunoglobulin-related adhesion molecule CD58. *J. Biol. Chem.* 272:15782-15788.
20. Dustin, M. L., D. E. Golan, D. M. Zhu, J. M. Miller, W. Meier, E. A. Davies, and P. A. van der Merwe. 1997. Low affinity interaction of human or rat T cell adhesion molecule CD2 with its ligand aligns adhering membranes to achieve high physiological affinity. *J. Biol. Chem.* 272:30889-30898.
21. Davis, S. J., and P. A. van der Merwe. 1996. The structure and ligand interactions of CD2: implications for T-cell function. *Immunol Today* 17:177-187.
22. Wilkins, A. L., W. Yang, and J. J. Yang. 2003. Structural biology of the cell adhesion protein CD2: from molecular recognition to protein folding and design. *Curr Protein Pept Sci* 4:367-373.
23. Trowbridge, I. S., and M. L. Thomas. 1994. CD45: an emerging role as a protein tyrosine phosphatase required for lymphocyte activation and development. *Annu Rev Immunol* 12:85-116.

24. Alexander, D. R. 2000. The CD45 tyrosine phosphatase: a positive and negative regulator of immune cell function. *Semin Immunol* 12:349-359.
25. Kwan Lim, G. E., L. McNeill, K. Whitley, D. L. Becker, and R. Zamoyska. 1998. Co-capping studies reveal CD8/TCR interactions after capping CD8 beta polypeptides and intracellular associations of CD8 with p56(lck). *Eur J Immunol* 28:745-754.
26. Mustelin, T., and K. Tasken. 2003. Positive and negative regulation of T-cell activation through kinases and phosphatases. *Biochem J* 371:15-27.
27. Palacios, E. H., and A. Weiss. 2004. Function of the Src-family kinases, Lck and Fyn, in T-cell development and activation. *Oncogene* 23:7990-8000.
28. Dustin, M. L. 2007. Cell adhesion molecules and actin cytoskeleton at immune synapses and kinapses. *Curr Opin Cell Biol* 19:529-533.
29. Billadeau, D. D., J. C. Nolz, and T. S. Gomez. 2007. Regulation of T-cell activation by the cytoskeleton. *Nat Rev Immunol* 7:131-143.
30. Fuller, C. L., V. L. Braciale, and L. E. Samelson. 2003. All roads lead to actin: the intimate relationship between TCR signaling and the cytoskeleton. *Immunol Rev* 191:220-236.
31. Samstag, Y., S. M. Eibert, M. Klemke, and G. H. Wabnitz. 2003. Actin cytoskeletal dynamics in T lymphocyte activation and migration. *J Leukoc Biol* 73:30-48.
32. Brdickova, N., T. Brdicka, P. Angelisova, O. Horvath, J. Spicka, I. Hilgert, J. Paces, L. Simeoni, S. Kliche, C. Merten, B. Schraven, and V. Horejsi. 2003. LIME: a new membrane Raft-associated adaptor protein involved in CD4 and CD8 coreceptor signaling. *J. Exp. Med.* 198:1453-1462.
33. Harder, T. 2004. Lipid raft domains and protein networks in T-cell receptor signal transduction. *Curr Opin Immunol* 16:353-359.
34. Magee, T., N. Pirinen, J. Adler, S. N. Pagakis, and I. Parmryd. 2002. Lipid rafts: cell surface platforms for T cell signaling. *Biol Res* 35:127-131.
35. Kabouridis, P. S. 2006. Lipid rafts in T cell receptor signalling. *Mol Membr Biol* 23:49-57.
36. He, H. T., A. Lellouch, and D. Marguet. 2005. Lipid rafts and the initiation of T cell receptor signaling. *Semin Immunol* 17:23-33.
37. Fahmy, T. M., J. G. Bieler, and J. P. Schneck. 2002. Probing T cell membrane organization using dimeric MHC-Ig complexes. *J. Immunol. Methods* 268:93-106.

38. Huang, J., L. J. Edwards, B. D. Evavold, and C. Zhu. 2007. Kinetics of MHC-CD8 interaction at the T cell membrane. *J Immunol* 179:7653-7662.
39. Kuhns, M. S., and M. M. Davis. 2007. Disruption of extracellular interactions impairs T cell receptor-CD3 complex stability and signaling. *Immunity* 26:357-369.
40. Kuhns, M. S., M. M. Davis, and K. C. Garcia. 2006. Deconstructing the form and function of the TCR/CD3 complex. *Immunity* 24:133-139.
41. Dustin, M. L., S. K. Bromley, M. M. Davis, and C. Zhu. 2001. Identification of self through two-dimensional chemistry and synapses. *Annu. Rev. Cell Dev. Biol.* 17:133-157.
42. McKeithan, T. W. 1995. Kinetic proofreading in T-cell receptor signal transduction. *Proc Natl Acad Sci U S A* 92:5042-5046.
43. Rabinowitz, J. D., C. Beeson, D. S. Lyons, M. M. Davis, and H. M. McConnell. 1996. Kinetic discrimination in T-cell activation. *Proc Natl Acad Sci U S A* 93:1401-1405.
44. Alam, S. M., P. J. Travers, J. L. Wung, W. Nasholds, S. Redpath, S. C. Jameson, and N. R. Gascoigne. 1996. T-cell-receptor affinity and thymocyte positive selection. *Nature* 381:616-620.
45. Kalergis, A. M., N. Boucheron, M. A. Doucey, E. Palmieri, E. C. Goyarts, Z. Vegh, I. F. Luescher, and S. G. Nathenson. 2001. Efficient T cell activation requires an optimal dwell-time of interaction between the TCR and the pMHC complex. *Nat Immunol* 2:229-234.
46. Rosette, C., G. Werlen, M. A. Daniels, P. O. Holman, S. M. Alam, P. J. Travers, N. R. Gascoigne, E. Palmer, and S. C. Jameson. 2001. The impact of duration versus extent of TCR occupancy on T cell activation: a revision of the kinetic proofreading model. *Immunity* 15:59-70.
47. Laugel, B., H. A. van den Berg, E. Gostick, D. K. Cole, L. Wooldridge, J. Boulter, A. Milicic, D. A. Price, and A. K. Sewell. 2007. Different T cell receptor affinity thresholds and CD8 coreceptor dependence govern cytotoxic T lymphocyte activation and tetramer binding properties. *J Biol Chem* 282:23799-23810.
48. Burroughs, N. J., Z. Lazic, and P. A. van der Merwe. 2006. Ligand detection and discrimination by spatial relocalization: A kinase-phosphatase segregation model of TCR activation. *Biophys J* 91:1619-1629.
49. Davis, S. J., and P. A. van der Merwe. 2006. The kinetic-segregation model: TCR triggering and beyond. *Nat Immunol* 7:803-809.

50. Gil, D., W. W. Schamel, M. Montoya, F. Sanchez-Madrid, and B. Alarcon. 2002. Recruitment of Nck by CD3 epsilon reveals a ligand-induced conformational change essential for T cell receptor signaling and synapse formation. *Cell* 109:901-912.
51. Gil, D., A. G. Schrum, B. Alarcon, and E. Palmer. 2005. T cell receptor engagement by peptide-MHC ligands induces a conformational change in the CD3 complex of thymocytes. *J. Exp. Med.* 201:517-522.
52. Risueno, R. M., D. Gil, E. Fernandez, F. Sanchez-Madrid, and B. Alarcon. 2005. Ligand-induced conformational change in the T-cell receptor associated with productive immune synapses. *Blood* 106:601-608.
53. Schamel, W. W., R. M. Risueno, S. Minguet, A. R. Ortiz, and B. Alarcon. 2006. A conformation- and avidity-based proofreading mechanism for the TCR-CD3 complex. *Trends Immunol* 27:176-182.
54. Levin, S. E., and A. Weiss. 2005. Twisting tails exposed: the evidence for TCR conformational change. *J Exp Med* 201:489-492.
55. Rudolph, M. G., and I. A. Wilson. 2002. The specificity of TCR/pMHC interaction. *Curr Opin Immunol* 14:52-65.
56. Reich, Z., J. J. Boniface, D. S. Lyons, N. Borochov, E. J. Wachtel, and M. M. Davis. 1997. Ligand-specific oligomerization of T-cell receptor molecules. *Nature* 387:617-620.
57. Bachmann, M. F., A. Gallimore, S. Linkert, V. Cerundolo, A. Lanzavecchia, M. Kopf, and A. Viola. 1999. Developmental regulation of Lck targeting to the CD8 coreceptor controls signaling in naive and memory T cells. *J Exp Med* 189:1521-1530.
58. Boniface, J. J., J. D. Rabinowitz, C. Wulfing, J. Hampl, Z. Reich, J. D. Altman, R. M. Kantor, C. Beeson, H. M. McConnell, and M. M. Davis. 1998. Initiation of signal transduction through the T cell receptor requires the multivalent engagement of peptide/MHC ligands [corrected]. *Immunity* 9:459-466.
59. Germain, R. N. 1997. T-cell signaling: the importance of receptor clustering. *Curr Biol* 7:R640-644.
60. Stone, J. D., and L. J. Stern. 2006. CD8 T cells, like CD4 T cells, are triggered by multivalent engagement of TCRs by MHC-peptide ligands but not by monovalent engagement. *J. Immunol.* 176:1498-1505.
61. Campi, G., R. Varma, and M. L. Dustin. 2005. Actin and agonist MHC-peptide complex-dependent T cell receptor microclusters as scaffolds for signaling. *J Exp Med* 202:1031-1036.

62. Varma, R., G. Campi, T. Yokosuka, T. Saito, and M. L. Dustin. 2006. T cell receptor-proximal signals are sustained in peripheral microclusters and terminated in the central supramolecular activation cluster. *Immunity* 25:117-127.
63. Block, M. S., A. J. Johnson, Y. Mendez-Fernandez, and L. R. Pease. 2001. Monomeric class I molecules mediate TCR/CD3 epsilon/CD8 interaction on the surface of T cells. *J Immunol* 167:821-826.
64. Rudolph, M. G., R. L. Stanfield, and I. A. Wilson. 2006. How TCRs bind MHCs, peptides, and coreceptors. *Annu. Rev. Immunol.* 24:419-466.
65. Wu, L. C., D. S. Tuot, D. S. Lyons, K. C. Garcia, and M. M. Davis. 2002. Two-step binding mechanism for T-cell receptor recognition of peptide MHC. *Nature* 418:552-556.
66. Valitutti, S., M. Dessing, K. Aktories, H. Gallati, and A. Lanzavecchia. 1995. Sustained signaling leading to T cell activation results from prolonged T cell receptor occupancy. Role of T cell actin cytoskeleton. *J Exp Med* 181:577-584.
67. Sykulev, Y., R. J. Cohen, and H. N. Eisen. 1995. The law of mass action governs antigen-stimulated cytolytic activity of CD8+ cytotoxic T lymphocytes. *Proc Natl Acad Sci U S A* 92:11990-11992.
68. McNeil, L. K., and B. D. Evavold. 2003. TCR reserve: a novel principle of CD4 T cell activation by weak ligands. *J Immunol* 170:1224-1230.
69. McNeil, L. K., and B. D. Evavold. 2002. Dissociation of peripheral T cell responses from thymocyte negative selection by weak agonists supports a spare receptor model of T cell activation. *Proc Natl Acad Sci U S A* 99:4520-4525.
70. Hogquist, K. A., S. C. Jameson, W. R. Heath, J. L. Howard, M. J. Bevan, and F. R. Carbone. 1994. T cell receptor antagonist peptides induce positive selection. *Cell* 76:17-27.
71. Yachi, P. P., J. Ampudia, T. Zal, and N. R. Gascoigne. 2006. Altered peptide ligands induce delayed CD8-T cell receptor interaction--a role for CD8 in distinguishing antigen quality. *Immunity* 25:203-211.
72. Kerry, S. E., J. Buslepp, L. A. Cramer, R. Maile, L. L. Hensley, A. I. Nielsen, P. Kavathas, B. J. Vilen, E. J. Collins, and J. A. Frelinger. 2003. Interplay between TCR affinity and necessity of coreceptor ligation: high-affinity peptide-MHC/TCR interaction overcomes lack of CD8 engagement. *J. Immunol.* 171:4493-4503.
73. Mamalaki, C., T. Norton, Y. Tanaka, A. R. Townsend, P. Chandler, E. Simpson, and D. Kioussis. 1992. Thymic depletion and peripheral

activation of class I major histocompatibility complex-restricted T cells by soluble peptide in T-cell receptor transgenic mice. *Proc. Natl. Acad. Sci. USA* 89:11342-11346.
74. Chesla, S. E., P. Selvaraj, and C. Zhu. 1998. Measuring two-dimensional receptor-ligand binding kinetics by micropipette. *Biophys. J.* 75:1553-1572.
75. Huang, J., J. Chen, S. E. Chesla, T. Yago, P. Mehta, R. P. McEver, C. Zhu, and M. Long. 2004. Quantifying the effects of molecular orientation and length on two-dimensional receptor-ligand binding kinetics. *J. Biol. Chem.* 279:44915-44923.
76. Long, M., J. Chen, N. Jiang, P. Selvaraj, R. P. McEver, and C. Zhu. 2006. Probabilistic modeling of rosette formation. *Biophys. J.* 91:352-363.
77. Burshtyn, D. N., and B. H. Barber. 1993. High occupancy binding of antigenic peptides to purified, immunoadsorbed H-2Db beta 2m molecules. *J. Immunol.* 151:3070-3081.
78. Wyer, J. R., B. E. Willcox, G. F. Gao, U. C. Gerth, S. J. Davis, J. I. Bell, P. A. van der Merwe, and B. K. Jakobsen. 1999. T cell receptor and coreceptor CD8 alphaalpha bind peptide-MHC independently and with distinct kinetics. *Immunity* 10:219-225.
79. Arcaro, A., C. Gregoire, T. R. Bakker, L. Baldi, M. Jordan, L. Goffin, N. Boucheron, F. Wurm, P. A. van der Merwe, B. Malissen, and I. F. Luescher. 2001. CD8beta endows CD8 with efficient coreceptor function by coupling T cell receptor/CD3 to raft-associated CD8/p56(lck) complexes. *J. Exp. Med.* 194:1485-1495.
80. Gakamsky, D. M., I. F. Luescher, A. Pramanik, R. B. Kopito, F. Lemonnier, H. Vogel, R. Rigler, and I. Pecht. 2005. CD8 kinetically promotes ligand binding to the T-cell antigen receptor. *Biophys. J.* 89:2121-2133.
81. Campanelli, R., B. Palermo, S. Garbelli, S. Mantovani, P. Lucchi, A. Necker, E. Lantelme, and C. Giachino. 2002. Human CD8 co-receptor is strictly involved in MHC-peptide tetramer-TCR binding and T cell activation. *Int. Immunol.* 14:39-44.
82. Daniels, M. A., and S. C. Jameson. 2000. Critical role for CD8 in T cell receptor binding and activation by peptide/major histocompatibility complex multimers. *J. Exp. Med.* 191:335-346.
83. Delon, J., C. Gregoire, B. Malissen, S. Darche, F. Lemaitre, P. Kourilsky, J. P. Abastado, and A. Trautmann. 1998. CD8 expression allows T cell signaling by monomeric peptide-MHC complexes. *Immunity* 9:467-473.

84. Lyons, G. E., T. Moore, N. Brasic, M. Li, J. J. Roszkowski, and M. I. Nishimura. 2006. Influence of human CD8 on antigen recognition by T-cell receptor-transduced cells. *Cancer Res.* 66:11455-11461.
85. Gao, G. F., J. Tormo, U. C. Gerth, J. R. Wyer, A. J. McMichael, D. I. Stuart, J. I. Bell, E. Y. Jones, and B. K. Jakobsen. 1997. Crystal structure of the complex between human CD8alpha(alpha) and HLA-A2. *Nature* 387:630-634.
86. Gao, G. F., Z. Rao, and J. I. Bell. 2002. Molecular coordination of alphabeta T-cell receptors and coreceptors CD8 and CD4 in their recognition of peptide-MHC ligands. *Trends Immunol.* 23:408-413.
87. Pecht, I., and D. M. Gakamsky. 2005. Spatial coordination of CD8 and TCR molecules controls antigen recognition by CD8+ T-cells. *FEBS Lett.* 579:3336-3341.
88. Yachi, P. P., J. Ampudia, N. R. Gascoigne, and T. Zal. 2005. Nonstimulatory peptides contribute to antigen-induced CD8-T cell receptor interaction at the immunological synapse. *Nat. Immunol.* 6:785-792.
89. Bosselut, R., S. Kubo, T. Guinter, J. L. Kopacz, J. D. Altman, L. Feigenbaum, and A. Singer. 2000. Role of CD8beta domains in CD8 coreceptor function: importance for MHC I binding, signaling, and positive selection of CD8+ T cells in the thymus. *Immunity* 12:409-418.
90. Chang, H. C., K. Tan, and Y. M. Hsu. 2006. CD8alphabeta has two distinct binding modes of interaction with peptide-major histocompatibility complex class I. *J. Biol. Chem.* 281:28090-28096.
91. Kern, P. S., M. K. Teng, A. Smolyar, J. H. Liu, J. Liu, R. E. Hussey, R. Spoerl, H. C. Chang, E. L. Reinherz, and J. H. Wang. 1998. Structural basis of CD8 coreceptor function revealed by crystallographic analysis of a murine CD8alphaalpha ectodomain fragment in complex with H-2Kb. *Immunity* 9:519-530.
92. Gangadharan, D., and H. Cheroutre. 2004. The CD8 isoform CD8alphaalpha is not a functional homologue of the TCR co-receptor CD8alphabeta. *Curr. Opin. Immunol.* 16:264-270.
93. Devine, L., D. Thakral, S. Nag, J. Dobbins, M. E. Hodsdon, and P. B. Kavathas. 2006. Mapping the binding site on CD8 beta for MHC class I reveals mutants with enhanced binding. *J. Immunol.* 177:3930-3938.
94. Sun, J., and P. B. Kavathas. 1997. Comparison of the roles of CD8 alpha alpha and CD8 alpha beta in interaction with MHC class I. *J. Immunol.* 159:6077-6082.

95. Leishman, A. J., O. V. Naidenko, A. Attinger, F. Koning, C. J. Lena, Y. Xiong, H. C. Chang, E. Reinherz, M. Kronenberg, and H. Cheroutre. 2001. T cell responses modulated through interaction between CD8alphaalpha and the nonclassical MHC class I molecule, TL. *Science* 294:1936-1939.
96. Kern, P., R. E. Hussey, R. Spoerl, E. L. Reinherz, and H. C. Chang. 1999. Expression, purification, and functional analysis of murine ectodomain fragments of CD8alphaalpha and CD8alphabeta dimers. *J. Biol. Chem.* 274:27237-27243.
97. Garcia, K. C., C. A. Scott, A. Brunmark, F. R. Carbone, P. A. Peterson, I. A. Wilson, and L. Teyton. 1996. CD8 enhances formation of stable T-cell receptor/MHC class I molecule complexes. *Nature* 384:577-581.
98. Moody, A. M., Y. Xiong, H. C. Chang, and E. L. Reinherz. 2001. The CD8alphabeta co-receptor on double-positive thymocytes binds with differing affinities to the products of distinct class I MHC loci. *Eur. J. Immunol.* 31:2791-2799.
99. Viret, C., and C. A. Janeway, Jr. 1999. MHC and T cell development. *Rev. Immunogenet.* 1:91-104.
100. Lee, N. A., D. Y. Loh, and E. Lacy. 1992. CD8 surface levels alter the fate of alpha/beta T cell receptor-expressing thymocytes in transgenic mice. *J. Exp. Med.* 175:1013-1025.
101. Robey, E. A., F. Ramsdell, D. Kioussis, W. Sha, D. Loh, R. Axel, and B. J. Fowlkes. 1992. The level of CD8 expression can determine the outcome of thymic selection. *Cell* 69:1089-1096.
102. Wu, L., B. Xiao, X. Jia, Y. Zhang, S. Lu, J. Chen, and M. Long. 2007. Impact of carrier stiffness and microtopology on two-dimensional kinetics of P-selectin and P-selectin glycoprotein ligand-1 (PSGL-1) interactions. *J. Biol. Chem.* 282:9846-9854.
103. Williams, T. E., S. Nagarajan, P. Selvaraj, and C. Zhu. 2001. Quantifying the impact of membrane microtopology on effective two-dimensional affinity. *J. Biol. Chem.* 276:13283-13288.
104. MacLachlan, J., A. T. Wotherspoon, R. O. Ansell, and C. J. Brooks. 2000. Cholesterol oxidase: sources, physical properties and analytical applications. *J. Steroid Biochem. Mol. Biol.* 72:169-195.
105. Cahuzac, N., W. Baum, V. Kirkin, F. Conchonaud, L. Wawrezinieck, D. Marguet, O. Janssen, M. Zornig, and A. O. Hueber. 2006. Fas ligand is localized to membrane rafts, where it displays increased cell death-inducing activity. *Blood* 107:2384-2391.

106. Xiong, Y., P. Kern, H. Chang, and E. Reinherz. 2001. T Cell Receptor Binding to a pMHCII Ligand Is Kinetically Distinct from and Independent of CD4. *J. Biol. Chem.* 276:5659-5667.
107. Gao, G. F., B. E. Willcox, J. R. Wyer, J. M. Boulter, C. A. O'Callaghan, K. Maenaka, D. I. Stuart, E. Y. Jones, P. A. Van Der Merwe, J. I. Bell, and B. K. Jakobsen. 2000. Classical and nonclassical class I major histocompatibility complex molecules exhibit subtle conformational differences that affect binding to CD8alphaalpha. *J. Biol. Chem.* 275:15232-15238.
108. Wooldridge, L., T. J. Scriba, A. Milicic, B. Laugel, E. Gostick, D. A. Price, R. E. Phillips, and A. K. Sewell. 2006. Anti-coreceptor antibodies profoundly affect staining with peptide-MHC class I and class II tetramers. *Eur. J. Immunol.* 36:1847-1855.
109. Denkberg, G., C. J. Cohen, and Y. Reiter. 2001. Critical role for CD8 in binding of MHC tetramers to TCR: CD8 antibodies block specific binding of human tumor-specific MHC-peptide tetramers to TCR. *J. Immunol.* 167:270-276.
110. Schott, E., and H. L. Ploegh. 2002. Mouse MHC class I tetramers that are unable to bind to CD8 reveal the need for CD8 engagement in order to activate naive CD8 T cells. *Eur. J. Immunol.* 32:3425-3434.
111. Wooldridge, L., S. L. Hutchinson, E. M. Choi, A. Lissina, E. Jones, F. Mirza, P. R. Dunbar, D. A. Price, V. Cerundolo, and A. K. Sewell. 2003. Anti-CD8 antibodies can inhibit or enhance peptide-MHC class I (pMHCI) multimer binding: this is paralleled by their effects on CTL activation and occurs in the absence of an interaction between pMHCI and CD8 on the cell surface. *J. Immunol.* 171:6650-6660.
112. Norment, A. M., R. D. Salter, P. Parham, V. H. Engelhard, and D. R. Littman. 1988. Cell-cell adhesion mediated by CD8 and MHC class I molecules. *Nature* 336:79-81.
113. Tolentino, T. P., J. Wu, V. I. Zarnitsyna, Y. Fang, M. L. Dustin, and C. Zhu. 2008. Measuring Diffusion and Binding Kinetics by Contact Area FRAP. *Biophys J* 4:4.
114. Long, M., H. Zhao, K. S. Huang, and C. Zhu. 2001. Kinetic measurements of cell surface E-selectin/carbohydrate ligand interactions. *Ann. Biomed. Eng.* 29:935-946.
115. Zhang, F., W. D. Marcus, N. H. Goyal, P. Selvaraj, T. A. Springer, and C. Zhu. 2005. Two-dimensional kinetics regulation of alphaLbeta2-ICAM-1 interaction by conformational changes of the alphaL-inserted domain. *J. Biol. Chem.* 280:42207-42218.

116. Williams, T. E., P. Selvaraj, and C. Zhu. 2000. Concurrent binding to multiple ligands: kinetic rates of CD16b for membrane-bound IgG1 and IgG2. *Biophys. J.* 79:1858-1866.
117. Williams, T. E., S. Nagarajan, P. Selvaraj, and C. Zhu. 2000. Concurrent and independent binding of Fcgamma receptors IIa and IIIb to surface-bound IgG. *Biophys. J.* 79:1867-1875.
118. Ding, Y. H., B. M. Baker, D. N. Garboczi, W. E. Biddison, and D. C. Wiley. 1999. Four A6-TCR/peptide/HLA-A2 structures that generate very different T cell signals are nearly identical. *Immunity* 11:45-56.
119. Devine, L., J. Sun, M. R. Barr, and P. B. Kavathas. 1999. Orientation of the Ig domains of CD8 alpha beta relative to MHC class I. *J. Immunol.* 162:846-851.
120. Daniels, M. A., L. Devine, J. D. Miller, J. M. Moser, A. E. Lukacher, J. D. Altman, P. Kavathas, K. A. Hogquist, and S. C. Jameson. 2001. CD8 binding to MHC class I molecules is influenced by T cell maturation and glycosylation. *Immunity* 15:1051-1061.
121. Jiang, N. 2005. Kinetic studies of Fcγ receptor III and T cell receptor. Georgia Institute of Technology, Atlanta, GA.
122. O'Rourke, A. M., J. Rogers, and M. F. Mescher. 1990. Activated CD8 binding to class I protein mediated by the T-cell receptor results in signalling. *Nature* 346:187-189.
123. Devine, L., M. E. Hodsdon, M. A. Daniels, S. C. Jameson, and P. B. Kavathas. 2004. Location of the epitope for an anti-CD8alpha antibody 53.6.7 which enhances CD8alpha-MHC class I interaction indicates antibody stabilization of a higher affinity CD8 conformation. *Immunol Lett* 93:123-130.
124. Bosselut, R., W. Zhang, J. M. Ashe, J. L. Kopacz, L. E. Samelson, and A. Singer. 1999. Association of the adaptor molecule LAT with CD4 and CD8 coreceptors identifies a new coreceptor function in T cell receptor signal transduction. *J Exp Med* 190:1517-1526.
125. Xavier, R., T. Brennan, Q. Li, C. McCormack, and B. Seed. 1998. Membrane compartmentation is required for efficient T cell activation. *Immunity* 8:723-732.
126. Chan, A. C., D. M. Desai, and A. Weiss. 1994. The role of protein tyrosine kinases and protein tyrosine phosphatases in T cell antigen receptor signal transduction. *Annu Rev Immunol* 12:555-592.
127. Hanke, J. H., J. P. Gardner, R. L. Dow, P. S. Changelian, W. H. Brissette, E. J. Weringer, B. A. Pollok, and P. A. Connelly. 1996. Discovery of a novel, potent, and Src family-selective tyrosine kinase

inhibitor. Study of Lck- and FynT-dependent T cell activation. *J Biol Chem* 271:695-701.
128. Lee, K., and T. R. Burke, Jr. 2003. CD45 protein-tyrosine phosphatase inhibitor development. *Curr Top Med Chem* 3:797-807.
129. Urbanek, R. A., S. J. Suchard, G. B. Steelman, K. S. Knappenberger, L. A. Sygowski, C. A. Veale, and M. J. Chapdelaine. 2001. Potent reversible inhibitors of the protein tyrosine phosphatase CD45. *J Med Chem* 44:1777-1793.
130. Zarnitsyna, V. I., J. Huang, F. Zhang, Y. H. Chien, D. Leckband, and C. Zhu. 2007. Memory in receptor-ligand-mediated cell adhesion. *Proc Natl Acad Sci U S A* 104:18037-18042.
131. Cho, B. K., K. C. Lian, P. Lee, A. Brunmark, C. McKinley, J. Chen, D. M. Kranz, and H. N. Eisen. 2001. Differences in antigen recognition and cytolytic activity of CD8(+) and CD8(-) T cells that express the same antigen-specific receptor. *Proc. Natl. Acad. Sci. USA* 98:1723-1727.
132. Drevot, P., C. Langlet, X. J. Guo, A. M. Bernard, O. Colard, J. P. Chauvin, R. Lasserre, and H. T. He. 2002. TCR signal initiation machinery is pre-assembled and activated in a subset of membrane rafts. *Embo J* 21:1899-1908.
133. Veillette, A., M. A. Bookman, E. M. Horak, and J. B. Bolen. 1988. The CD4 and CD8 T cell surface antigens are associated with the internal membrane tyrosine-protein kinase p56lck. *Cell* 55:301-308.
134. Barber, E. K., J. D. Dasgupta, S. F. Schlossman, J. M. Trevillyan, and C. E. Rudd. 1989. The CD4 and CD8 antigens are coupled to a protein-tyrosine kinase (p56lck) that phosphorylates the CD3 complex. *Proc Natl Acad Sci U S A* 86:3277-3281.
135. Turner, J. M., M. H. Brodsky, B. A. Irving, S. D. Levin, R. M. Perlmutter, and D. R. Littman. 1990. Interaction of the unique N-terminal region of tyrosine kinase p56lck with cytoplasmic domains of CD4 and CD8 is mediated by cysteine motifs. *Cell* 60:755-765.
136. Arcaro, A., C. Gregoire, N. Boucheron, S. Stotz, E. Palmer, B. Malissen, and I. F. Luescher. 2000. Essential role of CD8 palmitoylation in CD8 coreceptor function. *J. Immunol.* 165:2068-2076.
137. Gallagher, P. F., B. Fazekas de St Groth, and J. F. Miller. 1989. CD4 and CD8 molecules can physically associate with the same T-cell receptor. *Proc Natl Acad Sci U S A* 86:10044-10048.
138. Demotte, N., V. Stroobant, P. J. Courtoy, P. Van Der Smissen, D. Colau, I. F. Luescher, C. Hivroz, J. Nicaise, J. L. Squifflet, M.

Mourad, D. Godelaine, T. Boon, and P. van der Bruggen. 2008. Restoring the association of the T cell receptor with CD8 reverses anergy in human tumor-infiltrating lymphocytes. *Immunity* 28:414-424.
139. Mittler, R. S., S. J. Goldman, G. L. Spitalny, and S. J. Burakoff. 1989. T-cell receptor-CD4 physical association in a murine T-cell hybridoma: induction by antigen receptor ligation. *Proc Natl Acad Sci U S A* 86:8531-8535.
140. Rojo, J. M., K. Saizawa, and C. A. Janeway, Jr. 1989. Physical association of CD4 and the T-cell receptor can be induced by anti-T-cell receptor antibodies. *Proc Natl Acad Sci U S A* 86:3311-3315.
141. Abraham, N., M. C. Miceli, J. R. Parnes, and A. Veillette. 1991. Enhancement of T-cell responsiveness by the lymphocyte-specific tyrosine protein kinase p56lck. *Nature* 350:62-66.
142. Anel, A., A. M. O'Rourke, A. M. Kleinfeld, and M. F. Mescher. 1996. T cell receptor and CD8-dependent tyrosine phosphorylation events in cytotoxic T lymphocytes: activation of p56lck by CD8 binding to class I protein. *Eur. J. Immunol.* 26:2310-2319.
143. Holdorf, A. D., K. H. Lee, W. R. Burack, P. M. Allen, and A. S. Shaw. 2002. Regulation of Lck activity by CD4 and CD28 in the immunological synapse. *Nat Immunol* 3:259-264.
144. Tomonari, K., and S. Spencer. 1990. Epitope-specific binding of CD8 regulates activation of T cells and induction of cytotoxicity. *Int Immunol* 2:1189-1194.
145. Wooldridge, L., A. Lissina, J. Vernazza, E. Gostick, B. Laugel, S. L. Hutchinson, F. Mirza, P. R. Dunbar, J. M. Boulter, M. Glick, V. Cerundolo, H. A. van den Berg, D. A. Price, and A. K. Sewell. 2007. Enhanced immunogenicity of CTL antigens through mutation of the CD8 binding MHC class I invariant region. *Eur J Immunol* 37:1323-1333.
146. Cole, D. K., S. M. Dunn, M. Sami, J. M. Boulter, B. K. Jakobsen, and A. K. Sewell. 2008. T cell receptor engagement of peptide-major histocompatibility complex class I does not modify CD8 binding. *Mol Immunol* 45:2700-2709.
147. Buslepp, J., S. E. Kerry, D. Loftus, J. A. Frelinger, E. Appella, and E. J. Collins. 2003. High affinity xenoreactive TCR:MHC interaction recruits CD8 in absence of binding to MHC. *J. Immunol.* 170:373-383.
148. Stefanova, I., B. Hemmer, M. Vergelli, R. Martin, W. E. Biddison, and R. N. Germain. 2003. TCR ligand discrimination is enforced by

competing ERK positive and SHP-1 negative feedback pathways. *Nat Immunol* 4:248-254.
149. Santori, F. R., W. C. Kieper, S. M. Brown, Y. Lu, T. A. Neubert, K. L. Johnson, S. Naylor, S. Vukmanovic, K. A. Hogquist, and S. C. Jameson. 2002. Rare, structurally homologous self-peptides promote thymocyte positive selection. *Immunity* 17:131-142.
150. Anikeeva, N., T. Lebedeva, A. R. Clapp, E. R. Goldman, M. L. Dustin, H. Mattoussi, and Y. Sykulev. 2006. Quantum dot/peptide-MHC biosensors reveal strong CD8-dependent cooperation between self and viral antigens that augment the T cell response. *Proc Natl Acad Sci U S A* 103:16846-16851.
151. Sporri, R., and C. Reis e Sousa. 2002. Self peptide/MHC class I complexes have a negligible effect on the response of some CD8+ T cells to foreign antigen. *Eur J Immunol* 32:3161-3170.
152. De Magistris, M. T., J. Alexander, M. Coggeshall, A. Altman, F. C. Gaeta, H. M. Grey, and A. Sette. 1992. Antigen analog-major histocompatibility complexes act as antagonists of the T cell receptor. *Cell* 68:625-634.
153. Jameson, S. C., F. R. Carbone, and M. J. Bevan. 1993. Clone-specific T cell receptor antagonists of major histocompatibility complex class I-restricted cytotoxic T cells. *J Exp Med* 177:1541-1550.
154. Racioppi, L., F. Ronchese, L. A. Matis, and R. N. Germain. 1993. Peptide-major histocompatibility complex class II complexes with mixed agonist/antagonist properties provide evidence for ligand-related differences in T cell receptor-dependent intracellular signaling. *J Exp Med* 177:1047-1060.
155. Wylie, D. C., J. Das, and A. K. Chakraborty. 2007. Sensitivity of T cells to antigen and antagonism emerges from differential regulation of the same molecular signaling module. *Proc Natl Acad Sci U S A* 104:5533-5538.
156. Hogquist, K. A., A. J. Tomlinson, W. C. Kieper, M. A. McGargill, M. C. Hart, S. Naylor, and S. C. Jameson. 1997. Identification of a naturally occurring ligand for thymic positive selection. *Immunity* 6:389-399.
157. Yachi, P. P., C. Lotz, J. Ampudia, and N. R. Gascoigne. 2007. T cell activation enhancement by endogenous pMHC acts for both weak and strong agonists but varies with differentiation state. *J Exp Med* 204:2747-2757.

158. Evans, E., K. Ritchie, and R. Merkel. 1995. Sensitive force technique to probe molecular adhesion and structural linkages at biological interfaces. *Biophys J* 68:2580-2587.
159. Huse, M., L. O. Klein, A. T. Girvin, J. M. Faraj, Q. J. Li, M. S. Kuhns, and M. M. Davis. 2007. Spatial and temporal dynamics of T cell receptor signaling with a photoactivatable agonist. *Immunity* 27:76-88.
160. Wang, Y., E. L. Botvinick, Y. Zhao, M. W. Berns, S. Usami, R. Y. Tsien, and S. Chien. 2005. Visualizing the mechanical activation of Src. *Nature* 434:1040-1045.